



UNIVERSIDADE D
COIMBRA

Andreia Sofia Borges Cortês

**DESIGN AND DEVELOPMENT OF AN
INNOVATIVE GREEN VERTICAL SYSTEM**

**PhD thesis in Civil Engineering, Constructions, supervised by
Professor António José Barreto Tadeu, Professor Jorge Manuel
Caliço Lopes de Brito and PhD João António Soares de Almeida,
submitted to Department of Civil Engineering of the Faculty of
Sciences and Technology of the University of Coimbra**

December 2020

Faculty of Sciences and Technology of the University of Coimbra

Design and development of an innovative green vertical system

Andreia Sofia Borges Cortês

PhD thesis in Civil Engineering, Constructions, supervised by Professor António José Barreto Tadeu, Professor Jorge Manuel Calição Lopes de Brito and PhD João António Soares de Almeida, submitted to Department of Civil Engineering of the Faculty of Sciences and Technology of the University of Coimbra

December 2020



UNIVERSIDADE D
COIMBRA

Acknowledgements

The research work presented in this thesis was supported by the Portuguese Foundation for Science and Technology (FCT) under the Eco-Construction and Rehabilitation Programme (PhD grant PD/BD/127846/2016) for which I am extremely grateful. This work has also been developed under the Project GRLF (POCI-01-0145-FEDER-016852), co-funded by the Operational Program for Competitiveness and Internationalization (POCI) of Portugal 2020 with the support of the European Regional Development Fund (FEDER) and the Project EvaporCork (POCI-01-0247-FEDER-033357/ALG-01-0247-FEDER-033357) funded by the Operational Program for Competitiveness and Internationalization (POCI) of Portugal 2020, with the support of the European Regional Development Fund (FEDER). I also gratefully acknowledge the support provided by Amorim Cork Insulation.

I would like to express my deep gratitude to my supervisors, Professor António Tadeu, Professor Jorge de Brito and PhD João Almeida for their support, guidance and encouragement and for granting me the opportunity to carry out this work at the Institute for Research and Technological development in Construction, Energy, Environment and Sustainability (Itecons).

I would also like to extend my appreciation to all of my colleagues at Itecons, in particular to Maria Inês Santos, Ana Azevedo, Michael Brett, Saúl Martins, Miguel Esteves, André Santos, Mónica Marques, Bruna Santos and Rosário Fino for all their precious help.

Finally, I could not fail to thank all my family and friends for always encouraging me, in particular to my parents for always believing in me and for being an inspiration, to my sister for her patience and for all the wise advices, to my boyfriend for always being there and for his unconditional support and to my uncles and grandparents for all the affection.

Abstract

Urban centres are facing several challenges resulting from their quick expansion and from climate change. As a consequence, some areas have been experiencing flash floods, degradation of air quality, and an increase in temperatures. Buildings also represent a high burden in terms of greenhouse gas emission and energy consumption. It is therefore extremely important to invest in finding solutions that could help to mitigate the effects of some of these problems. In this context, the European Commission has encouraged countries and regions to adopt nature-based solutions, particularly green vertical systems (GVSs), that can improve daily living and environmental conditions.

Green vertical systems are construction solutions that use vegetation to cover a building surface. The benefits that have been attributed to them include an improvement in buildings' thermal insulation, the mitigation of the urban heat island effect, better air quality, the restoration of urban biodiversity, and the support of rainwater management. However, several questions have also been raised concerning the sustainability of these solutions. The use of materials with high environmental burdens and the high irrigation and maintenance needs of such systems are being pointed out as key aspects. Additionally, the design and implementation of GVSs can be much more complex than other green infrastructure since the plants and/or growing media must be fixed to a vertical surface.

The main goal of this research work was to design and develop an innovative green vertical system, with improved environmental performance over its life-cycle. The expanded cork agglomerate was the main material. Thermal insulation and water retention are two of the characteristics recognized in this natural material that turned it into a suitable option.

Tests were initially performed to quantify the water retention capacity and drainage capability of the insulation cork boards (ICB). The results showed that the material allows a suitable moistening and a good retention capacity, and at the same time it can quickly drain the excess water. A new ICB module was then designed, based on a set of environmental and functional aspects discussed beforehand. The ICB modules then underwent a series of mechanical tests to evaluate the behaviour of the proposed solution in wet conditions and after wetting-drying cycles. These experiments also intended to help to choose the most suitable material density to use in the new GVS. The results showed that the medium density ICB modules (140–160 kg/m³) fully meet the environmental and functional requirements, and are therefore an appropriate choice.

Afterwards, a real-scale prototype was built, consisting of four façades (facing north, south, east, and west) and two plant species (*Thymus pulegioides* and *Festuca glauca*) were selected for the system. The prototypes were monitored for one year to check the coverage area, carbon sequestration capacity, and thermal behaviour. The results showed that the system and the plant species performed well. The overall environmental profile of the system was evaluated through a life-cycle study and it was found that the new modular living wall can be an eco-friendly choice, contributing especially to mitigate global warming.

Keywords: Green vertical systems, expanded cork agglomerate, water retention, life cycle assessment, carbon sequestration, thermal performance

Resumo

Os centros urbanos enfrentam diversos desafios decorrentes da sua rápida expansão e das alterações climáticas. Como resultado, algumas destas áreas têm vindo a deparar-se com inundações repentinas, uma degradação da qualidade do ar e um aumento da temperatura. Os edifícios representam também uma grande preocupação pelas elevadas emissões de gases com efeito de estufa e pelo elevado consumo energético. Considerando todos estes aspetos, torna-se extremamente importante investir na procura de soluções que possam ajudar a mitigar alguns dos efeitos destes problemas. Neste contexto, a Comissão Europeia tem vindo a incentivar países e regiões a adotarem soluções baseadas na natureza, nomeadamente as fachadas verdes, que têm a capacidade de melhorar a qualidade de vida das populações e as condições ambientais.

As fachadas verdes são soluções construtivas que utilizam a vegetação para recobrir a fachada de um edifício. Os benefícios que lhes têm sido atribuídos incluem uma melhoria do isolamento térmico dos edifícios, a mitigação do efeito ilha de calor urbana, uma melhoria da qualidade do ar, a recuperação da biodiversidade urbana e o apoio à gestão das águas pluviais. No entanto, várias questões têm também surgido em relação à sustentabilidade destas soluções. A utilização de materiais com elevados impactes ambientais e as elevadas necessidades de irrigação e manutenção têm vindo a ser apontados como aspetos importantes. Além disso, a conceção e a implementação das fachadas verdes podem também tornar-se tarefas muito complexas quando comparadas com as de outras infraestruturas verdes uma vez que, no caso das fachadas verdes as plantas e/ou os meios de cultivo têm de ser fixados numa superfície vertical.

O objetivo principal deste trabalho de investigação foi conceber e desenvolver uma solução de fachada verde inovadora com um melhor desempenho ambiental ao longo do seu ciclo de vida. Para tal, foi utilizado como material principal o aglomerado de cortiça expandida. A capacidade de isolamento térmico e de retenção de água são duas das características reconhecidas a este material natural que o tornaram numa opção adequada.

Inicialmente foram realizados testes para quantificar a capacidade de retenção de água e de drenagem das placas de aglomerado de cortiça expandida (ICB). Os resultados mostraram que o material permite um adequado humedecimento e uma boa retenção, demonstrando simultaneamente a capacidade de escoar de forma rápida o excesso de água. A conceção de um novo módulo de ICB foi, então, realizada com base num conjunto de aspetos ambientais e funcionais discutidos anteriormente. Os módulos de ICB foram posteriormente submetidos a uma série de testes mecânicos para avaliar o comportamento da solução proposta em condições húmidas e após os ciclos de humedecimento-secagem. Esta campanha experimental teve também como objetivo ajudar na escolha da densidade do material mais adequada para usar no novo sistema de fachada verde. Os resultados mostraram que os módulos de ICB de média densidade (140–160 kg/m³) cumprem totalmente os requisitos ambientais e funcionais, mostrando-se uma escolha adequada.

Posteriormente, foi construído um protótipo em escala real constituído por quatro fachadas (orientadas a norte, sul, este e oeste) e foram selecionadas duas espécies de plantas (*Thymus pulegioides* e *Festuca glauca*) para integrarem o sistema. Os protótipos foram monitorizados durante um ano em termos da área de cobertura, do sequestro de carbono e do comportamento térmico. Os resultados revelaram um bom desempenho do sistema e das espécies vegetativas selecionadas. O perfil ambiental e global do sistema foi avaliado por meio de um estudo de ciclo de vida. Os resultados mostraram que a nova fachada verde pode ser uma escolha ecologicamente correta, contribuindo principalmente para mitigar o aquecimento global.

Palavras-chave: Fachadas verdes, aglomerado de cortiça expandida, retenção de água, avaliação de ciclo de vida, sequestro de carbono, desempenho térmico

Table of contents

CHAPTER 1	1
1. Introduction.....	3
1.1. Context and motivation	3
1.2. Objectives	5
1.3. Thesis structure	5
References	7
CHAPTER 2	9
2. Water retention and drainage capability of expanded cork agglomerate boards intended for application in green vertical systems.....	11
2.1. Introduction	11
2.2. Experimental setup.....	13
2.3. Results and discussion	15
2.3.1. Fully confined tests.....	16
2.3.2. Partially confined tests.....	20
2.3.3. Microscopic analysis	23
2.4. Conclusions.....	24
References	25
CHAPTER 3	29
3. Innovative module of expanded cork agglomerate for green vertical system.....	31
3.1. Introduction	31
3.2. Methods	34
3.2.1. Life cycle analysis	34
3.2.2. Mechanical tests	37
3.3. Results and discussion	39
3.3.1. Design process	39
3.3.2. Mechanical characterization.....	44
3.4. Conclusions.....	55
References	56
CHAPTER 4	61
4. Environmental performance of a cork-based modular living wall from a life-cycle perspective.....	63
4.1. Introduction	63
4.2. Methodologies.....	65
4.2.1. Prototype description	66
4.2.2. Carbon sequestration analysis	67

4.2.3.	Area covered with vegetation.....	68
4.2.4.	Life cycle assessment of the modular living wall system	68
4.3.	Results and discussion.....	69
4.3.1.	Carbon sequestration	69
4.3.2.	Covered area.....	73
4.3.3.	Environmental performance	76
4.4.	Conclusions	81
	References	82
	CHAPTER 5.....	87
5.	The effect of a cork-based modular living wall on the energy performance of buildings and local microclimate	89
5.1.	Introduction	89
5.2.	Methodology	92
5.3.	Results	95
5.3.1.	Temperature profiles	95
5.3.2.	Microclimate effect	100
5.3.3.	Comparison with an ETICS insulated wall.....	102
5.3.4.	Simulation of energy savings	104
5.4.	Conclusions	105
	References	106
	CHAPTER 6.....	111
6.	Final remarks	113
6.1.	Overview and main conclusions.....	113
6.2.	Future work.....	115

Index of figures

Figure 2.1 - Experimental setup used to study water retention and drainage capability of expanded cork agglomerate boards of varying height (H), thickness (T) and density: a) fully confined tests; b) partially confined tests (50% of the front removed).....	15
Figure 2.2 - Drainage curves for fully confined test specimens: a) (H=2000 mm; T=200 mm); b) (H=1000 mm; T=200 mm); c) (H=1000 mm; T=100 mm).....	17
Figure 2.3 - Runoff time for fully confined test specimens: a) H=2000 mm; T=200 mm; b) H=1000 mm; T=200 mm; c) H=1000 mm; T=100 mm.....	18
Figure 2.4 - Water retention for fully confined test specimens: a) H=2000 mm; T=200 mm; b) H=1000 mm; T=200 mm; c) H=1000 mm; T=100 mm.....	19
Figure 2.5 - Drainage curves for partially confined test specimens with H=1000 mm and T=200 mm: a) Facade; b) Interior.....	20
Figure 2.6 - Drainage curves for partially confined test specimens with H=1000 mm and T=100 mm: a) Facade; b) Interior.....	21
Figure 2.7 - Runoff time for partially confined test specimens: a) H=1000 mm; T=200 mm; b) H=1000 mm; T=100 mm.	22
Figure 2.8 - Water retention for partially confined test specimens: a) H=1000 mm; T=200 mm; b) H=1000 mm; T=100 mm.	23
Figure 2.9 - Scanning electron microscopy (SEM) images obtained for expanded cork agglomerate boards of different density.	24
Figure 3.1 - Schematic representation of green vertical systems (adapted from [2]).....	32
Figure 3.2 - System boundaries of the life cycle of GVSs.	35
Figure 3.3 - Illustration of: (a) a person climbing the living wall, simulating the loads generated by doing so; (b) a ladder propped against the living wall, representing a maintenance operation.	38
Figure 3.4 - LCA impacts of product stage for systems S1 to S5.	40
Figure 3.5 - Schematic representation of the new ICB module for living walls.	43
Figure 3.6 - Illustration of a modular living wall built with the new ICB modules.....	44
Figure 3.7 - Force-extension curves for dry specimens and compression behaviour apparatus.	45
Figure 3.8 - Force-extension curves for dry specimens and bending behaviour apparatus.....	47
Figure 3.9 - Force-extension curves for dry specimens and tensile strength perpendicular to faces apparatus.	48
Figure 3.10 - Force-extension curves for dry specimens and shear behaviour apparatus.	49
Figure 3.11 - Force-extension curves for a distributed load applied to the outer edge of the module specimens.	50
Figure 3.12 - Force-displacement curves recorded when point loads are applied to the centre of the outer edge of the module specimens.	51

Figure 3.13 - Force-displacement curves recorded when point loads are applied to the corners of the outer edge of the module specimens.	51
Figure 4.1 - Side view of the new cork-based module with all the components.....	66
Figure 4.2 - Schematic illustration of the prototype preparation: (a) bearing wall; (b) cork-based modules; (c) geotextile filter and technical substrate; (d) drip irrigation lines; (e) side covers; (f) plants.	67
Figure 4.3 - Living wall prototype showing <i>Thymus pulegioides</i> (left side) and <i>Festuca glauca</i> (right side).67	
Figure 4.4 - Total carbon content per square meter of façade (g/m ²) in the aboveground biomass samples.	71
Figure 4.5 - Total carbon content per square meter of façade (g/m ²) in the belowground biomass samples.	72
Figure 4.6 - Cumulative carbon uptake in above and belowground biomass over one year.	73
Figure 4.7 - Representative images of the north-facing test façade for <i>Festuca glauca</i> processed with the aim of estimating the covering area (%).	74
Figure 4.8 - Representative images of the north-facing test façade for <i>Thymus pulegioides</i> processed with the aim of estimating the covering area (%).	74
Figure 4.9 - Area of the façade (%) covered by <i>Thymus pulegioides</i> and <i>Festuca glauca</i> during one year.	75
Figure 4.10 - System boundaries of the LCA study.	76
Figure 4.11 - Potential environmental impacts for the product stage of the cork-based living wall normalized for 100%.	78
Figure 4.12 - Potential environmental impacts for the entire life cycle of the cork-based living wall normalized for 100%.	79
Figure 4.13 - Potential environmental impacts for the entire life cycle for the reference wall (RW) and the wall improved with the new modular living wall (RW+GVS).	81
Figure 5.1 - Schematic representation of the cork-based module: (A) Plants; (B) Drip irrigation lines; (C) Technical substrate; (D) Geotextile filter; (E) Cork-based modules; (F) Adhesive mortar; (G) Bearing wall.	93
Figure 5.2 - Plant species used: a) <i>Thymus pulegioides</i> ; b) <i>Festuca glauca</i>	93
Figure 5.3 - Schematic representation of the thermocouples positions: a) Cross-section view b) Longitudinal view: T – <i>Thymus pulegioides</i> area and F – <i>Festuca glauca</i> area.	94
Figure 5.4 - Temperatures recorded during three consecutive days representative of winter season (January 2020).	96
Figure 5.5 - Temperatures recorded during three consecutive days representative of summer season (July 2020).	99
Figure 5.6 - Temperatures recorded in a summer day, when the outer surface of the ICB layer was kept dry.	101
Figure 5.7 - Temperatures recorded in a summer day with, when the outer surface of the ICB layer was sprayed with water.	101

Figure 5.8 - Surface temperatures of the modular living walls and of the reference walls with ETICS (summer)	102
Figure 5.9 - Surface temperatures of the modular living walls, when the outer surface of the ICB layer was sprayed with water, and of the reference walls with ETICS (summer)	103

Index of tables

Table 2.1 - Nominal dimensions of the expanded cork agglomerate boards	14
Table 3.1 - Materials used in each system and respective amounts according to the defined functional unit.....	36
Table 3.2 - Compressive strength tests: results for dry specimens.....	46
Table 3.3 - Flexural strength tests: results for dry specimens	47
Table 3.4 - Tensile strength perpendicular to faces tests: results for dry specimens.....	48
Table 3.5 - Shear strength tests: results for dry specimens	49
Table 3.6 - Results obtained when the outer edge of the module specimens is subjected to distributed load tests.....	50
Table 3.7 - Results obtained when the outer edge is subjected to point loads at the centre of the module specimens	51
Table 3.8 - Results obtained when the outer edge is subjected to point loads at the corners of the module specimens	52
Table 3.9 - Medium density ICB tests results performed on specimens that were dry, wet, and had undergone 30 wetting-drying cycles	54
Table 3.10 - Results of the adhesion tests performed on dry MD specimens and MD specimens after 30 wetting-drying cycles	54
Table 4.1 - Dry mass of the aboveground biomass per square meter of façade (g/m ²) from week 0 (W0) to week 55 (W55).....	69
Table 4.2 - Dry mass of the belowground biomass per square meter of façade (g/m ²) from week 0 (W0) to week 55 (W55).....	70
Table 4.3 - Carbon content ± standard deviation, %(m/m)	71
Table 4.4 - Input and output flows of the new modular living wall according to the functional unit defined	77
Table 4.5 - Potential environmental impacts for the entire life cycle of the cork-based living wall	79
Table 5.1 - Average maximum and minimum temperatures recorded during three consecutive days in January 2020.....	97
Table 5.2 - Average maximum and minimum temperatures recorded during three consecutive days in July 2020.....	100
Table 5.3 - Heating and cooling needs for a reference building and a modified building containing ICB boards of 50 mm and 200 mm thickness covering the outer walls.....	104

CHAPTER 1

INTRODUCTION

1. Introduction

1.1. Context and motivation

Urban centres concentrate a wide range of economic activities, infrastructure elements, and people, increasing the vulnerabilities and challenges associated with the sustainable management of these territories. Recent figures indicate that about 75% of the European Union population lives in cities and by 2050 this number will be reaching nearly 85% [1], [2]. The fast expansion of cities has been increasing the built-up areas and changing their morphology as it increases the soil sealed areas. As a result, some cities are already facing changes in the water cycle, biodiversity, and local climate conditions, making, for example, episodes of flash floods much more frequent. Climate changes have also contributed to exacerbating all of these problems and turned towns and cities into vulnerable areas [3]. Additionally, urban centres around the world are responsible for 72% of all global greenhouse gas emissions. In Europe, buildings account for 36% of greenhouse gas emissions and 40% of the energy consumption. Nearly 75% of EU buildings are considered energy inefficient [4].

For these reasons, cities are seen as key areas for interventions that will not only increase the resilience of these territories, but will also help to make these problems less significant [2], [3]. The European Commission has proposed to reduce greenhouse gas emissions by 55% by 2030, relative to the 1990 levels. To meet this objective, buildings will have to reduce their greenhouse gas emissions by 60%, their final energy consumption by 14%, and the energy used for acclimatization by 18%, relative to 2015 levels [5]. The European Green Deal also states that efforts should be made to improve the resilience of buildings and to create climate adaptation strategies that promote public and private investment, especially in the nature based-solutions [6]. The EU biodiversity

strategy for 2030 also sets targets for green cities that should be achieved through the implementation of several solutions, among which are green roofs and walls [7]. Additionally, investment in sustainable solutions has been considered crucial for Europe's economy [2].

Several authors had previously demonstrated the benefits enhanced by green infrastructures, which were also recognized in the Final Report of the Horizon 2020 Expert Group on "Nature-Based solutions". Green infrastructure, in particular green vertical systems, have important features that could help to improve building thermal insulation, mitigate the UHI effect, increase air quality, reduce noise levels, restore urban biodiversity, and help in rainwater management, by reducing the peak flows [8]. In this context, some countries are already establishing policies and guidelines to promote the adoption of green strategies, making them mandatory by legislation in some situations [9]–[13].

However, as far as green vertical systems are concerned, important questions have been raised concerning the sustainability of these infrastructure elements, when assessed from a life cycle perspective. The materials used, the vegetative species selected and the irrigation and maintenance needs are key factors that have to be carefully studied to secure the sustainability of these elements [14]–[16]. Specifically, several challenges have been reported related to the design and implementation of GVSs. Green vertical systems are much more complex solutions in terms of design than green roofs. This is because the plants and/or growing media must be fixed to a vertical surface, for which metal or plastic components are often used. Moreover, GVSs often require more systematic watering since they contain less substrate (or no substrate at all) [17]. Despite that, a building's façade could have a much larger area than its green roof, which extends the possibility for greening these surfaces.

Designing and developing an innovative green vertical system, with improved environmental performance throughout its life cycle, is the main focus of this research. It will be achieved by using expanded cork agglomerate, which is a natural material whose water retention and thermal insulation capacity is recognized. Expanded cork agglomerate is an insulation material made by agglomerating the by-products of the cork industry and the waste resulting from the pruning the cork oaks that is agglomerated with the resins naturally present. The cork is taken from the bark of the cork-oak without harming any trees, and it is therefore considered a sustainable practice. Cork also retains carbon as the cork oak trees grow and it is estimated that the cork forests sequester up to 14 million tons of CO₂, every year [18]. The use of expanded cork agglomerate as a base material for a green vertical system should help to reduce the environmental burden of the common raw materials. It is thus intended, in this work, to develop a feasible design with expanded cork agglomerate boards and then characterize the new green vertical system performance in terms of the benefits provided and its overall environmental profile.

1.2. Objectives

This research work was intended to design and develop an innovative green vertical system with improved environmental performance throughout its life cycle. Expanded cork agglomerate was used to improve the environmental performance of the proposed solution. To accomplish this main goal, the following specific objectives were defined:

- Evaluation of the behaviour of expanded cork agglomerate in terms of its water retention and drainage capability to use in a green vertical system by studying different densities, heights, and thicknesses of the material;
- Comparison of different GVS solutions to identify the environmental hotspots and establish design guidelines for the new GVS;
- Design of a new GVS based on the environmental and functional requirements and using expanded cork agglomerate as the main material;
- Evaluation of the mechanical performance of the proposed GVS design under different test conditions;
- Experimental monitoring of the new green vertical system under field conditions, particularly in terms of plant development;
- Quantification of carbon sequestration potential provided by the new GVS for different plant species and geographical orientations;
- Application of life cycle methodologies to evaluate the environmental performance of the new GVS in a cradle-to-grave perspective;
- Assessment of thermal performance of the new GVS in terms of its insulation capacity;
- Assessment of the proposed GVS on the local micro-climate.

The research work needed to meet these objectives was carried out at Itecons - Institute for Research and Technological Development for Construction Sciences, Energy, Environment and Sustainability, in Coimbra. It is a laboratory that offers a great many experimental tests accredited by IPAC - Instituto Português de Acreditação (member of EA - European Cooperation for Accreditation and ILAC - International Laboratory Accreditation Cooperation).

1.3. Thesis structure

The research work reported in this thesis is organized into six chapters that include this introduction (Chapter 1), the design and characterization of the innovative green vertical system (Chapters 2 to 5) and final remarks (Chapter 6). Once the main chapters correspond to manuscripts already published or submitted to indexed journals, they follow a structure of an article, comprising an

introduction, description of methods, discussion of the results, conclusions, and references. This means that each chapter can be accessed as a complete unit without needing to seek information in other chapters.

Chapter 2 describes the experimental tests carried out to evaluate the water retention and drainage capability of expanded cork agglomerate boards of varying density, height, and thickness for application in a green vertical system. Board specimens were fully confined laterally in a watertight box with open ends at the top and bottom, with successive water discharges being carried out on the top. Other tests were performed with the front of the box removed, thus allowing the water to drain from the façade, too.

Chapter 3 describes the design process for a new modular GVS based on insulation cork boards (ICBs). A comparative life cycle analysis (LCA) of several GVSs was first carried out to identify the environmental hotspots of most concern with respect to the product phase. Based on the conclusions of the LCA and a set of additional functional requirements, a new ICB module to build a GVS with better environmental performance was created. Since ICBs can be produced with different mass densities, with distinct environmental impacts and manufacturing costs, a full mechanical characterization was also carried out to assist in choosing the most suitable ICB density.

Chapter 4 presents an extended characterization of the new GVS to assess its performance in real conditions, with different plant species, geographical orientations, and in different seasons. For this purpose, a prototype was built with four façades, facing north, south, east, and west. The area of façade covered by vegetation and the carbon sequestration provided by two different plant species were then monitored for over a year. LCA methodologies were used to evaluate the environmental performance of the new GVS from a cradle-to-grave perspective. Annual values of carbon uptake, experimentally determined, were further used to update the environmental life cycle model of the system. A comparative LCA was also performed to assess the benefits of installing the new GVS on a building façade.

In Chapter 5 the thermal performance of the new GVS was evaluated experimentally under real conditions. For that purpose, the prototype described in Chapter 4 was used. The temperatures were recorded at different points on the façades facing north, south, east, and west using a set of thermocouples. The ambient temperature in the vicinity of the façade was also monitored. This study was carried out for over a year to assess the performance of the new GVS in winter and summer conditions. Real climate data were further used to update a model in the DesignBuilder and the results obtained discussed in terms of energy savings.

Chapter 6 summarizes the main conclusions of the research work performed and suggests the sort of work that could usefully be done to continue this study.

References

- [1] The world bank, “Urban population (% of total population) - European Union”. [Online]. Available: <https://data.worldbank.org/indicator/SP.URB.TOTL.IN.ZS?locations=EU>.
- [2] European Commission, “Proposed Mission: 100 Climate-neutral Cities by 2030 – by and for the Citizens”, 2020. [Online]. Available: https://ec.europa.eu/info/publications/100-climate-neutral-cities-2030-and-citizens_en.
- [3] European Environment Agency, “Urban adaptation in Europe : how cities and towns respond to climate change”, 2020. [Online]. Available: <https://climate-adapt.eea.europa.eu/metadata/publications/urban-adaptation-in-europe-how-cities-and-towns-respond-to-climate-change>.
- [4] European Commission, “Energy efficiency in buildings”, 2020. [Online]. Available: https://ec.europa.eu/info/publications/100-climate-neutral-cities-2030-and-citizens_en.
- [5] European Commission, “Communication from the Commission to the European Parliament, the Council, the European Economic and Social Committee and the Committee of the Regions - A Renovation Wave for Europe - greening our buildings, creating jobs, improving lives”, COM(2020) 662 final. [Online]. Available: https://ec.europa.eu/energy/topics/energy-efficiency/energy-efficient-buildings/renovation-wave_en.
- [6] European Commission, “Communication from the Commission to the European Parliament, the Council, the European Economic and Social Committee and the Committee of the Regions - The European Green Deal”, COM(2019) 640 final. [Online]. Available: https://ec.europa.eu/info/strategy/priorities-2019-2024/european-green-deal_en.
- [7] European Commission, “Communication from the Commission to the European Parliament, the Council, the European Economic and Social Committee and the Committee of the Regions - EU Biodiversity Strategy for 2030 - Bringing nature back into our lives”, COM(2020) 380 final. [Online]. Available: https://ec.europa.eu/environment/nature/biodiversity/strategy/index_en.htm.
- [8] European Commission, “Towards an EU Research and Innovation policy agenda for Nature-Based Solutions & Re-Naturing Cities”, 2015. [Online]. Available: <http://bookshop.europa.eu/en/towards-an-eu-research-and-innovation-policy-agenda-for-nature-based-solutions-re-naturing-cities-pbKI0215162/>.

- [9] UNEP, AITF, FFP, HORTIS, and L. V. D. L. V. ARRDHOR, “Recommandations professionnelles B.C.3-R0: Conception, réalisation et entretien de solutions de végétalisation de façades par bardage rapporté”, 2016.
- [10] UNEP, AITF, FFP, HORTIS, and L. V. D. L. V. ARRDHOR, “Recommandations professionnelles B.C.5-R0: Conception, réalisation et entretien de solutions de végétalisation de façades par plantes grimpantes”, 2016.
- [11] Fll - Landscape Development and Landscaping Research Society e. V., “Fassadenbegrünungsrichtlinien – Richtlinien für die Planung, Bau und Instandhaltung von Fassadenbegrünungen”, 2018.
- [12] Urban Greening and N. build Landscapes, “UK Guide to Green Walls - An introductory guide to designing and constructing green walls in the UK”.
- [13] State Government of Victoria, “Growing Green Guide: A guide to green roofs, walls and facades in Melbourne and Victoria”, Australia. 2014.
- [14] M. Ottel , K. Perini, A. L. A. Fraaij, E. M. Haas, and R. Raiteri, “Comparative life cycle analysis for green facades and living wall systems”, *Energy and Buildings*, vol. 43, pp. 3419–3429, 2011.
- [15] H. Feng and K. Hewage, “Lifecycle assessment of living walls: Air purification and energy performance”, *Journal of Cleaner Production*, vol. 69, pp. 91–99, 2014.
- [16] V. Oquendo-Di Cosola, F. Olivieri, L. Ruiz-García, and J. Bacenetti, “An environmental Life Cycle Assessment of Living Wall Systems”, *Journal of Environmental Management*, vol. 254, p. 109743, 2020.
- [17] A. Medl, F. Florineth, S. B. Kikuta, and S. Mayr, “Irrigation of ‘Green walls’ is necessary to avoid drought stress of grass vegetation (*Phleum pratense* L.)”, *Ecological Engineering*, vol. 113, pp. 21–26, 2018.
- [18] Amorim cork insulation, “The forest. Life hotspot.”. [Online]. Available: <https://www.amorimcorkinsulation.com/en/cork/the-forest/>.

CHAPTER 2

WATER RETENTION AND DRAINAGE CAPABILITY OF
EXPANDED CORK AGGLOMERATE BOARDS INTENDED
FOR APPLICATION IN GREEN VERTICAL SYSTEMS

2. Water retention and drainage capability of expanded cork agglomerate boards intended for application in green vertical systems

2.1. Introduction

The increasing numbers of people living in urban areas are creating several challenges regarding the sustainable management of available resources and maintenance of the quality of life. It is estimated that 75% of the European Union population live in urban areas [1]. This high concentration of people and economic activities also contribute to transforming urban centres into areas sensitive to extreme weather phenomena resulting from the climate changes [2]. Furthermore, the reduction of green areas and the intensive anthropogenic activities in many cities are also threatening the quality of life and people's state of health as several European cities still do not comply with EU air quality directives regarding the most concerning air pollutants: PM, NO_x, O₃ and NH₃ [1], [3]. Alongside this reality, the building and construction sector is responsible for 36% of global energy use and 39% of energy related CO₂ emissions [4]. As a result, governments and decision makers are looking forward to finding solutions that can either minimize or adapt urban areas to answer these challenges. The European Commission is also encouraging the adoption of what are known as Nature-Based Solutions (NBS). These are engineered solutions inspired and supported by nature itself. ReNaturing cities is a strategy to bring green areas to urban centres again to meet the challenges presently faced by cities. Regarding this, some countries have already

established politics and guidelines to promote the adoption of these green strategies, making them legally compulsory in some cases [5], [6].

Green vertical systems (GVS) are among the solutions suggested within this concept [6]. GVS are engineered solutions that involve covering walls with vegetation. The large number of designs and constructive solutions make it difficult to categorize them using standard classifications. According to Manso and Gomes [7] the GVS can be divided into two large categories: green facades and living walls. Green facades are systems in which plants are attached directly to the wall (direct green facades) or to a specific structure such as cables or guides (indirect green facades). Living walls are solutions that enable plants to grow on a vertical surface, either with or without substrate, and are designated as continuous or modular systems according to their characteristics [7].

Green vertical systems may improve a building's thermal and acoustic performance in several ways [8]–[11]. Furthermore, covering the building envelope with vegetation can also greatly benefit the urban environment by reducing the urban heat island effect (UHI) [12], [13], improving the air quality [14]–[16], delaying water peak flows [17], [18] and restoring urban biodiversity [19], [20]. However, despite the benefits described, the sustainability of these systems is often questioned because of the maintenance, irrigation and fertilization they need. Moreover, many of the materials used represent a high environmental burden. They often include plastic (e.g. PE, PVC, PP and polyamide) and metal components (e.g. steel and Al alloy) specifically designed to hold plants and fix the GVS to the wall, respectively [21]–[24]. A variety of felts and other fabrics are also very often used to keep the plants perpendicular to the wall and prevent the substrate from falling out [21], [22]. Green vertical systems also have a steep slope which means that the irrigation water drains away quickly rather than being retained for use by the vegetation. Additionally, these systems generally make use of small quantities of substrate, increasing the need for a correct irrigation system. In fact, a water failure is one of the main reasons that compromises the feasibility of GVS [25]. Medl et al [26] studied the necessity to use an artificial irrigation system by comparing two test plots, one with an activated irrigation system and other with a deactivated one. The authors concluded that irrigation systems are mandatory components to assure the viability of the vegetation.

In this chapter, studies have been performed to evaluate expanded cork agglomerate as a sustainable alternative to conventional materials used in GVS. Expanded cork agglomerate, which has been widely used as thermal and acoustic insulation in buildings, could help to reduce the environmental burden of the usual raw materials if it is used instead of some of the plastic, metal and felt components. Furthermore, expanded cork agglomerate could also regulate drainage and enhance water retention, thus helping to reduce the need for irrigation. Some authors have already enhanced the environmental performance of this material compared with conventional alternatives [27]–[29].

The influence of water absorption by the expanded cork agglomerate boards on the heat transferred across the wall has also been studied [30]–[32].

An example of a living wall using expanded cork agglomerate has already been proposed and characterized in terms of thermal and environmental performance [33], [34]. In addition to the expanded cork boards that help to keep the substrate and plants in circular openings, that system also contains a geopolymer base plate to minimize water loss and irrigation needs. On vertical or sloping surfaces, it might be necessary to ensure the continuity and stability of the system by inserting a support structure in the gaps between modules. In this work, however, it was explored the possibility of making a GVS entirely of expanded cork boards and study the water retention and drainage capability provided by this material in such circumstances.

Expanded cork agglomerate boards are produced from by-products of the cork industry and from the waste resulting from the pruning of the cork oak. The industrial production starts with sieving and screening operations to prepare the raw material of an adequate grain size. The cork granules are then placed in autoclaves to process the agglomeration of the material into large boards by the natural resins contained in the cork. After a period of stabilization the boards are rectified and cut to the required dimensions [35]. Note that the incorporation of such boards in GVS solutions is not expected to increase the overall cost per square meter compared with other, more conventional, solutions.

The next section describes the experimental setup used to the study water retention and drainage capability of expanded cork agglomerate boards of varying density, height and thickness. Since water can percolate a cork board in different directions, two different tests were performed to assess the vertical percolation capacity within and near the free surfaces of the boards. Within the board the water mainly drains in the vertical direction, under the action of the gravity forces and given the lateral confinement; near the free surfaces some water might escape from the board and form a film of water on the surface. The results are presented and discussed in terms of drainage profiles, runoff times and retention capacity. Finally, some comments on the potential benefits for GVS applications are presented.

2.2. Experimental setup

The water retention and drainage capability of expanded cork agglomerate boards for application in GVS were assessed using test specimens of varying height, thickness and density, provided by Amorim Cork Insulation (a business unit of the Amorim Group). Nominal dimensions of the

expanded cork agglomerate boards are presented in Table 2.1. All the boards were kept in a climatic chamber at 23 °C and 50% relative humidity for 48 hours before the tests.

Two tests were performed to study the behaviour of expanded cork boards when water is discharged on them. In the first, board specimens were laterally confined in a watertight marine plywood box with open ends at the top and bottom (fully confined tests). In the second, the front of the box had an extra opening, allowing the drainage to occur also through the facade (partially confined tests). In both cases, to ensure that the drainage occurs only through the ICB board, silicone wires were passed horizontally every 200 mm between the plywood and the ICB board. A small device containing a flush valve was also used to ensure a reproducible quick discharge of water over the specimen. These boxes were supported by a structure placed on a calibrated scale with a sensitivity of ± 0.02 kg, connected to a computer with a frequency of acquisition of 5 readings per second. For the partially confined tests, a second calibrated scale connected to the same acquisition system was used to weigh the water collected from the facade separately. Figure 2.1 shows the experimental setup.

Table 2.1 - Nominal dimensions of the expanded cork agglomerate boards

Ref.	Height (H) (mm)	Thickness (T) (mm)	Volume (m ³)	Density (kg/m ³)
Standard density (ST)	2000	200	0.20	90 – 110
	1000	200	0.10	
	1000	100	0.05	
Medium density (MD)	2000	200	0.20	140 - 160
	1000	200	0.10	
	1000	100	0.05	
High density (HD)	2000	200	0.20	170 - 190
	1000	200	0.10	
	1000	100	0.05	

The volume of water discharged on the top of the agglomerate cork board was specified to ensure that the board achieved maximum retention and excess water was released from the bottom. Additionally, the volume of water discharged was adjusted to maintain the same hydraulic load (260 mm water column) along the different tests. Thus, approximately 26.6 l were used for the 200 mm thick specimens, while 13.3 l were used for the 100 mm thick specimens. The tests were conducted in a laboratory at controlled temperature ($20\pm 3^\circ\text{C}$) and relative humidity ($50\pm 5\%$).

Each test specimen was subjected to 4 repeated flushes over 24 hours or 48 hours, in the case of specimens of 1000 mm or 2000 mm height, respectively, to simulate consecutive watering episodes. Note that a longer period was necessary for the 2000 mm specimens to ensure the complete drainage of water.

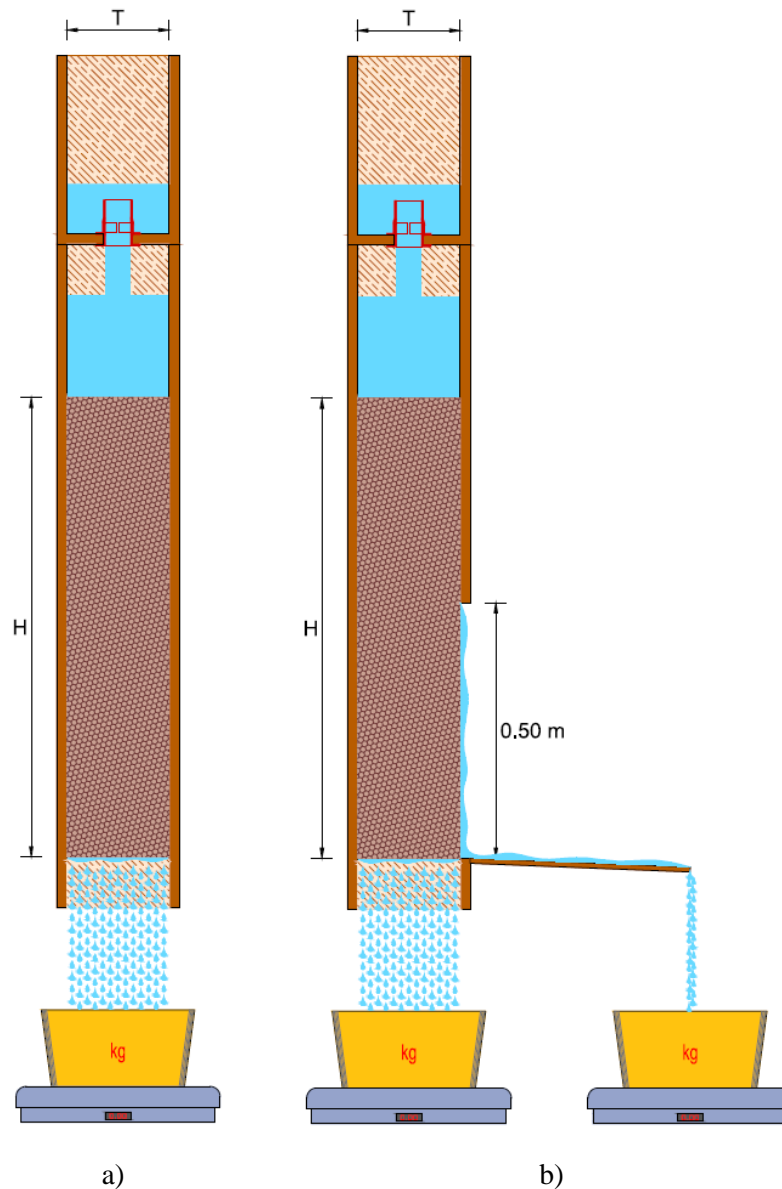


Figure 2.1 - Experimental setup used to study water retention and drainage capability of expanded cork agglomerate boards of varying height (H), thickness (T) and density: a) fully confined tests; b) partially confined tests (50% of the front removed).

2.3. Results and discussion

Drainage profiles obtained for the fully confined and partially confined tests are fully described in this section. Results for the four flushes are discussed in terms of accumulated drained water, drainage velocity, water retention and runoff time, taking into account differences of height, thickness and density of the test specimens. Note that results are discussed in terms of drainage velocity instead of flow, since the cross-sectional area of the test specimens varies to allow the results to be compared for different board thicknesses.

2.3.1. Fully confined tests

Drainage profiles

As noted above, board specimens of varying height, thickness and density were fully laterally confined in a watertight box and successive discharges of water were applied to them. The drainage profiles obtained are presented in Figure 2.2. For easier comparison of the results, the graphics are presented as a matrix with density variation along the columns and height and thickness variation along the rows. In each graphic, the drainage velocity is represented on the left axis, while the accumulated drained water is represented on the right axis. Note that a different maximum axis limit was used to represent the drainage velocity for standard density specimens since their results are significantly higher than those for the medium and high density specimens.

All the drainage profiles tend to show a similar behaviour, with water velocity decreasing with both flush number and density. These results suggest that the smaller intergranular spaces in denser cork boards make water drainage more difficult. Concomitantly, the expansion of cork granules caused by the presence of water contributes to making the intergranular spaces smaller and thus reduces drainage velocity.

Differences in the final amount of accumulated drained water result from the amount of water retained by each specimen. Thus, it can be seen that more water from the first flushes on dry specimens is retained compared with the subsequent flushes on wet specimens.

Looking now at the effect of specimen height on the drainage profiles, it is found that, in general, the water velocity decreases for the taller specimens, which is probably caused by the resistance that the expanded cork agglomerate produces to the drainage flow. However, this effect is not noticeable for the densest specimens, where the drainage resistance is much higher and the natural variability of the material predominates.

Regarding thickness variation, it can be seen that water velocity decreases for decreasing thickness, suggesting greater wall effects promoted by the box panels on the thinner specimens. Meanwhile, for the denser specimens, greater resistance to drainage flow is provided by the material, and these wall effects are less marked.

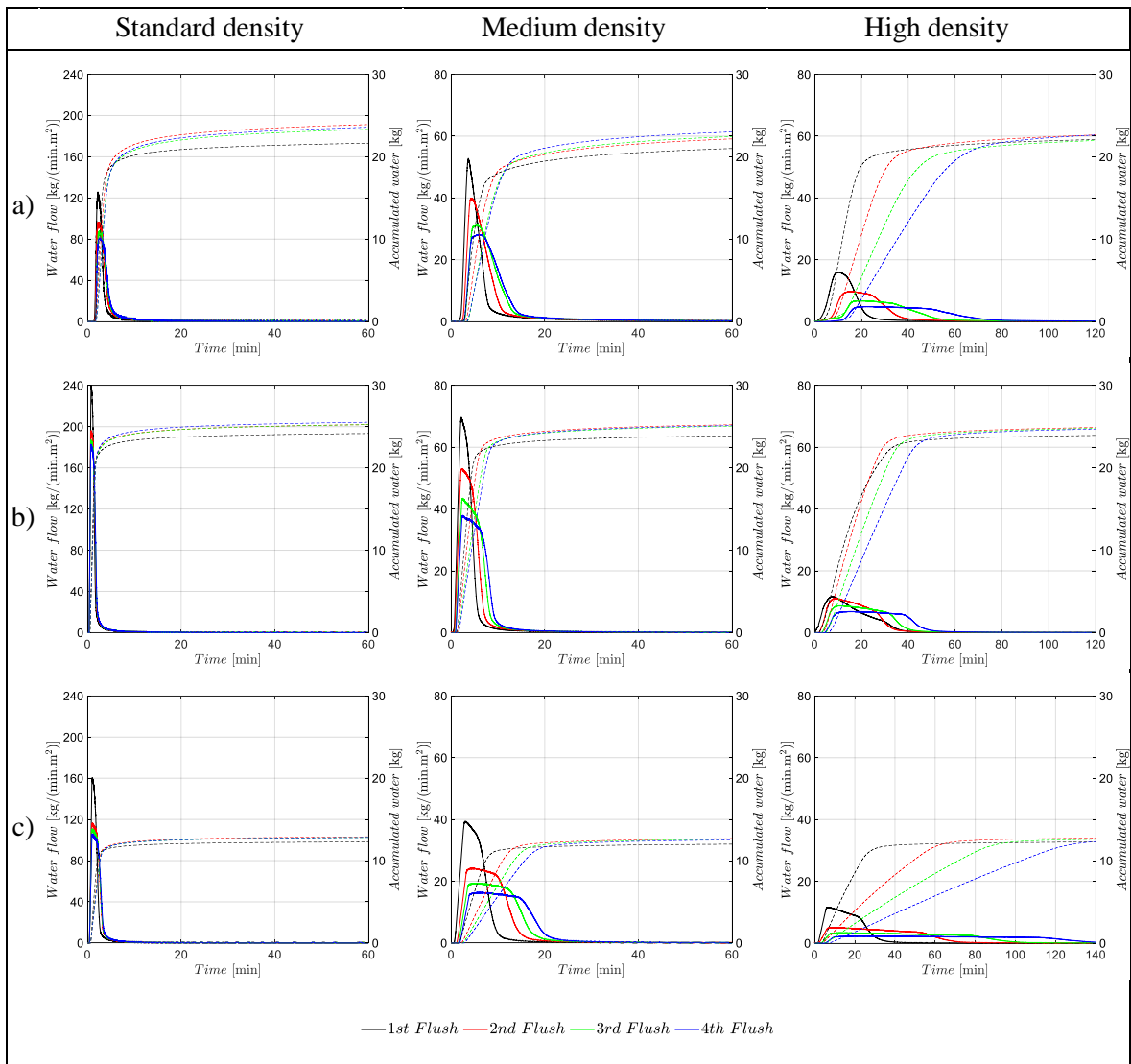


Figure 2.2 - Drainage curves for fully confined test specimens: a) (H=2000 mm; T=200 mm); b) (H=1000 mm; T=200 mm); c) (H=1000 mm; T=100 mm).

Runoff time

Since drainage velocity influences the performance of irrigation and the capacity of the system to slow water peak flows, it is important to analyse the runoff time provided by the different cork boards. Thus, the time taken to drain 15%, 40% and 65% of the total water discharged on the specimens has been calculated (Figure 2.3). Note that runoff times were not compared for higher water percentages because of the amount of water retained by some specimens.

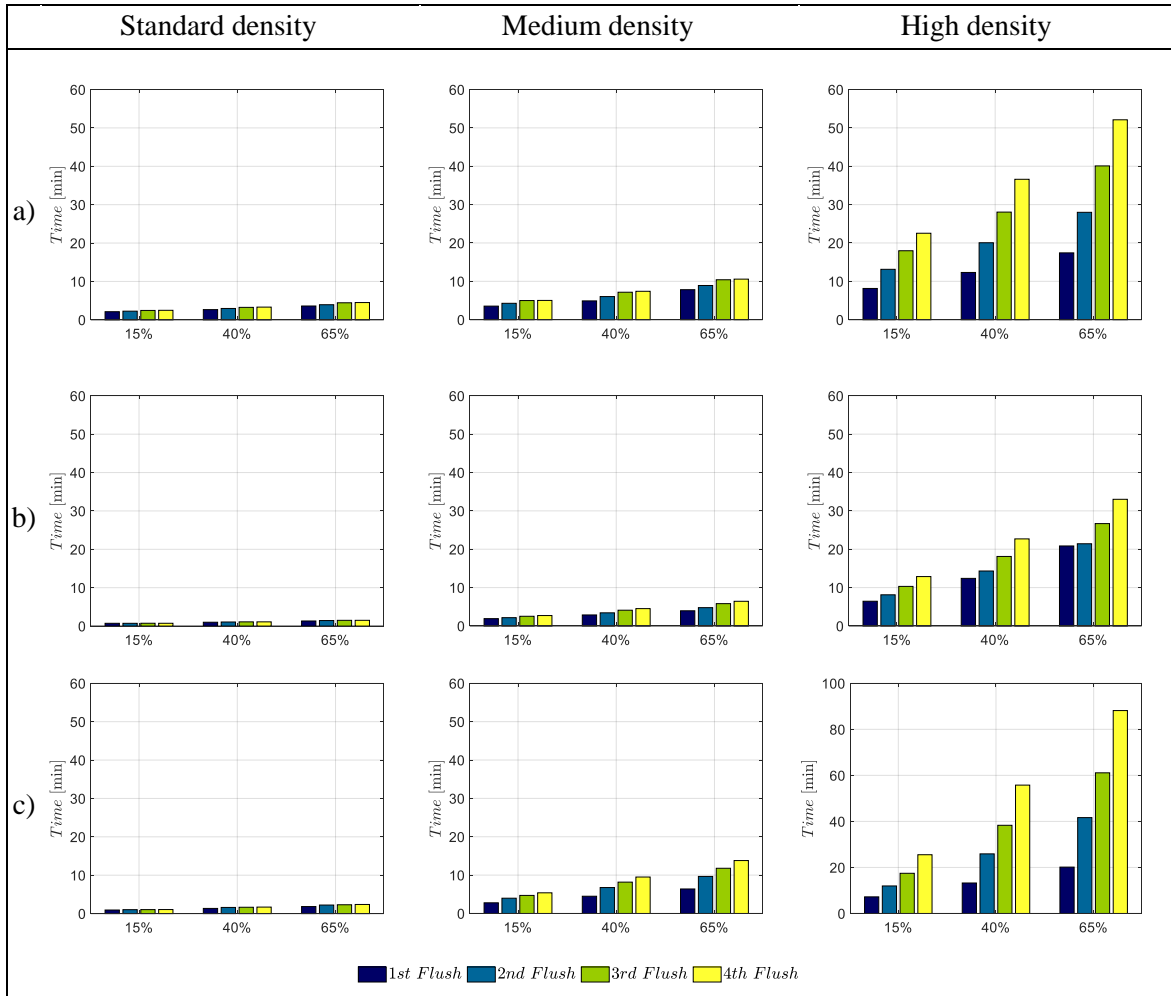


Figure 2.3 - Runoff time for fully confined test specimens: a) H=2000 mm; T=200 mm; b) H=1000 mm; T=200 mm; c) H=1000 mm; T=100 mm.

The results show that, in general, the time taken to drain the same quantity of water increases with the number of flushes. Analysing the variation in specimen height, it is possible to observe that water drainage is faster for the shorter specimens. For example, 1000 mm height specimens are 3, 4 and 19 minutes faster than 2000 mm height specimens at draining 65% of the fourth flush for the standard, medium and high density specimens, respectively. As previously mentioned, this is likely to be caused by the resistance of the expanded cork agglomerate to drainage flow.

Regarding the variation in thickness, it is possible to see that water drainage is faster for the thicker specimens. For example, 200 mm thick specimens are 1, 7 and 55 minutes faster than 100 mm thick specimens at draining 65% of the fourth flush for the standard, medium and high density specimens, respectively. In this case, it is expected that more significant wall effects will be produced by the box panels for the thinner specimens.

Water retention

As previously mentioned, an important aspect of the green facades concerns their water retention capacity, which must be optimized to reduce irrigation needs in drier periods. In order to analyse the retention capacity of the different types of expanded cork agglomerate boards more carefully, water retention in kg/m^3 is presented in Figure 2.4.

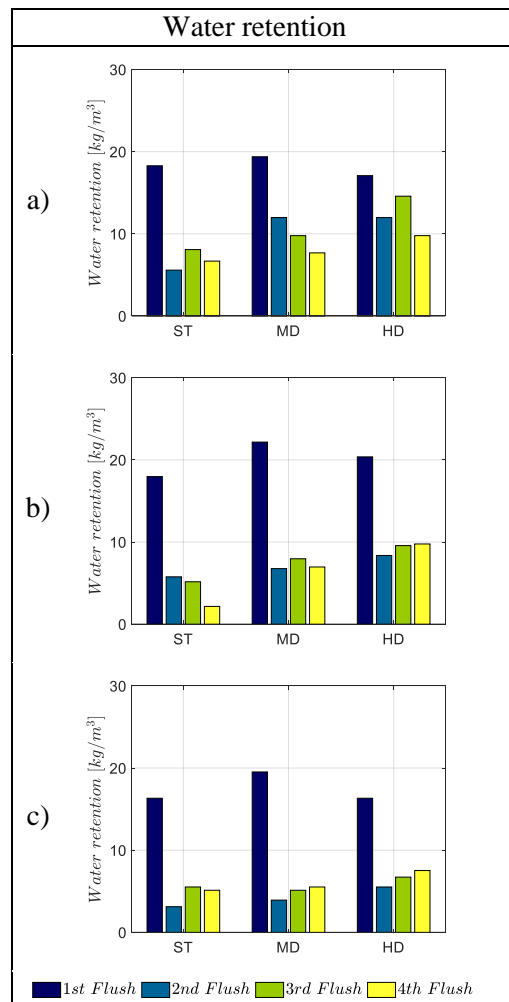


Figure 2.4 - Water retention for fully confined test specimens: a) H=2000 mm; T=200 mm; b) H=1000 mm; T=200 mm; c) H=1000 mm; T=100 mm.

As expected, the results show that dry specimens (first flush) retain significantly higher amounts of water per cubic meter than wet specimens (second and following flushes). See, for example, medium density specimens that were able to retain $20 \pm 2 \text{ kg/m}^3$ on average in the first flush, but only $7.3 \pm 2 \text{ kg/m}^3$ in the following flushes.

Although slightly higher water retention capacity is obtained for medium and high density cork boards, small differences can be noted between specimens of different density. This may be because higher density cork boards contain a greater amount of absorbent material but, simultaneously,

fewer empty spaces. It could also result, though to a lesser extent, from the intrinsic heterogeneity of expanded cork agglomerate, which is produced from by-products whose composition is variable.

2.3.2. Partially confined tests

Drainage profiles

Partially confined tests were performed aiming to achieve a situation in which the water could escape not only from the bottom but also from the front of the specimens. Drainage profiles obtained for board specimens 200 mm and 100 mm thick are presented in Figure 2.5 and Figure 2.6, respectively. Once again, drainage velocity is represented on the left axis, while accumulated drained water is represented on the right axis.

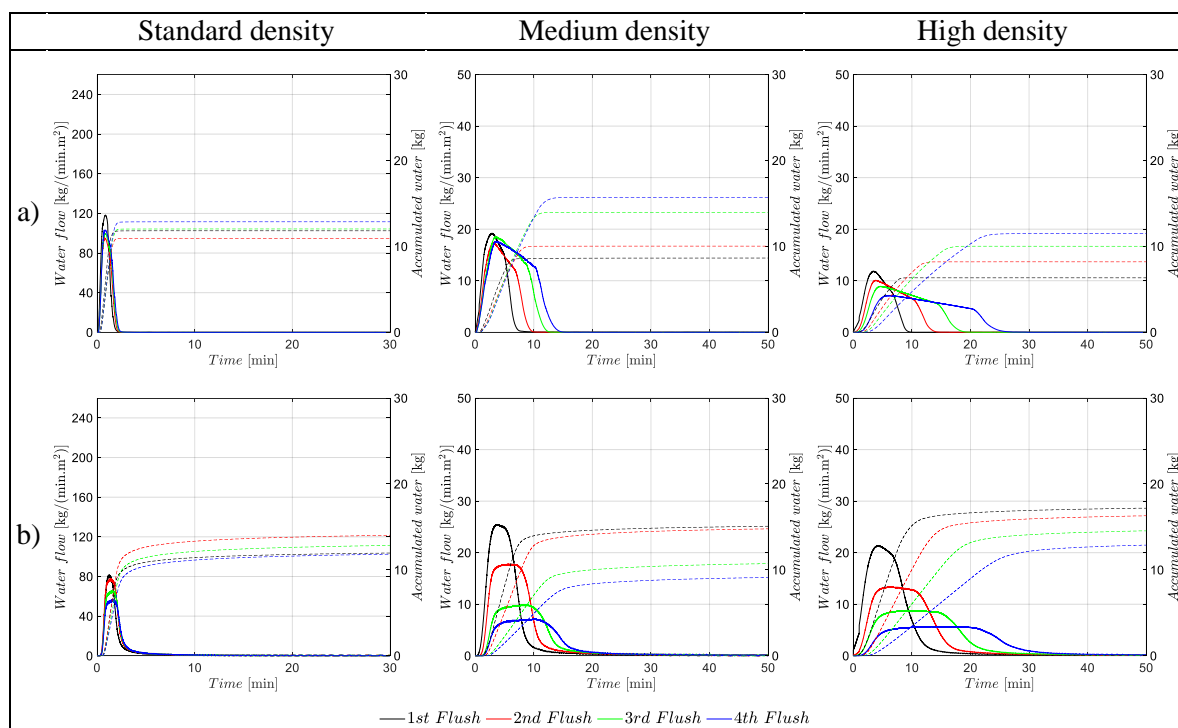


Figure 2.5 - Drainage curves for partially confined test specimens with $H=1000$ mm and $T=200$ mm: a) Facade; b) Interior.

As with the fully confined tests, a decrease in drainage velocity as the number of flushes increases is observed for water drained both from the facade and from the bottom of the cork boards due to the greater flow resistance caused by the expansion of cork granules in the presence of water. This behaviour becomes more pronounced as the density increases because this property influences the flow resistance.

Also, in general, the accumulated water drained from the facade tends to increase with the number of flushes, while that drained from the bottom tends to decrease. This behaviour is again related to the increased flow resistance helped by the expansion of cork granules in the presence of water,

though this is less marked for the thinner specimens where the percolated water is more accessible to the facade, escaping more easily this way from the first flush.

Furthermore, for the thinner specimens, the amount of accumulated water drained from the facade increases with the increase of density, while the amount of accumulated water drained from the bottom decreases. Once again, this behaviour could result from the greater resistance that the denser expanded cork agglomerate produces to the drainage flow. This increases the propensity of water to be released by the facade, a process that is more likely to occur in thinner boards. This behaviour is therefore very significant for the highest density specimens, in which the vertical flow resistance is more pronounced. In this case, almost all the water discharged on these specimens escapes via the facade.

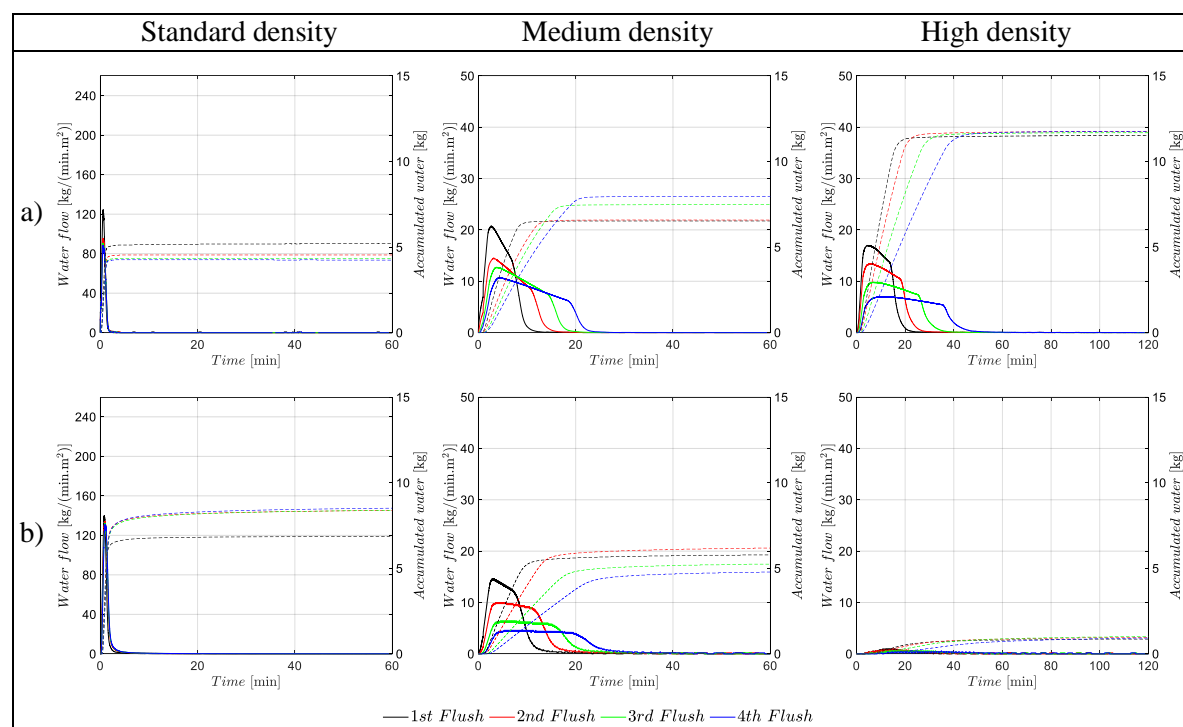


Figure 2.6 - Drainage curves for partially confined test specimens with $H=1000$ mm and $T=100$ mm: a) Facade; b) Interior.

Runoff time

Time taken to drain 15%, 40% and 65% of the total water discharged on the specimens was also calculated for these partially confined tests, adding the water drained both from the bottom and the facade (Figure 2.7). It can be seen that the behaviour in terms of runoff times is similar for the fully and partially confined test (Figure 2.3 and Figure 2.7). Thus, the time taken to drain a certain amount of water increases with the increasing number of flushes, although considerably faster runoff times were obtained for the partially confined tests in which water could drain from the bottom and from the facade. It is also noted that water drainage is faster for the thicker specimens and slower for denser specimens. For example, 200 mm thick specimens are 5 and 10 minutes faster than 100 mm thick specimens at draining 65% of the fourth flush for the medium and high density

specimens, respectively. Regarding the standard specimens, no significant differences were found between runoff time for the specimens with different thickness, which might be because of the lower resistance to water flow.

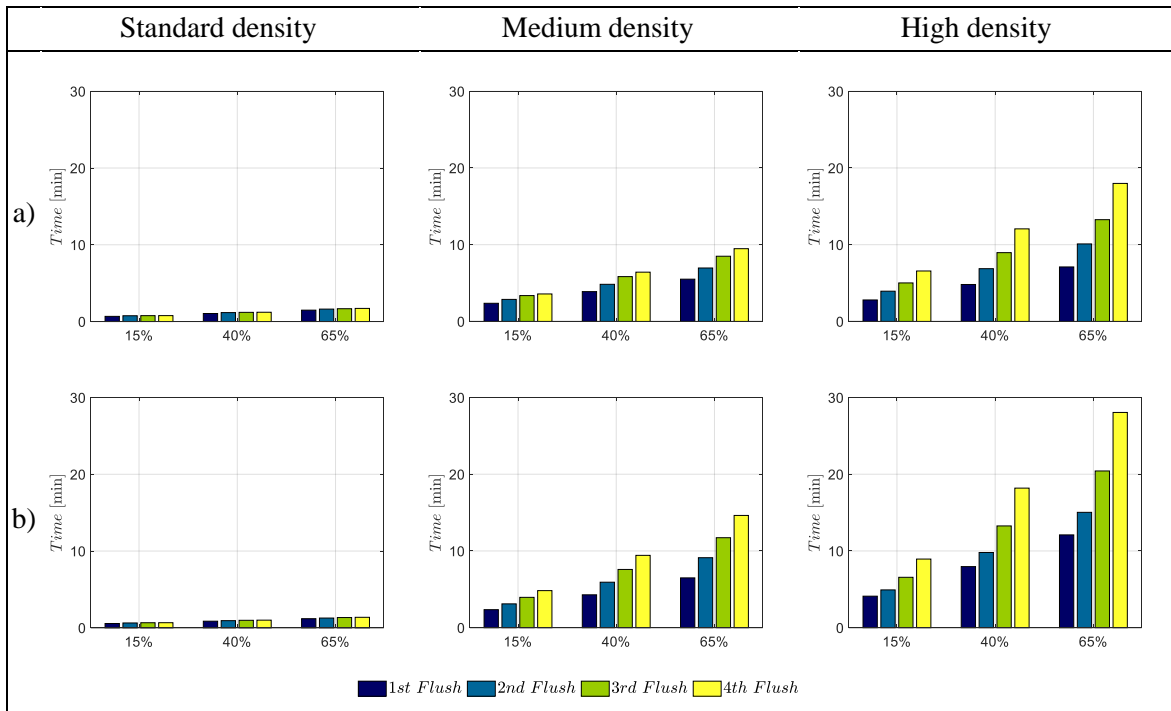


Figure 2.7 - Runoff time for partially confined test specimens: a) H=1000 mm; T=200 mm; b) H=1000 mm; T=100 mm.

Water retention

Water retention was also calculated for the partially confined tests and the results are given in Figure 2.8.

Retention results provided by the partially confined tests do not differ much from those obtained in the fully confined tests, either qualitatively or quantitatively. Thus, the first flushes have a higher water retention capacity compared with the subsequent flushes. In this case, for example, medium density specimens retain $20 \pm 4 \text{ kg/m}^3$ on average in the first flush, but only $8.6 \pm 2 \text{ kg/m}^3$ in the following flushes. Additionally, thicker specimens generally have greater retention capacity than thinner specimens. Small differences are observed between specimens of different density. As previously mentioned, this may result from the combined effect of a greater amount of absorbent material and fewer intergranular spaces.

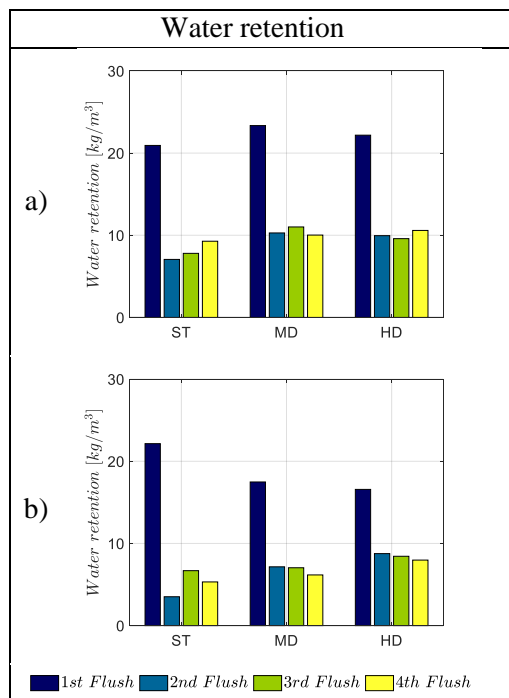


Figure 2.8 - Water retention for partially confined test specimens: a) H=1000 mm; T=200 mm; b) H=1000 mm; T=100 mm.

2.3.3. Microscopic analysis

To provide a better understanding of the water retention and drainage phenomena observed, expanded cork agglomerate boards of variable density were inspected by scanning electron microscopy (SEM) using a Phenon Pro instrument with a magnification of 690x. Although not very different from the macroscopic point of view, relevant differences were found in the microstructure of expanded cork agglomerate specimens. SEM images (Figure 2.9) show that cells are smaller in denser specimens, with the size of the cells increasing with the decrease of density. A systematic analysis of these images, performed with Phenom Poro-Metric software, showed that the internal area of the cells range from 339 to 1949 μm^2 , 87 to 927 μm^2 and 44 to 756 μm^2 for standard, medium and high density specimens, respectively. The densest specimens also exhibit distortion and even the collapse of some cells. According to the literature, such modification of the microstructure is induced by expansion phenomena occurring at cell level as a consequence of high temperatures, and compression phenomena occurring at the board level, due to the high pressures involved in the production process [36].

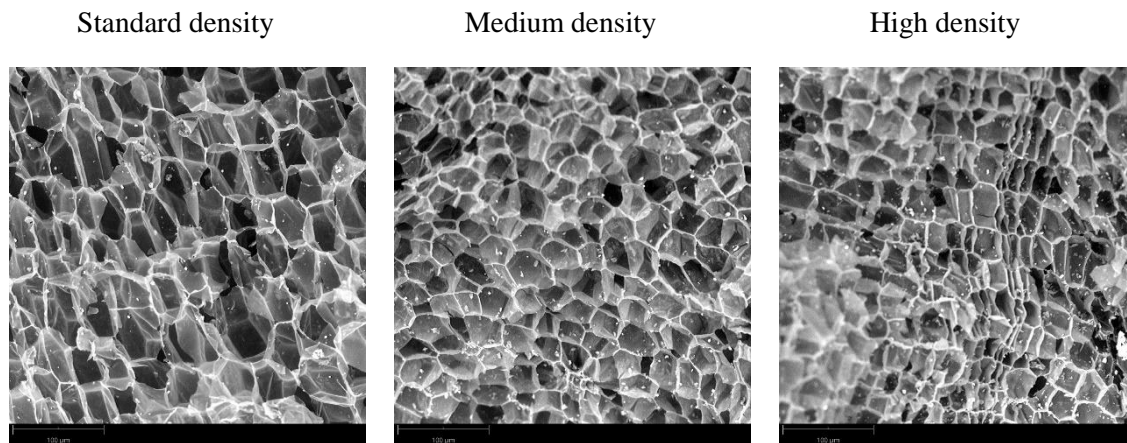


Figure 2.9 - Scanning electron microscopy (SEM) images obtained for expanded cork agglomerate boards of different density.

The microstructure exhibited by expanded cork agglomerate explains the water retention and drainage behaviour detailed in previous sections. In fact, considering that the observed cells work as water reservoirs, it could be said that denser boards contain a larger number of small reservoirs, while less dense boards contain a smaller number of large reservoirs. Therefore, a similar amount of water can be expected to be retained, regardless of the density. However, distinct drainage velocities are expected for boards of different density, since water is expected to percolate more easily through the boards containing a smaller number of cells with larger internal area (less dense specimens) than it does through the boards containing a larger number of cells with smaller internal area (denser specimens).

Another important factor that seems to affect water drainage is related to the expansion of cork granules when exposed to water. To assess this effect, two cubic specimens (10 cm^3) of each density were examined in 20 different spots under a stereo microscope (magnification 6.5x) before and after immersion in water for 2 hours. Intergranular spaces were measured, suggesting a significant size reduction for all the densities ($14 \pm 10\%$, $10 \pm 5\%$ and $15 \pm 6\%$ for standard, medium and high density, respectively). This result also corroborates the drainage profiles previously analysed, in which higher drainage velocities were observed for the first flush on the dry specimens than for the subsequent flushes on wet specimens.

2.4. Conclusions

In this chapter, it was explored the possibility of making a GVS entirely of expanded cork agglomerate and perform tests to assess the water retention and drainage capability of boards of

different density, height and thickness. Drainage profiles were obtained for fully confined and partially confined boards. The results in terms of water retention and runoff time were discussed.

The results suggest that expanded cork agglomerate allows a suitable moistening and a retention capacity up to 20 kg/m³, which helps to reduce irrigations needs when used in green vertical systems. The results also suggest that expanded cork agglomerate is able to quickly drain the excess water, even if denser specimens are used, thereby avoiding soil saturation. Board specimens of different density were further examined by scanning electron microscopy, which provided microstructural information useful to describing the results.

Overall, the results show that expanded cork agglomerate is a viable and eco-friendly alternative that can be used in green vertical systems, offering the possibility of optimizing the retention and drainage properties by changing the manufactured density to suit local weather conditions.

From the end-user perspective, it is also important to note that a GVS made entirely of expanded cork agglomerate is expected to perform better in thermal, acoustic and environmental terms than conventional solutions made essentially of plastic and metal components. In terms of cost, a GVS solution made of expanded cork agglomerate should compare well with other, conventional, solutions. Moreover, those combined benefits should help to offset the cost per square meter of an expanded cork agglomerate facade.

References

- [1] The world bank, “Urban population (% of total population) - European Union”. [Online]. Available: <https://data.worldbank.org/indicator/SP.URB.TOTL.IN.ZS?locations=EU>.
- [2] European Environment Agency EEA, “Urban adaptation to climate change in Europe 2016,” no. 12. 2016.
- [3] European Environment Agency EEA, “Air Quality in Europe - 2016 report”. European Environment Agency Report, no. 28. 2016.
- [4] United Nations Environment Programme, Global Status Report 2017 - Towards a zero-emission, efficient, and resilient buildings and construction sector. 2017.
- [5] K. Vijayaraghavan, “Green roofs: A critical review on the role of components, benefits, limitations and trends”, *Renewable and Sustainable Energy Reviews*, vol. 57, pp. 740–752, 2016.

- [6] European Commission, Towards an EU Research and Innovation policy agenda for Nature-Based Solutions & Re-Naturing Cities. 2015.
- [7] M. Manso and J. Castro-Gomes, “Green wall systems: A review of their characteristics”, *Renewable and Sustainable Energy Reviews*, vol. 41, pp. 863–871, 2015.
- [8] E. A. Eumorfopoulou and K. J. Kontoleon, “Experimental approach to the contribution of plant-covered walls to the thermal behaviour of building envelopes”, *Building and Environment*, vol. 44, no. 5, pp. 1024–1038, 2009.
- [9] I. Susorova, M. Angulo, P. Bahrami, and Brent Stephens, “A model of vegetated exterior facades for evaluation of wall thermal performance”, *Building and Environment*, vol. 67, pp. 1–13, 2013.
- [10] U. Mazzali, F. Peron, P. Romagnoni, R. M. Pulselli, and S. Bastianoni, “Experimental investigation on the energy performance of Living Walls in a temperate climate”, *Building and Environment*, vol. 64, pp. 57–66, 2013.
- [11] T. Van Renterghem, M. Hornikx, J. Forssen, and D. Botteldooren, “The potential of building envelope greening to achieve quietness”, *Building and Environment*, vol. 61, pp. 34–44, 2013.
- [12] U. Berardi, “The outdoor microclimate benefits and energy saving resulting from green roofs retrofits”, *Energy and Buildings*, vol. 121, pp. 217–229, 2016.
- [13] M. P. de Jesus, J. M. Lourenço, R. M. Arce, and M. Macias, “Green façades and in situ measurements of outdoor building thermal behaviour”, *Building and Environment*, vol. 119, pp. 11–19, 2017.
- [14] K. L. Getter, D. B. Rowe, G. P. Robertson, B. M. Cregg, and J. A. Andresen, “Carbon sequestration potential of extensive green roofs”, *Environmental science & technology*, vol. 43, no. 19, pp. 7564–7570, 2009.
- [15] K. Perini, M. Ottel , S. Giulini, A. Magliocco, and E. Roccotiello, “Quantification of fine dust deposition on different plant species in a vertical greening system”, *Ecological Engineering*, vol. 100, pp. 268–276, 2017.
- [16] T. Pettit, P. J. Irga, P. Abdo, and F. R. Torpy, “Do the plants in functional green walls contribute to their ability to filter particulate matter?”, *Building and Environment*, vol. 125, pp. 299–307, 2017.
- [17] A. Tiwary, K. Godsmark, and J. Smethurst, “Field evaluation of precipitation interception potential of green façades”, *Ecological Engineering*, vol. 122, no. July, pp. 69–75, 2018.

-
- [18] P. M. F. van de Wouw, E. J. M. Ros, and H. J. H. Brouwers, “Precipitation collection and evapo(transpi)ration of living wall systems: A comparative study between a panel system and a planter box system”, *Building and Environment*, vol. 126, no. October, pp. 221–237, 2017.
- [19] R. Collins, M. Schaafsma, and M. D. Hudson, “The value of green walls to urban biodiversity”, *Land Use Policy*, vol. 64, pp. 114–123, 2017.
- [20] F. Madre, P. Clergeau, N. Machon, and A. Vergnes, “Building biodiversity: Vegetated façades as habitats for spider and beetle assemblages”, *Global Ecology and Conservation*, vol. 3, pp. 222–233, 2015.
- [21] M. Ottelé, K. Perini, A. L. A. Fraaij, E. M. Haas, and R. Raiteri, “Comparative life cycle analysis for green façades and living wall systems”, *Energy and Buildings*, vol. 43, pp. 3419–3429, 2011.
- [22] H. Feng and K. Hewage, “Lifecycle assessment of living walls: Air purification and energy performance”, *Journal of Cleaner Production*, vol. 69, pp. 91–99, 2014.
- [23] M. S. de L. Brajkovich, “Comparative life cycle assessment for Green walls systems”, *International Green Wall Conference – 4–5th September 2014*.
- [24] R. Giordano, “Eco-innovation based on Quick-Life Cycle Assessment in designing and manufacturing a Living Wall System”, *World SB14 Barcelona Conference*, 2014.
- [25] State Government of Victoria, “Growing Green Guide: A guide to green roofs, walls and facades in Melbourne and Victoria”, Australia. 2014.
- [26] A. Medl, F. Florineth, S. B. Kikuta, and S. Mayr, “Irrigation of ‘Green walls’ is necessary to avoid drought stress of grass vegetation (*Phleum pratense* L.)”, *Ecological Engineering*, vol. 113, pp. 21–26, 2018.
- [27] A. S. Tártaro, T. M. Mata, A. A. Martins, and J. C. G. Esteves da Silva, “Carbon footprint of the insulation cork board”, *Journal of Cleaner Production*, vol. 143, pp. 925–932, 2017.
- [28] N. Pargana, M. D. Pinheiro, J. D. Silvestre, and J. de Brito, “Comparative environmental life cycle assessment of thermal insulation materials of buildings”, *Energy and Buildings*, vol. 82, pp. 466–481, 2014.
- [29] J. D. Silvestre, N. Pargana, J. de Brito, M. D. Pinheiro, and V. Durão, “Insulation cork boards-environmental life cycle assessment of an organic construction material”, *Materials*, vol. 9, pp. 1–16, 2016.

- [30] R. Fino, A. Tadeu, and N. Simões, “Influence of a period of wet weather on the heat transfer across a wall covered with uncoated medium density expanded cork”, *Energy and Buildings*, vol. 165, pp. 118–131, 2018.
- [31] A. Tadeu, L. Š, N. Simões, and R. Fino, “Simulation of heat and moisture flow through walls covered with uncoated medium density expanded cork”, *Building and Environment*, vol. 142, pp. 195–210, 2018.
- [32] N. Simões, R. Fino, and A. Tadeu, “Uncoated medium density expanded cork boards for building façades and roofs: Mechanical, hygrothermal and durability characterization”, *Construction and Building Materials*, vol. 200, pp. 447–464, 2019.
- [33] M. Manso and J. P. Castro-Gomes, “Thermal analysis of a new modular system for green walls”, *Journal of Building Engineering*, vol. 7, pp. 53–62, 2016.
- [34] M. Manso, J. Castro-Gomes, B. Paulo, I. Bentes, and C. A. Teixeira, “Life cycle analysis of a new modular greening system”, *Science of the Total Environment*, vol. 627, pp. 1146–1153, 2018.
- [35] Amorim Cork Insulation [Online]. Available: <https://www.amorimisolamentos.com/oprocesso/processo-productivo/> (accessed 11.04.2018).
- [36] H. Pereira and E. Ferreira, “Scanning electron microscopy observations of insulation cork agglomerates”, *Materials Science and Engineering: A*, vol. 111, pp. 217–225, 1989.

CHAPTER 3

INNOVATIVE MODULE OF EXPANDED CORK
AGGLOMERATE FOR GREEN VERTICAL SYSTEM

3. Innovative module of expanded cork agglomerate for green vertical system

3.1. Introduction

Green vertical systems (GVSs) are construction solutions that make use of vegetation to cover a vertical surface [1]. Different names, such as “vertical garden”, “vertical greening systems”, “vertical greenery systems”, “green walls”, “biowalls” or “vertical landscaping”, have also been used by different authors to describe these systems [1], [2]. Although they serve similar purposes, a wide range of designs and constructive solutions can be found, making classification of GVSs into categories difficult [3], [4]. Manso et al. [2] proposed a classification that generically places GVSs into green façades (direct or indirect) and living walls (continuous or modular). The design process described in this chapter follows this classification. A simplified adapted schematic representation is presented in Figure 3.1.

Green vertical systems can provide many services, contributing to improve the quality of life in urban centres. Not only do they increase the thermal and acoustic insulation of buildings, but they also enhance the biodiversity, improve the air quality and reduce the heat island effect.

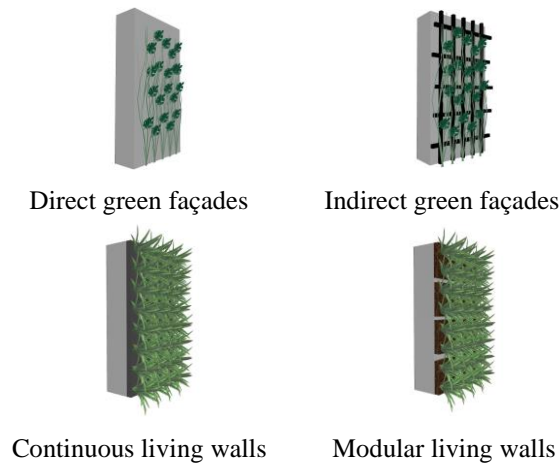


Figure 3.1 - Schematic representation of green vertical systems (adapted from [2]).

The thermal benefits of GVSs are difficult to generalize, since the overall behaviour of these systems strongly depends on the building design, plant species and local climate conditions, to mention only the key factors [5]–[8]. A number of authors have tried to show the efficiency of GVSs for insulating building façades and blocking solar radiation [9]–[10]. Having substrate and vegetation on the façade can also improve the acoustic insulation of buildings. For example, differences between 1 dB for traffic noise and 2 and 3 dB for pink noise were found with the installation of a GVS with a thickness of 20–30 cm [11].

Furthermore, covering buildings with vegetation within urban centres could help to enhance the biodiversity by attracting small animals and birds that would otherwise avoid towns and cities [12], [13], and to mitigate the urban heat island effect by reducing the accumulation of heat in the building envelope when it is sunny and the consequent release of heat during the rest of the day [14], [15], [16]. Additionally, plants can retain airborne pollutants, thereby helping to improve urban air quality [17], [18]. The phytoremediation of indoor air pollutants has also been reported [19].

However, despite all the benefits described so far, questions have been raised about the effective sustainability of GVSs when assessed from a life cycle perspective. In the last decade, several studies have tried to answer this simple question, suggesting that major environmental impacts of GVSs may arise from the materials used, and also from the irrigation and maintenance needs [20]–[22]. Additionally, several challenges have been reported related to the design and implementation of GVSs. In fact, green vertical systems are much more complex solutions in terms of design than green roofs. This is because the plants and/or growing media must be fixed to a vertical surface, for which metal or plastic components are often used, and these are known to be responsible for significant environmental impacts during the product phase of the life cycle [20], [21]. Thus, choosing eco-friendlier materials could contribute to improve the sustainability of GVSs.

Moreover, GVSs often require more systematic watering, since they contain less substrate (or no substrate at all) and water tends to escape more quickly through the façade [23]. In the summer, for example, the irrigation needs might be three or four times higher than in winter [24]. Therefore, it is important to create an appropriate design that contains more water-absorbent materials. Other strategies may be used to save water, such as the integration of greywater recovery systems [25]. Another important aspect that should not be overlooked is maintenance. The operations involved are not just related to pruning and weed control; they include replacing components from time to time, too. Avoiding materials with a short lifetime can therefore also help to increase the environmental performance and lower the cost of GVSs by reducing the frequency of maintenance operations [20], [26].

Although some countries have already established guidelines to support the implementation of GVSs, including France [27], [28], Germany [29], the United Kingdom [30], and Australia [31], most of these guidelines are relatively general and offer little help for the design. Additionally, significant differences can be found between the various systems. Direct and indirect green façades are both expected to use small amounts of materials and have lower irrigation needs. However, they could take anything from between 3 and 20 years to fully cover the façade, depending on the plant species selected, local climate conditions and maintenance interventions [2], [20], [21], [32]. This could compromise not only the long-term aesthetics of the façade, but also all the other benefits that are expected from the vegetation layer. Likewise, continuous living walls are known to need a constant supply of water and nutrients. An exterior hydroponic GVS could require up to 20 litres of water blend per square meter per day for a dry climate, as described in an Australian guide to green roofs, walls and façades with Melbourne and Victoria [31]. The absence of substrate also leads to an increase in the rate of plant replacement [20], [21]. A modular living wall is therefore expected to achieve a better trade-off between all the pros and cons. Furthermore, the modularity will facilitate the production process, transportation, and installation.

Given all the challenges implicit in the implementation of GVSs, particularly those with improved environmental performance, this chapter describes the design process of a new modular living wall system made of insulation cork boards (ICBs). Note that ICB is a natural insulation material made from by-products of the cork industry, and it has a better environmental performance than other insulation materials [33]–[35]. Several thermal benefits have been demonstrated when ICB has been used in external insulation coating systems [36]–[38]. Additionally, its water retention capacity was previously studied in chapter 1 and it was found that when applied to vertical façades this material can retain significant amounts of water, while quickly draining the excess [39]. The expanded cork agglomerate also has a long lifetime compatible with the lifespan of a GVS, even when exposed to the atmospheric agents over prolonged periods of time, which is something that other natural materials, including wood-based materials, very rarely achieve without specific chemical treatment. Finally, ICB can be easily modelled by computer numerical controlled (CNC)

processes to create new three-dimensional shapes. This could help to reduce the environmental and economic burdens of fabrication and maintenance operations.

Although ICB has previously been used in green roofs to replace conventional water retention and drainage layers [40], [41], and in GVSs to replace conventional vegetation supports [42], [43], there is still a lack of knowledge on the viability of new modular living walls made of such material, especially with regard to the mechanical strength needed to bear the weight of the plants and substrate under the maximum water capacity, and sustain the mechanical stresses caused by transport, installation, and maintenance operations.

To ascertain the features that should guide the design process of the new ICB based living wall, a comparative life cycle analysis (LCA) of five existing modular living walls was carried out, followed by a systematic survey about additional functional requirements. A new ICB module (the main building block of a living wall) was then developed based on these assumptions. To assist in choosing the most suitable ICB density and to ensure that the new ICB based living wall should withstand the effects of wind, rain, and accidental impacts, a full mechanical characterization was performed. The methods used and results obtained are presented and discussed in the following sections. The main conclusions are summarized at the end.

3.2. Methods

The materials and methods used in this work regarding life cycle analysis and mechanical tests are fully described in the following subsections.

3.2.1. Life cycle analysis

An LCA was carried out according to the ISO 14000 series of standards. Based on this methodology, all the input and output flows of mass and energy over the life cycle of a product can be systematically analysed. Once the boundaries and other assumptions for the study have been established and a functional unit has been defined, it was possible to estimate and compare the potential environmental impacts of different products.

Aim and boundaries of the LCA

This study intended to identify the most critical environmental hotspots of the product phase of five existing modular living wall systems (S1 to S5) based on the classification presented in Figure 3.1. One square meter of a modular living wall with a lifetime of 50 years was established as the functional unit. Characteristics of the systems and the data used to build the life cycle inventories were taken directly from the literature.

A cradle-to-gate LCA was performed, covering the life cycle stages from the extraction of raw materials to the production of GVS components. Other LCA stages were not included due to the lack of quantitative data. Figure 3.2 illustrates the life cycle stages considered. Although outside the boundaries of the study, relevant aspects for the construction, use, and end-of-life stages were also considered.

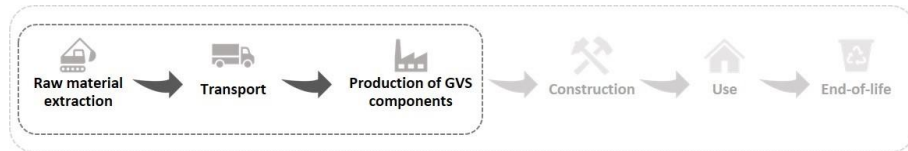


Figure 3.2 - System boundaries of the life cycle of GVSs.

LCA inventory

The input data used in the LCA modelling were taken directly from the literature. A brief description of the main materials used in the different systems is now presented. System S1 [20], [21] is made of HDPE modules supported on a steel structure. System S2 [43] consists of modules comprising an underlayer made of alkali-activated precast slab and a top layer of expanded cork agglomerate, fixed to the façade using a stainless-steel structure. System S3 [44] uses HDPE planter boxes supported on a structure made of stainless steel and galvanized iron. System S4 [22] consists of plastic modules supported on an aluminium structure and other layers made of polyester and polypropylene. System S5 [22] is based on felt material with gaps, supported on an aluminium structure. The substrate, vegetation, and irrigation components of all the systems were also taken into account in the LCA study to better reflect the results of the real impacts. Since no information about the irrigation system for S4 and S5 was found in the literature, it was assumed the same material was used as in the other systems, with a total weight corresponding to the average of those systems. Further data to model the production process were obtained from the Ecoinvent database v3.6, environmental product declarations, and other literature sources.

To facilitate the discussion, materials in the inventory were grouped into these five categories: fastening components, vegetation support elements, substrate, vegetation, and irrigation system. Fastening components are used to support the modular living wall and to fasten it to the façade. Vegetation support elements include all the components used to contain the substrate and plants, including the waterproofing layer, if needed. The materials used in each system and the respective amounts according to the defined functional unit are summarized in Table 3.1.

Table 3.1 - Materials used in each system and respective amounts according to the defined functional unit

	Material	Total weight (kg)
System - S1 [20], [21]		
Fastening components	Steel S235	5.21
Vegetation support elements	HDPE ¹	13.20
Substrate	Potting soil	75.60
Vegetation	<i>Pteropsida</i>	8.00
Irrigation systems	PE ²	0.26
System - S2 [43]		
Fastening components	Stainless steel	3.20
Vegetation support elements	Mine waste mud; Milled waste glass; Black cork granules Sodium silicate; Sodium hydroxide; ICB Glue; EPDM ³	24.40
Substrate	Light weight substrate	29.70
Vegetation	<i>Sedum album</i>	5.90
Irrigation systems	PE	0.80
System - S3 [44]		
Fastening components	Stainless steel; Galvanized iron	40.50
Vegetation support elements	HDPE	6.00
Substrate	Sandy soil; Expanded clay aggregate	3.60
Vegetation	<i>P. claviformis</i>	18.00
Irrigation systems	PE	0.50
System - S4 [22]		
Fastening components	Aluminium	0.60
Vegetation support elements	Polyester; PP ⁴	2.09
Substrate	Coconut fibre; Turf; Humus	4.00
Vegetation	<i>Hedera h. stems</i>	1.50
Irrigation systems	PE	0.52
System - S5 [22]		
Fastening components	Aluminium	3.90
Vegetation support elements	PP; Viscose; Polycarbonate	5.68
Substrate	Raw soil; SAP; Coco-coir; Peat moss	2.10
Vegetation	<i>Lonicera n. stems</i>	1.66
Irrigation systems	PE	0.52

¹ HDPE - High-density polyethylene

² PE – Polyethylene

³ EPDM - Ethylene propylene diene monomer rubber

⁴ PP - Polypropylene

Impact assessment

The potential environmental impacts were calculated using SimaPro (version 9.0). The impact assessment made use of the CML-IA v.4.7 method [45], considering the following categories: depletion of abiotic resources - elements (ADP-elements), depletion of abiotic resources - fossil (ADP-fossil), global warming (GWP), ozone depletion (ODP), photochemical ozone creation (PCOP), acidification (AP), and eutrophication (EP).

3.2.2. Mechanical tests

Experimental mechanical tests were performed on ICB specimens provided by the Amorim Cork Insulation business unit. The three densities tested were: 90 - 110 kg/m³ (standard density - ST); 140 - 160 kg/m³ (medium density - MD); and 170 - 190 kg/m³ (high density - HD). Three series of mechanical tests were performed to select the most appropriate density to use for the modular living wall component. Another series of tests were performed on the selected density to characterize the mechanical performance after wetting and after being subjected to wetting-drying cycles. The mechanical tests are described in the following subsections. Detailed information on the conditions of each test is also provided throughout the results section to facilitate the interpretation of the results.

Mechanical behaviour of ICB

The first series of tests were performed to evaluate the mechanical behaviour of the expanded cork agglomerate under dry conditions. For this, expanded cork agglomerate boards, 50 mm thick (the same thickness as the outer edge of the module) were studied with respect to their compressive, flexural, shear, and tensile strength perpendicular to faces.

Mechanical behaviour of the new GVS modules

A second series of tests were carried out to characterize the mechanical behaviour of the modules, in particular the resistance of its outer edge, which is known to be the weakest part of the structure. Point and distributed loads were used to simulate the actions generated by maintenance operations (such as leaning a ladder against a wall with modules fixed to it) or inappropriate actions (namely climbing and hanging from the modules). Figure 3.3 illustrates these examples. Figure 3.3 (a) shows the example of a person stepping on the outer edge of the module. In the subsequent discussion, it is assumed that the person has a mass of 100.0 kg. In Figure 3.3 (b), a person with the same mass is climbing a 15 kg ladder. The distance between the ladder and the wall on the ground is a quarter of the height. The person on the ladder is assumed to be close to the wall (to check the worst scenario situation).

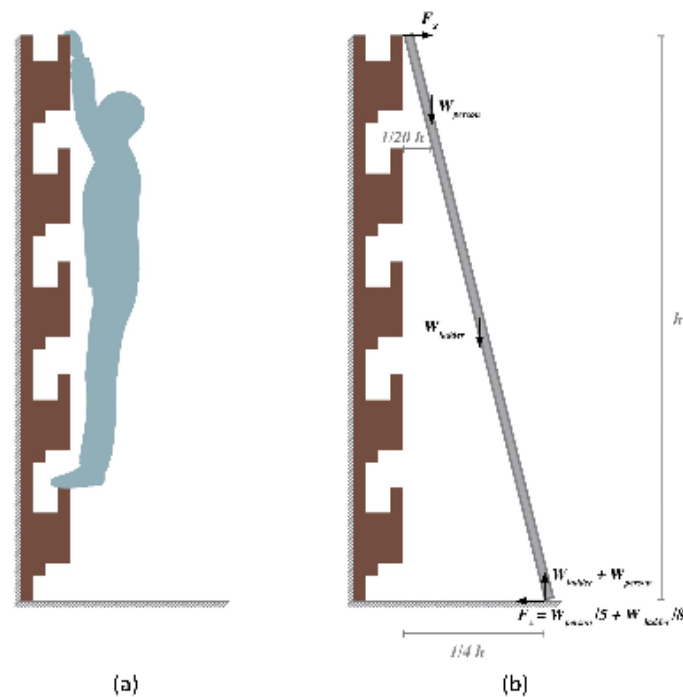


Figure 3.3 - Illustration of: (a) a person climbing the living wall, simulating the loads generated by doing so; (b) a ladder propped against the living wall, representing a maintenance operation.

Adhesion of the ICB to the substrate

The third series of tests were introduced to study the adhesion of the ICB to the substrate. For this, a commercially available bonding mortar was selected (Webertherm flex P [46]) that ensures both watertightness and vapour permeability, as proved in previous studies [37]. In this case, pull-out and shear tests were performed to evaluate the adhesion of the modules to concrete vertical supports.

Wetting and wetting-drying cyclic tests

The fourth set of tests determined the mechanical performance of the expanded cork agglomerate with the selected density after wetting and after being subjected to wetting-drying cycles, intended to replicate the ageing effect of rainfall and watering. For testing under wet conditions, the specimens were first immersed in water at $T = (23 \pm 2)^\circ\text{C}$. After 24 h, the test specimens were removed from the water, left to drain for 1 hour and tested again. Regarding the wetting-drying tests, each cycle lasted 48 h, corresponding to 24 h immersed in water and 24 h when the specimens were left to drain. The test specimens were subjected to a total of 30 cycles over 60 days. After those cycles, the specimens were left to dry at room temperature and tested. In these tests, ICB specimens glued to concrete boards were submerged up to the mortar layer (not completely submerged). This protocol was intended to replicate a real situation, where the water might reach the mortar by percolation through the expanded cork agglomerate.

3.3. Results and discussion

A comparative life cycle analysis of several GVSs was carried out first to identify the environmental hotspots of greatest concern regarding the components and materials used to produce different types of GVS. Based on the environmental hotspots thus identified, along with a set of additional functional requirements, it was then proposed a new ICB module that could be used to build a GVS that offers a better environmental performance. Since ICBs with different mass densities can be produced, and these may have different manufacturing costs and lead to distinct environmental impacts, a full mechanical characterization was also carried out to help choose the most suitable ICB density. The design process and mechanical results are presented and discussed in the following subsections.

3.3.1. Design process

Environmental hotspots

As described above, a comparative cradle-to-gate LCA was performed for five existing modular living wall systems (S1 to S5) based on data gathered directly from the literature to identify key environmental hotspots. To make comparing the different systems easier and facilitate the discussion, materials were inventoried into five categories (fastening components, vegetation support elements, substrate, vegetation, and irrigation system). The results for each impact category are presented in Figure 3.4. Once again, to facilitate comparison between the different systems, the results of each impact category were normalized to 100%.

The results for S1 show that the fastening components and substrate contribute most to the impact category of ADP-elements (45.7% and 45.4%, respectively). The fastening components are made of structural steel, whose production involves a large consumption of resources. Additionally, the large amount of substrate (c. 76 kg/m²) used by this system explains its high contribution for this impact category. As far as the other impact categories are concerned, the worst components are the vegetation support elements that are made of HDPE plastic, which is produced from non-renewable resources (ADP fossil: 80.6%, GWP: 64.0%, ODP: 51.4%, POCP: 48.8%, AP: 53.7%, EP: 41.6%).

Regarding S2, the largest contribution to the impact category of ADP-elements comes from the fastening components (74.5%) that are made of stainless steel, which is also known to consume significant resources in the production process. In terms of the other impact categories, the vegetation support elements always make the highest contribution (ADP fossil: 68.4%, GWP: 54.5%, ODP: 73.6%, POCP: 64.4%, AP: 72.9%, EP: 68.2%). These components are made from mine and glass waste, black cork granules, and others.

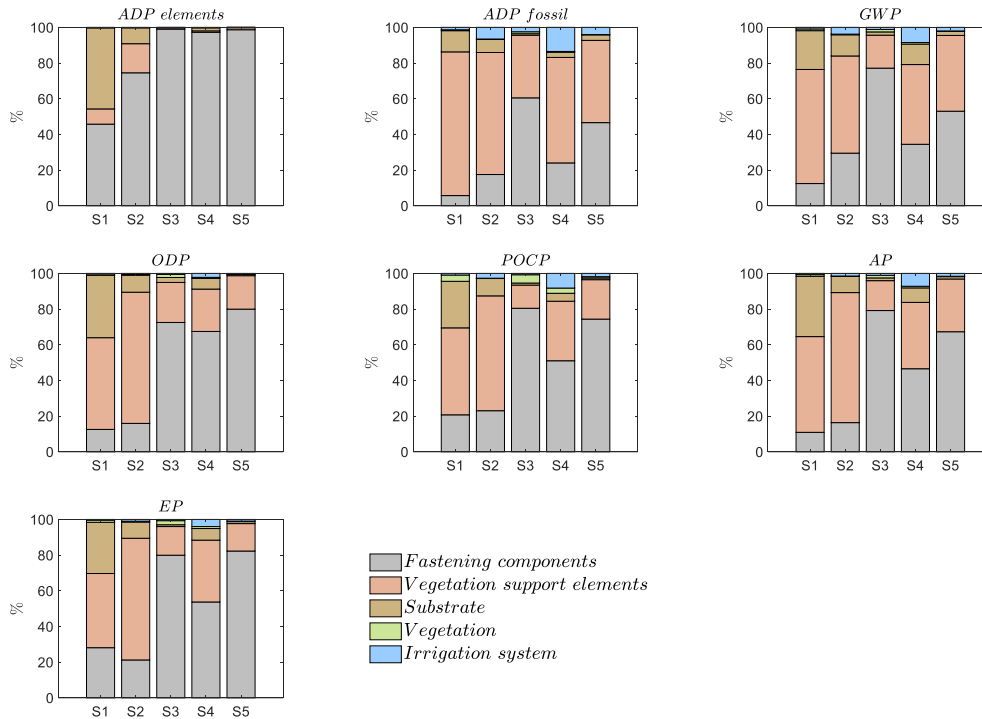


Figure 3.4 - LCA impacts of product stage for systems S1 to S5.

Regarding S3, the fastening components (made of stainless steel and galvanized iron) make the highest contribution to all the impact categories (ADP elements: 99.0%, ADP fossil: 60.5%, GWP: 77.1%, ODP: 72.5%, POCP: 80.5%, AP: 79.2%, EP: 79.9%). This is probably because of the large mass of material used (c. 41 kg/m²).

For S4, it was found that the fastening components make the highest contribution to several impact categories (ADP elements: 97.2%, ODP: 67.5%, POCP: 51.0%, AP: 46.5%, EP: 53.7%), because of the large consumption of resources during the manufacturing of aluminum. Regarding the categories of ADP fossil and GWP, the largest contribution comes from the vegetation support elements, since they are made of plastic (polyester and PP) produced from non-renewable resources.

Finally, observing the results obtained for S5, it was observed that the fastening components make the highest contribution to all the impact categories (ADP elements: 98.7%, ADP fossil: 46.6%, GWP: 53.0%, ODP: 80.0%, POCP: 74.4%, AP: 67.3%, EP: 82.3%). Again, these components are made of aluminium.

In conclusion, using metal fastening components and plastic vegetation support elements leads to major environmental impacts on the overall performance of the modular living wall systems analysed. Regarding this, in the new living wall the use of fastening components and vegetation support elements should be specifically optimized and replaced by eco-friendlier materials when possible. Other minor impacts are also related to the substrate and irrigation components. Finally,

the results show that vegetation has very little influence on the environmental performance of any of the systems.

It is important to note that other aspects could contribute to the overall performance of these systems over the entire life cycle. Thus, for the new living wall, materials with a longer lifetime should be selected to mitigate environmental impacts related to having to replace some components during the use phase. For example, irrigation systems and waterproofing layers often need to be replaced during the service life of these systems. Also, the selection of substrate could influence the fertilization needs during the life cycle [22], [31]. Concerning the end-of-life, systems also benefit if materials can be easily removed and separated, and if they can be reused and/or recycled.

As pointed out in the Introduction section, the environmental performance of ICB makes it a good option to replace the plastic and metal components most commonly used in conventional living walls. In fact, ICB is an insulation material made exclusively from the by-products of the cork industry and provides several thermal and acoustic benefits for buildings when used in external cladding systems. In addition, since it is made from the bark of the cork oak tree, ICB has been shown to retain its properties after decades of exposure to the outside environment. Finally, and no less important, it can be easily recycled.

Functional requirements

The design process of a new modular living wall should consider several functional aspects that go beyond the environmental performance.

The protection of the bearing wall is an essential aspect since plant roots and permanent humidity can often damage it. One major strategy to prevent physical damage focuses on selecting plants whose roots are unable to penetrate the system and reach the bearing wall. Note, however, that such a strategy can, in principle, be followed regardless of the living wall design. What is desirable in terms of GVS design is that plants do not come into direct contact with the bearing wall. A waterproofing layer may also be necessary to prevent the deterioration of the bearing wall caused by moisture and dissolved salts [31].

Modular living walls use substrate as a growing medium. In this case, the substrate should be lightweight, be able to retain a given amount of water and promote aeration. In terms of chemical composition, it should be ensured that at least the pH, the organic matter content and the amount of extractable micronutrients are within the appropriate range of values [47].

An efficient irrigation system that can uniformly moisten the growing medium is another key factor in the design of a modular living wall, since insufficient water is one of the commonest reasons why these systems fail [23]. However, defining an appropriate irrigation system for a GVS could be more challenging than creating one for a green roof due to the drop in pressure that occurs with the height of the living wall. Furthermore, vertical drainage makes uniformly moistening the

growing medium difficult. For this reason, several irrigation lines with individual pressure control and located at different heights are often chosen for watering living walls. Although several irrigation systems are commercially available, localized systems such as drip lines (with a water flow $< 8 \text{ l/m}^2$) are among the most recommended for saving water [48].

The correct moistening of the substrate is important, but too much watering associated with poor drainage will certainly compromise the vigour and viability of vegetation [26]. For that reason, the design process of a modular living wall should include the appropriate drainage of any excess water, to prevent waterlogging of the substrate. Some living walls have holes in the structure that supports the vegetation to promote the water drainage [48]. Drip trays could also be installed to recover the excess water. However, to avoid wastage, it is recommended to aim for lower water flows for short periods of time and to increase the frequency of irrigation [49], [50].

With the passage of time, maintenance operations are unavoidable. These may involve replacing plants, fertilizing, pruning, controlling weeds and disease, adding substrate, inspecting the irrigation system and replacing it if necessary [31], [48]. For tall living façades, such interventions can be complex and mechanically demanding. Therefore, this aspect should be anticipated in the design phase.

Still looking at mechanical strength, modular living walls must support loads resulting from their own weight and the weight generated by the plants and substrate under the maximum water capacity. Additionally, they must withstand additional mechanical stresses caused by transport, installation, and maintenance operations, as well as strong winds.

New ICB module proposed

Bearing in mind the environmental hotspots and the functional requirements previously identified, a new ICB module to build living walls was developed.

Since it favours the use of natural materials with low environmental impact, the new system makes use of insulation cork board (ICB) modules to support the vegetation, instead of the plastic components most often used. As it was shown in the previous chapter, ICB will also ensure the adequacy of both water retention and the drainage of excess water [39].

Additionally, ICB modular blocks were developed so that they could be fastened directly to the bearing wall by means of a waterproofing (though permeable to vapour) adhesive mortar. This made it unnecessary to use metal fastening components, which were found to have a strong negative impact on the overall environmental performance of GVSs analysed.

The design of the new module is illustrated in Figure 3.5. This modular block is made from the regular ICBs used for external building insulation purposes [51], with nominal dimensions of 500 mm x 1000 mm x 200 mm, resorting to optimized computer numerical controlled (CNC) processes.

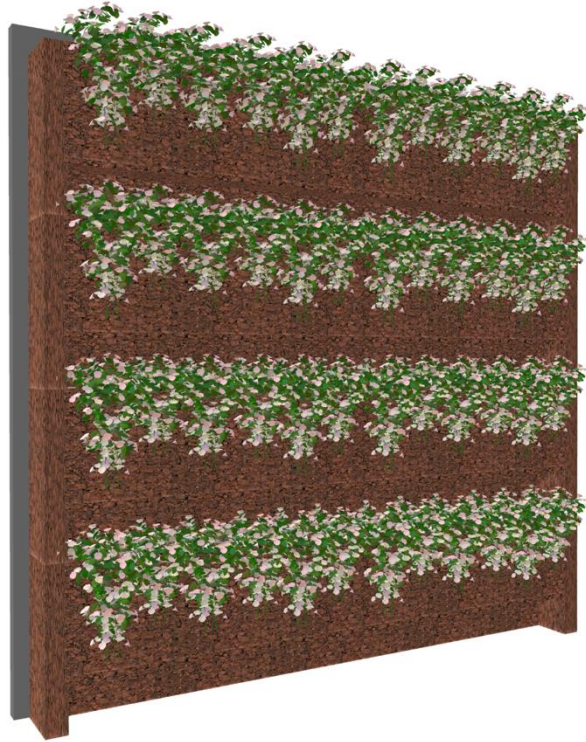


Figure 3.6 - Illustration of a modular living wall built with the new ICB modules.

Taking advantage of a natural insulation material made from by-products of the cork industry, these new ICB modules are expected to enhance the thermal insulation and the water retention properties of the living wall simultaneously. However, as previously mentioned, a new modular living wall like this must ensure mechanical resistance to its own weight and to actions generated during transport, installation, and maintenance operations. Moreover, since it corresponds to an external application, the modular living wall system will also be exposed to the effects of wind, rain, and accidental impacts. It is therefore essential to fully evaluate the behaviour of the constructive solutions, regarding both the performance of the material and the strength of the adhesion to the substrate. Since ICB can be produced in different mass densities, with distinct environmental impacts and manufacturing costs, the optimal density for the application must also be chosen (i.e. the lowest density that still fulfils the mechanical requirements). For this purpose, ICB specimens with three different densities were tested for both dry and wet conditions and after 30 wetting-drying cycles (60 days). The results obtained are presented and fully discussed in the next section.

3.3.2. Mechanical characterization

As previously noted, a full mechanical characterization was performed on ICB with 90 - 110 kg/m³ (ST), 140 - 160 kg/m³ (MD), and 170 - 190 kg/m³ (HD) with the aim of selecting the most appropriate density. Another series of tests were performed on the selected density after wetting

and after being subjected to wetting-drying cycles. The results are described in the following subsections.

Tests performed on ICB boards

This section presents the results of the mechanical tests performed on dry test specimens. Specific procedures for evaluating products made of expanded cork agglomerate based on EN 13170:2012+A1:2015 were used. To better understand the results, a brief description of the methodology used in each test is presented at the beginning of each subsection. Each sample is composed of six test specimens. The tests were performed using a calibrated universal testing machine (Instron 59R5884). The force-displacement curves, and the mean and standard deviation values obtained for each test are presented.

- Compressive strength

The compression behaviour of the specimens was evaluated based on the procedure described in EN 826:2013. Each test specimen, with nominal size of 100 mm x 100 mm x 50 mm, was preloaded with a load that generated a pressure of (250 ± 10) Pa. A compressive force was then applied at a constant rate of $(0.1 \text{ d/min} \pm 25\%)$, in which d is the thickness of the test specimen, in mm). The test ended when 50% deformation was reached. The load was measured using a calibrated load cell of 30 kN. Figure 3.7 presents the registered force-extension curves, while Table 3.2 summarizes the results.

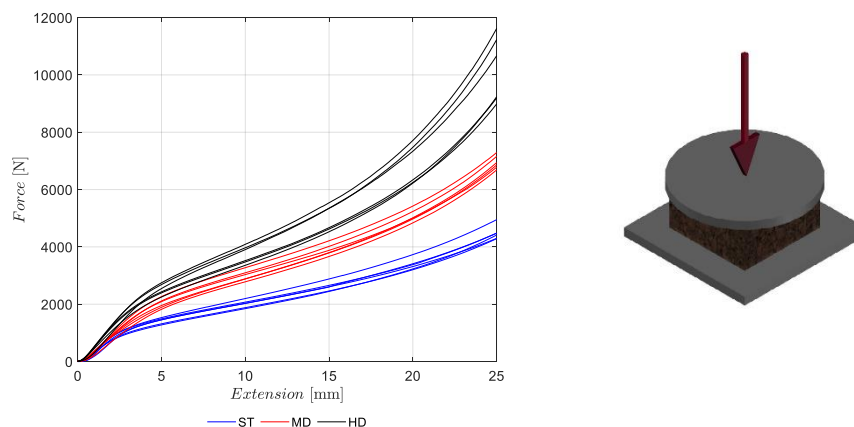


Figure 3.7 - Force-extension curves for dry specimens and compression behaviour apparatus.

Table 3.2 - Compressive strength tests: results for dry specimens

Ref	Density (kg/m ³)	Force at 50% of strain F ₅₀ (N)	Compressive stress at 50% of strain σ_{50} (kPa)
ST	110±3	4490±248	448±28
MD	151±5	6984±243	698±24
HD	194±15	10043±1068	1003 ±104

The results show a clear separation of the curves according to the material density, with the higher densities showing higher resistance to compressive loads. Additionally, the results for the medium density samples have a lower standard deviation. The compressive strength of the material is particularly important because of the loads that are generated by stepping on the outer edge of the module. A compressive stress of 187 kPa would be generated assuming the full weight of a 100 kg person supported on one foot (with a foot breadth of 0.107 m [52]) (see Figure 3.3a). This value is much smaller than the compressive stresses recorded for all ICB test specimens at 50% of strain.

- Flexural strength

The bending behaviour was evaluated based on the procedure described in EN 12089:2013, method B. Each specimen, with nominal size of 150 mm x 250 mm x 50 mm, was placed symmetrically upon two supporting edges with a span of 200 mm. The test consisted of applying a force to the loading edge at a rate of 10 mm/min±10% until failure occurred. The load was measured using a calibrated load cell of 10 kN. The force-extension curves recorded are presented in Figure 3.8. The maximum force (F_m) and the corresponding bending stress (σ_b) are listed in Table 3.3.

The curves obtained are grouped according to the density of the ICB. As expected, higher density test specimens are also more resistant to bending loads. The bending behaviour is particularly relevant when it is generated by the growing medium (which could be saturated by water) and vegetation. Assuming a saturated substrate with a density of 700 kg/m³ [53] it would generate a maximum bending stress of 2.78 kPa, which is very small compared with flexural strength.

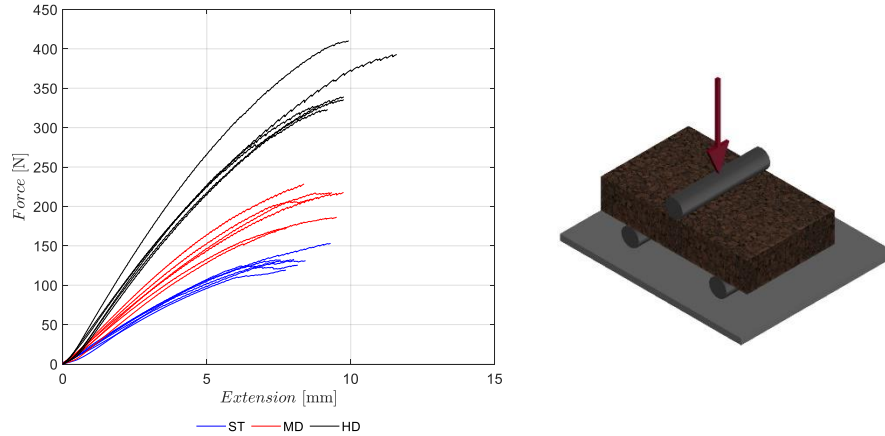


Figure 3.8 - Force-extension curves for dry specimens and bending behaviour apparatus.

Table 3.3 - Flexural strength tests: results for dry specimens

Ref.	Density (kg/m ³)	Maximum force F_m (N)	Bending stress σ_b (kPa)
ST	106±5	132±10	108±8
MD	143±3	205±20	165±16
HD	182±5	355±34	288±27

- Tensile strength perpendicular to faces

The tensile strength perpendicular to faces was evaluated based on the test method described in EN 1607:2013. Specimens with nominal size of 100 mm x 100 mm x 50 mm were previously bonded at two rigid plates. The testing machine, equipped with a load cell of 5 kN, applied a tensile force that pulled apart the two rigid plates at a speed of (10±1) mm/min until failure occurred. Force-extension curves recorded are presented in Figure 3.9. The maximum force (F_m) and the corresponding tensile strength perpendicular to faces (σ_{mt}) are indicated in Table 3.4.

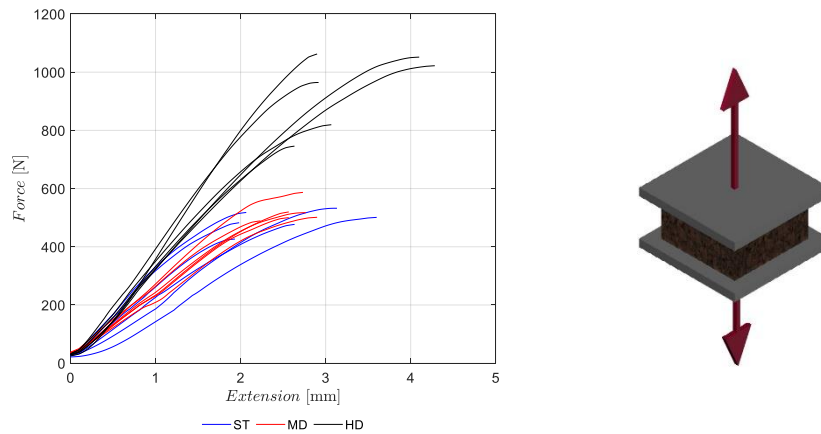


Figure 3.9 - Force-extension curves for dry specimens and tensile strength perpendicular to faces apparatus.

Table 3.4 - Tensile strength perpendicular to faces tests: results for dry specimens

Ref.	Density (kg/m ³)	Maximum force F_m (N)	Tensile strength perpendicular to faces σ_{mt} (kPa)
ST	106±6	490±34	49±4
MD	146±7	519±32	51±3
HD	175±8	943±120	92±12

The separation of the force-displacement curves according to the density of the test specimens can again be seen. However, this separation is not so clear for ST and MD density as in previous tests. As before, increasing the expanded cork density improves its ability to withstand higher tensile loads. It is important to characterize the tensile strength perpendicular to faces because the modules have to withstand tension forces generated by the wind. The values found are much higher than the tensile stresses induced by high velocity wind (less than 2 kPa, obtained for a mean wind velocity of 36.9 m/s applied to a façade 10 m above the ground for the worst scenario [54]).

- Shear strength

The shear strength was determined according to the single test method described in the standard EN 12090:2013. Specimens with nominal size of 200 mm x 50 mm x 50 mm were glued to two flat rigid supports measuring 330 mm x 50 mm. The supports were fixed to the test machine equipped with a 5 kN load cell. A continuously increasing force was applied in order to produce vertical movement at a rate of (3±0.5) mm/min until failure occurs. The force-extension curves recorded are presented in Figure 3.10. The maximum force (F_m) and the corresponding shear strength (τ) are indicated in Table 3.5.

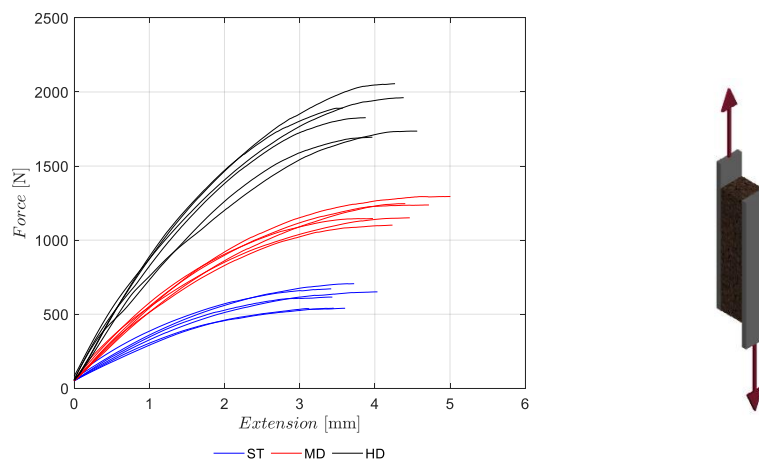


Figure 3.10 - Force-extension curves for dry specimens and shear behaviour apparatus.

Table 3.5 - Shear strength tests: results for dry specimens

Ref.	Density (kg/m ³)	Maximum force F_m (N)	Shear strength τ (kPa)
ST	105±5	621±63	50±5
MD	140±5	1196±68	96±5
HD	195±8	1861±125	149±10

The curve results are clearly grouped according to the material's density. Once more, higher density testing samples can withstand higher shear loads. The shear strength of the material is again relevant with respect to the forces acting on the lower cross section of the outer edge of the module, by maintenance operations, particularly when a ladder leans against the vertical wall (Figure 3.3b). In the conditions described above, it would generate a shear stress of 43.75 kPa, assuming a simplified model that only considers the mobilization of two sections of 0.05 m x 0.05 m, which result from the contact of the two supports of the ladder.

Although the results obtained for the various mechanical tests suggest that all densities can be used, the ST ICB may fail under certain circumstances, taking into account the expected generation of shear stresses during maintenance operations.

Tests performed on ICB modules

The mechanical resistance of the modules to distributed loads and to point loads (at the corners and centre) applied to the outer edge was also evaluated. Each sample is composed of three specimens. The tests were performed using a hydraulic actuator.

- Effect of a distributed load

The maximum distributed load that the outer edge of the module can withstand was evaluated experimentally. The load was applied through a solid metal beam, 50 mm thick and measured using the load cell of 5 kN. An increasing load was applied at a constant rate of 4 mm/min until failure occurred. The force-extension curves are presented in Figure 3.11, while the maximum force (F_m) and the displacement at maximum force (X_m) obtained are listed in Table 3.6.

The results indicate a tendency of higher densities to withstand higher distributed loads. This test defined the maximum distributed load that could be applied perpendicular to the outer edge of the module.

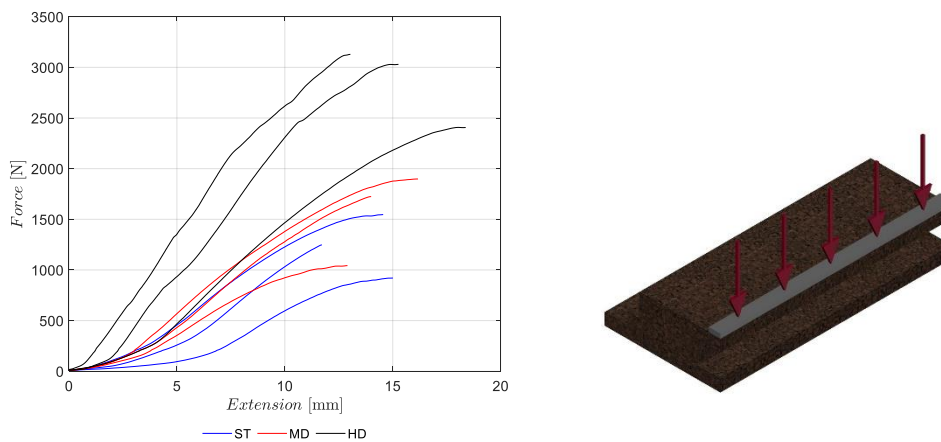


Figure 3.11 - Force-extension curves for a distributed load applied to the outer edge of the module specimens.

Table 3.6 - Results obtained when the outer edge of the module specimens is subjected to distributed load tests

Ref.	Density (kg/m ³)	Maximum force F_m (N)	Displacement at maximum force X_m (mm)
ST	106±5	1238±256	14±1
MD	156±7	1555±369	14±1
HD	174±4	2855±319	15±2

- Effect of point load

The resistance of the outer edge of the modules to point loads was determined by applying a load that increased at a constant rate of 4 mm/min until failure occurred. The force was applied using a 50 mm steel cube placed between a 5 kN calibrated load cell and the hydraulic actuator. The registered force-extension curves for loads applied to the centre and the corners of the outer edge

of the module specimens are presented in Figure 3.12 and Figure 3.13, respectively. Table 3.7 and Table 3.8 list the corresponding maximum force (F_m) and the associated displacement (X_m).

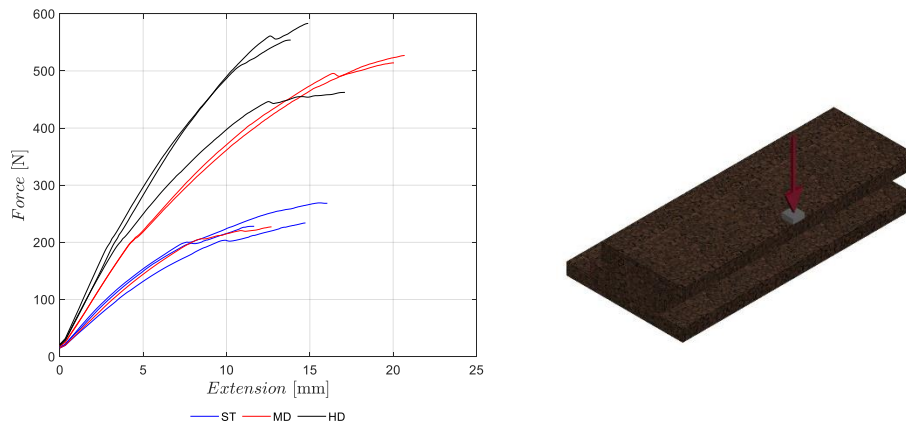


Figure 3.12 - Force-displacement curves recorded when point loads are applied to the centre of the outer edge of the module specimens.

Table 3.7 - Results obtained when the outer edge is subjected to point loads at the centre of the module specimens

Ref.	Density (kg/m ³)	Maximum force F_m (N)	Displacement at maximum force X_m (mm)
ST	112±0	244±18	14±2
MD	154±9	423±138	18±4
HD	182±5	533±51	15±1

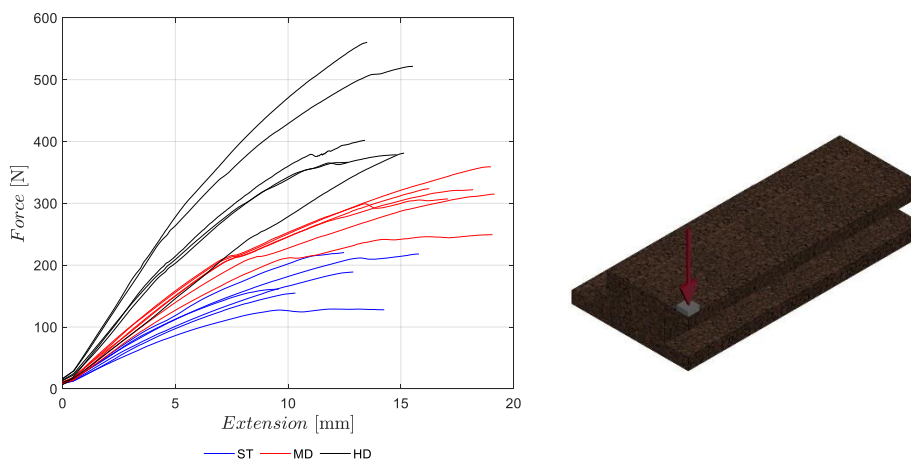


Figure 3.13 - Force-displacement curves recorded when point loads are applied to the corners of the outer edge of the module specimens.

Table 3.8 - Results obtained when the outer edge is subjected to point loads at the corners of the module specimens

Ref.	Density (kg/m ³)	Maximum force F_m (N)	Displacement at maximum force X_m (mm)
ST	111±6	179±33	12±2
MD	162±2	313±33	18±1
HD	175±3	435±76	14±1

As expected, regardless of the density of the ICB, the outer edge of the module specimens withstands higher point loads applied away from its corner. Furthermore, test specimens with higher density withstand higher point loads.

Assuming a ladder is leaned against the wall in the above-described conditions (Figure 3.3b)), it would result in the application of a point load of 218.75 N. This load would be compatible with the use of an MD or HD ICB module. Once again, ST ICB may fail, given the loads that are expected to be applied to the outer edge of the modules during maintenance operations.

Adhesive tests on the bond between ICB and the substrate

This section describes the set of tests carried out to study the adhesion of the ICB to the substrate. Pull-out and shear tests were performed to study the adherence of specimens glued to a concrete substrate with the adhesive mortar. The mortar was applied to both bonding surfaces (ICB and concrete surfaces) and left to dry for three days in a controlled environment at 23 °C and 50% humidity. Each sample was composed of six test specimens. The tests were performed using a calibrated universal testing machine (Instron 59R5884), equipped with a calibrated load cell of 10 kN.

Regarding the pull-out strength, this was evaluated using specimens with nominal size of 100 mm x 100 mm x 50 mm. Each external specimen face was bonded to a metal plate with the same area dimensions and fixed to the testing machine. Then an increasing tensile force, at a rate of (10±1) mm/min was applied until failure occurred.

As expected, the failure always occurred in the ICB test specimen and not in the adhesive mortar; as the pull-out loads were similar to those found in the tests to determine the tensile strength perpendicular to faces, they are not shown.

The shear strength adhesion was evaluated using specimens with nominal size of 200 mm x 50 mm x 50 mm. The external ICB face of each specimen was bonded to a metal plate measuring 330 mm x 50 mm and fixed to the testing machine. The shear load was applied by applying a vertical movement at a rate of (3±0.5) mm/min until failure.

Once more, the failure always occurred in the ICB test specimen and not in the adhesive mortar, with shear strength values similar to those previously obtained and thus not shown.

As a general conclusion, all the mechanical results obtained so far point towards a better performance of the higher densities. However, lower densities tend to have lower environmental impacts, since smaller amounts of raw materials are used. Moreover, in economic terms, lower densities cost significantly less to produce. Given all these aspects, the best choice is the MD material (140–160 kg/m³). Although slightly less resistant than HD, MD modules provided a good mechanical performance, meeting the required strength to cope with the dead weight, wind, maintenance operations and other potential actions, as previously discussed. Additionally, they are a better option in both environmental and economic terms. Note that the ST material should be avoided, since it does not fully comply with the above-mentioned requirements.

Mechanical characterization of ICB in the presence of water

Since a living wall is expected to be exposed to cycles of wetting and drying over a full year, it was relevant to characterize the mechanical behaviour of the modules under these conditions. Thus, further experimental tests were carried out on wet ICB specimens and on ICB specimens subjected to 30 wetting-drying cycles (60 days), considering only the previously selected density (MD). For each condition, the ICB was tested under compression, bending, tensile strength perpendicular to faces, and shear loads. Pull-out and shear tests were also performed to assess the adhesion of the specimens to the concrete substrate. The same testing procedures described in the previous sections were followed. Each sample was composed of six specimens.

Table 3.9 summarizes the average values obtained for each test performed on ICB boards. For comparison purposes, all the results previously obtained with dry medium density (MD) samples are included.

In general, no significant differences were found between the results for the dry specimens and those that were wetted and underwent wetting-drying cycles, except for the compressive tests. The decrease of the compressive strength for the wet specimens is likely to be caused by the increased elasticity of the cork fibres in the presence of water. In addition, the slight decrease in compressive strength recorded for the ICB specimens after the wetting-drying cycles may suggest that the ICB specimens were not completely dry. Note, however, that the compressive stress values fully meet the mechanical requirements discussed earlier.

Table 3.9 - Medium density ICB tests results performed on specimens that were dry, wet, and had undergone 30 wetting-drying cycles

ICB tests		Dry	Wet	30 wetting-drying cycles
Compressive strength	Density (kg/m ³)	151±5	167±5	158±7
	Force at 50% strain F ₅₀ (N)	6984±243	5525±202	5720±179
	Compressive stress at 50% strain σ_{50} (kPa)	698±24	553±21	575±20
Flexural strength	Density (kg/m ³)	143±3	154±8	154±6
	Maximum force F _m (N)	205±20	213±15	211±13
	Bending stress σ_b (kPa)	165±16	168±12	167±10
Tensile strength perpendicular to the faces	Density (kg/m ³)	146±7	147±2	154±7
	Maximum force F _m (N)	519±32	523±101	512±62
	Tensile strength perpendicular to faces σ_{mt} (kPa)	51±3	52±10	51±6
Shear strength	Density (kg/m ³)	140±5	155±9	157±6
	Maximum force F _m (N)	1196±68	1068±68	1178±74
	Shear strength, τ (kPa)	96±5	85±5	94±6

Table 3.10 summarizes the results for each test performed to evaluate the adhesion of the ICB to the concrete substrate. Once again, the results for the dry medium density (MD) samples are included to facilitate the comparison.

Table 3.10 - Results of the adhesion tests performed on dry MD specimens and MD specimens after 30 wetting-drying cycles

Adhesion tests		Dry	30 wetting-drying cycles
Pull-out	Density (kg/m ³)	157±12	157±8
	Maximum force F _m (N)	522±47	505±70
	Pull-out strength (kPa)	52±5	51±7
Shear	Density (kg/m ³)	154±11	152±11
	Maximum force F _m (N)	1178±47	1123±43
	Shear strength (kPa)	94±3	90±4

No significant differences were found between the dry and wetting-drying cycle results. Furthermore, as previously found for the dry specimens, in the pull-out tests, failure of the

specimens subjected to the wetting-drying cycles always occurred in the ICB, suggesting that mortar adhesion is resistant to the ageing conditions.

It is thus possible to conclude that a living wall made of only MD ICB and fixed with a suitable mortar adhesive can both meet the mechanical requirements and be a good environmental choice. As noted above, ICB is a natural material, with relevant thermal insulation and water retention properties that can be used instead of the less eco-friendly materials very often used in living walls.

3.4. Conclusions

In this chapter the design process of a new ICB module for building eco-friendlier living walls have been described. This was done considering the key environmental hotspots extracted from a comparative LCA performed for the product stage of five distinct modular living wall systems. The results of the LCA study clearly showed that the metal and plastic materials used for the fastening components and vegetation support elements represent the major impact on the overall environmental performance. To assist the design process, a number of additional functional requirements have also been discussed, including aspects related to the protection of the bearing wall, water retention and drainage capacity, and the mechanical resistance to face loads generated by the dead weight, wind, maintenance operations, and other potential actions.

Favouring the use of natural materials with low environmental impact, good water retention, and the ability to quickly drain off any excess water, the proposed living wall system makes use of ICB modules to support the vegetation layer, instead of the plastic components most commonly used. In addition, the ICB module was developed so that it could be fastened directly to the bearing wall by means of a waterproof adhesive mortar, replacing the metal fixing components more often used. Furthermore, the new module was designed to ensure that the supporting wall will benefit from a continuous layer that has both thermal and acoustic insulation properties, and protection functions.

A full mechanical characterization was also carried out to assist in choosing the most suitable ICB density and to evaluate the behaviour of the construction solutions in wet conditions and after wetting-drying cycles. The results suggest that the medium density (140 - 160 kg/m³) ICB modular system could well be an appropriate eco-friendlier alternative to current plastic- and metal-based GVS, since it fully meets the environmental and functional requirements that would be expected for a living wall system.

The practical implications of using the proposed ICB modules in GVSs are the simultaneous enhancement of thermal insulation and water retention properties, without compromising the mechanical performance, taking advantage of a natural insulation material made from by-products of the cork industry.

References

- [1] A. B. Besir and E. Cuce, “Green roofs and facades: A comprehensive review”, *Renewable and Sustainable Energy Reviews*, vol. 82, pp. 915–939, 2018.
- [2] M. Manso and J. Castro-Gomes, “Green wall systems: A review of their characteristics”, *Renewable and Sustainable Energy Reviews*, vol. 41, pp. 863–871, 2015.
- [3] G. Pérez, J. Coma, I. Martorell, and L. F. Cabeza, “Vertical Greenery Systems (VGS) for energy saving in buildings: A review”, *Renewable and Sustainable Energy Reviews*, vol. 39, pp. 139–165, 2014.
- [4] A. Medl, R. Stangl, and F. Florineth, “Vertical greening systems – A review on recent technologies and research advancement”, *Building and Environment*, vol. 125, pp. 227–239, 2017.
- [5] S. Flores Larsen, C. Filippín, and G. Lesino, “Modeling double skin green façades with traditional thermal simulation software”, *Solar Energy*, vol. 121, pp. 56–67, 2015.
- [6] X. Nan, H. Yan, R. Wu, Y. Shi, and Z. Bao, “Assessing the thermal performance of living wall systems in wet and cold climates during the winter”, *Energy and Buildings*, vol. 208, p. 109680, 2020.
- [7] L. Zhang et al., “Thermal behavior of a vertical green facade and its impact on the indoor and outdoor thermal environment”, *Energy and Buildings*, vol. 204, 2019.
- [8] L. Pan, S. Wei, P. Y. Lai, and L. M. Chu, “Effect of plant traits and substrate moisture on the thermal performance of different plant species in vertical greenery systems”, *Building and Environment*, vol. 175, no. March, p. 106815, 2020.
- [9] L. S. H. Lee and C. Y. Jim, “Energy benefits of green-wall shading based on novel-accurate apportionment of short-wave radiation components”, *Applied Energy*, vol. 238, pp. 1506–1518, 2019.
- [10] J. Coma, G. Pérez, A. de Gracia, S. Burés, M. Urrestarazu, and L. F. Cabeza, “Vertical greenery systems for energy savings in buildings: A comparative study between green walls and green facades”, *Building and Environment*, vol. 111, pp. 228–237, 2017.
- [11] G. Pérez et al., “Acoustic insulation capacity of Vertical Greenery Systems for buildings”, *Applied Acoustics*, vol. 110, pp. 218–226, 2016.
- [12] R. Collins, M. Schaafsma, and M. D. Hudson, “The value of green walls to urban biodiversity”, *Land Use Policy*, vol. 64, pp. 114–123, 2017.

-
- [13] F. Madre, P. Clergeau, N. Machon, and A. Vergnes, "Building biodiversity: Vegetated façades as habitats for spider and beetle assemblages", *Global Ecology and Conservation*, vol. 3, pp. 222–233, 2015.
- [14] L. L. H. Peng, Z. Jiang, X. Yang, Y. He, T. Xu, and S. S. Chen, "Cooling effects of block-scale facade greening and their relationship with urban form", *Building and Environment*, vol. 169, no. November 2019, p. 106552, 2020.
- [15] E. Shafiee, M. Faizi, S. A. Yazdanfar, and M. A. Khanmohammadi, "Assessment of the effect of living wall systems on the improvement of the urban heat island phenomenon", *Building and Environment*, vol. 181, no. January, p. 106923, 2020.
- [16] C. L. Tan, N. H. Wong, and S. K. Jusuf, "Effects of vertical greenery on mean radiant temperature in the tropical urban environment", *Landscape and Urban Planning*, vol. 127, pp. 52–64, 2014.
- [17] M. Marchi, R. M. Pulselli, N. Marchettini, F. M. Pulselli, and S. Bastianoni, "Carbon dioxide sequestration model of a vertical greenery system", *Ecological Modelling*, vol. 306, pp. 46–56, 2015.
- [18] A. F. Speak, J. J. Rothwell, S. J. Lindley, and C. L. Smith, "Urban particulate pollution reduction by four species of green roof vegetation in a UK city", *Atmospheric Environment*, vol. 61, pp. 283–293, 2012.
- [19] P. J. Irga, T. J. Pettit, and F. R. Torpy, "The phytoremediation of indoor air pollution: a review on the technology development from the potted plant through to functional green wall biofilters", *Reviews in Environmental Science and Biotechnology*, vol. 17, no. 2, pp. 395–415, 2018.
- [20] M. Ottelé, K. Perini, A. L. A. Fraaij, E. M. Haas, and R. Raiteri, "Comparative life cycle analysis for green façades and living wall systems", *Energy and Buildings*, vol. 43, pp. 3419–3429, 2011.
- [21] H. Feng and K. Hewage, "Lifecycle assessment of living walls: Air purification and energy performance", *Journal of Cleaner Production*, vol. 69, pp. 91–99, 2014.
- [22] V. Oquendo-Di Cosola, F. Olivieri, L. Ruiz-García, and J. Bacenetti, "An environmental Life Cycle Assessment of Living Wall Systems", *Journal of Environmental Management*, vol. 254, p. 109743, 2020.
- [23] A. Medl, F. Florineth, S. B. Kikuta, and S. Mayr, "Irrigation of 'Green walls' is necessary to avoid drought stress of grass vegetation (*Phleum pratense* L.)", *Ecological Engineering*, vol. 113, pp. 21–26, 2018.

- [24] V. Prodanovic, A. Wang, and A. Deletic, “Assessing water retention and correlation to climate conditions of five plant species in greywater treating green walls”, *Water Research*, vol. 167, p. 115092, 2019.
- [25] V. Prodanovic, B. Hatt, D. McCarthy, and A. Deletic, “Green wall height and design optimisation for effective greywater pollution treatment and reuse”, *Journal of Environmental Management*, vol. 261, no. January, p. 110173, 2020.
- [26] B. Riley, “The state of the art of living walls: Lessons learned”, *Building and Environment*, vol. 114, pp. 219–232, 2017.
- [27] UNEP, AITF, FFP, HORTIS, and L. V. D. L. V. ARRDHOR, “Recommandations professionnelles B.C.3-R0: Conception, réalisation et entretien de solutions de végétalisation de façades par bardage rapporté”, 2016.
- [28] UNEP, AITF, FFP, HORTIS, and L. V. D. L. V. ARRDHOR, “Recommandations professionnelles B.C.5-R0: Conception, réalisation et entretien de solutions de végétalisation de façades par plantes grimpantes”, 2016.
- [29] Fll - Landscape Development and Landscaping Research Society e. V., “Fassadenbegrünungsrichtlinien – Richtlinien für die Planung, Bau und Instandhaltung von Fassadenbegrünungen”, 2018.
- [30] Urban Greening and N. build Landscapes, UK Guide to Green Walls - An introductory guide to designing and constructing green walls in the UK [Online]. Available: <https://www.urbangreening.info>.
- [31] State Government of Victoria, “Growing Green Guide: A guide to green roofs, walls and facades in Melbourne and Victoria”, Australia. 2014.
- [32] K. Perini and P. Rosasco, “Is greening the building envelope economically sustainable? An analysis to evaluate the advantages of economy of scope of vertical greening systems and green roofs”, *Urban Forestry and Urban Greening*, vol. 20, pp. 328–337, 2016.
- [33] A. S. Tártaro, T. M. Mata, A. A. Martins, and J. C. G. Esteves da Silva, “Carbon footprint of the insulation cork board”, *Journal of Cleaner Production*, vol. 143, pp. 925–932, 2017.
- [34] N. Pargana, M. D. Pinheiro, J. D. Silvestre, and J. de Brito, “Comparative environmental life cycle assessment of thermal insulation materials of buildings”, *Energy and Buildings*, vol. 82, pp. 466–481, 2014.

-
- [35] J. D. Silvestre, N. Pargana, J. de Brito, M. D. Pinheiro, and V. Durão, “Insulation cork boards-environmental life cycle assessment of an organic construction material”, *Materials*, vol. 9, pp. 1–16, 2016.
- [36] N. Simões, R. Fino, and A. Tadeu, “Uncoated medium density expanded cork boards for building façades and roofs: Mechanical, hygrothermal and durability characterization”, *Construction and Building Materials*, vol. 200, pp. 447–464, 2019.
- [37] R. Fino, A. Tadeu, and N. Simões, “Influence of a period of wet weather on the heat transfer across a wall covered with uncoated medium density expanded cork”, *Energy and Buildings*, vol. 165, pp. 118–131, 2018.
- [38] A. Tadeu, L. Š, N. Simões, and R. Fino, “Simulation of heat and moisture flow through walls covered with uncoated medium density expanded cork”, *Building and Environment*, vol. 142, pp. 195–210, 2018.
- [39] A. Cortês, J. Almeida, J. de Brito, and A. Tadeu, “Water retention and drainage capability of expanded cork agglomerate boards intended for application in green vertical systems”, *Construction and Building Materials*, vol. 224, pp. 439–446, 2019.
- [40] A. Tadeu, N. Simões, R. Almeida, and C. Manuel, “Drainage and water storage capacity of insulation cork board applied as a layer on green roofs”, *Construction and Building Materials*, vol. 209, pp. 52–65, 2019.
- [41] R. Almeida, N. Simões, A. Tadeu, P. Palha, and J. Almeida, “Thermal behaviour of a green roof containing insulation cork board. An experimental characterization using a bioclimatic chamber”, *Building and Environment*, vol. 160, p. 106179, 2019.
- [42] M. Manso and J. P. Castro-Gomes, “Thermal analysis of a new modular system for green walls”, *Journal of Building Engineering*, vol. 7, pp. 53–62, 2016.
- [43] M. Manso, J. Castro-Gomes, B. Paulo, I. Bentes, and C. A. Teixeira, “Life cycle analysis of a new modular greening system”, *Science of the Total Environment*, vol. 627, pp. 1146–1153, 2018.
- [44] L. Pan and L. M. Chu, “Energy saving potential and life cycle environmental impacts of a vertical greenery system in Hong Kong: A case study”, *Building and Environment*, vol. 96, pp. 293–300, 2016.
- [45] PRé, “SimaPro Database Manual Methods Library”, 4.14.2, 2019.
- [46] “Webertherm flex P - Technical file”, 2018. [Online]. Available: <https://www.pt.weber/revestimento-e-renovacao-de-fachadas/webertherm-flex-p>.

[47] Fll - Landscape Development and Landscaping Research Society e. V., “FLL - Green Roof Guidelines - Guidelines for the Planning, Construction and Maintenance of Green Roofing”, 2018.

[48] L. Perez-Urrestarazu and M. Urrestarazu, “Vertical Greening Systems: Irrigation and Maintenance”, in *Nature Based Strategies for Urban and Building Sustainability*, G. Pérez and K. Perini, Eds. Butterworth-Heinemann, Elsevier, 2018, pp. 55–63.

[49] L. Pérez-Urrestarazu, G. Egea, A. Franco-Salas, and R. Fernández-Cañero, “Irrigation systems evaluation for living walls”, *Journal of Irrigation and Drainage Engineering*, vol. 140, no. 4, 2014.

[50] D. A. Segovia-Cardozo, L. Rodríguez-Sinobas, and S. Zubelzu, “Living green walls: Estimation of water requirements and assessment of irrigation management”, *Urban Forestry and Urban Greening*, vol. 46, no. April, p. 126458, 2019.

[51] Amorim Isolamentos S.A., “Declaração Ambiental de Produto - Aglomerado de cortiça expandida (ICB)”, Sistema DAPHabitat, DAP 002:2016, 2016.

[52] Man-Systems Integration Standards (NASA-STD-3000), Revision B, July 1995, Volume I, Section 3 - Anthropometry and Biomechanics [Online]. Available: <https://msis.jsc.nasa.gov/sections/section03.htm>.

[53] Siro-roof - Technical file [Online]. Available: <https://portal.siro.pt/pt/programs/cindex.aspx>.

[54] EN 1991-1-4 - Eurocode 1: Actions on structures - Part 1-4: General actions - Wind actions.

CHAPTER 4

ENVIRONMENTAL PERFORMANCE OF A CORK- BASED MODULAR LIVING WALL FROM A LIFE-CYCLE PERSPECTIVE

4. Environmental performance of a cork-based modular living wall from a life-cycle perspective

4.1. Introduction

Engineering solutions inspired and supported by nature, such as green vertical systems (GVSs), have long been suggested to improve the performance of buildings and mitigate some of the environmental problems observed in cities [1]. Although all GVSs make use of vegetation to cover building façades, there is a wide variety of systems with specific characteristics. Thus, to facilitate the discussion, a classification based on that proposed by Manso et al. [2] is assumed in this work. According to this classification, GVSs are divided into two main systems: green façades and living walls. Green façades are then subdivided into direct green façades and indirect green façades, if plants are fixed directly to the wall or to a purpose-built supporting structure, respectively. Living walls are also subdivided into modular or continuous systems, depending on whether they are built using a limited number of pieces arranged side by side, or not, respectively.

Regarding the performance of buildings, GVSs can act as an external layer capable of improving acoustic and thermal behaviour. A recent study performed by Romanova et al. [3] shows that plants with high leaf area density can improve the sound absorption of a living wall, particularly for medium and high frequencies. The results also reveal that plants with high leaf area density can reduce acoustic resonances. Djedjig et al. [4] also show that GVSs can lower the temperature of

building skins, due to evapotranspiration and shading effects, reporting a reduction of 37% in the cooling loads of nearby buildings. An experimental study performed by Cheng et al. [5] also discusses the importance of the area covered by living plants and moisture of the growing medium for the cooling effect, stressing the value of maintaining a healthy vegetation cover.

Green vertical systems can also act as biofilters and capture different atmospheric pollutants. A study performed by Pettit et al. [6] shows that several plant species are able to filter the air and outperforms biofilters consisting only of substrate. Perini et al. [7] also compared the performance of four evergreen plant species commonly used in GVSs, concluding that the amount of dust removed could depend to a significant extent on the plant species' shape and surface of the leaves. In a study performed by Weerakkody et al. [8], using 17 living wall plant species, it was found that small, hairy and waxy leaves can increase the particulate matter fixation. Another study by the same authors [9] found that a 100 cm² living wall is able to remove about 122×10⁷ PM₁, 8.24×10⁷ PM_{2.5} and 4.45×10⁷ PM₁₀. Weerakkody et al. [10] further studied the biofiltration capacity of four evergreen plants in a GVS by washing-off particles from the leaves. The results show that the simulated rainfalls were able to restore the biofiltration capacity.

Plants also have the ability to capture carbon dioxide (CO₂) from the atmosphere via photosynthesis and store it in the form of biomass for many years. Under given circumstances, a fraction of this carbon may be transferred to the soil and stored in other forms (e.g. phytoliths) for even longer periods of time. It is estimated that about 3170 gigatons of C are kept in terrestrial systems, 2500 gigatons in soil, 560 gigatons in plants and the rest in microbial biomass [11]. However, several factors could influence the carbon uptake capacity of plants. Tall, fast-growing woody plants with large stems are normally responsible for high carbon uptake rates. More complex roots may also help to increase the rate of carbon transfer to the soil. Physiological and biological features of plants could also influence the sequestration capacity [12].

A study by Getter et al. [13] on an extensive green roof with four sedum species found the carbon sequestration capacity at the end of the second growing season varied between 64 and 239 gCm⁻² for the aboveground biomass, and between 37 and 185 gCm⁻² for belowground biomass. A substrate sequestration rate of 100 gCm⁻² was also found, regardless of the species. As far as GVSs are concerned, Charoenkit and Yiemwattana [14] compared the carbon sequestration capacity of three herbaceous plants. They found that those with the densest foliage, smallest leaves and woody branches perform better, with carbon sequestered over six months varying between 4.35 and 30.26 gCm⁻². Another study conducted by Marchi et al. [15] on a model of vertical garden shows that the mean yearly uptakes rates by plant biomass varies between 0.44 and 3.18 kg CO₂eq.m⁻². However, the number of studies on the carbon sequestration potential of green vertical systems is relatively small, suggesting that further research is necessary.

Apart from the benefits, the estimation of the environmental impacts from a life cycle perspective is crucial to assess the overall performance of GVSs. In this context, a life cycle analysis (LCA) could be a useful tool to understand the environmental performance of such systems in a more comprehensive way [16]–[18]. However, the lack of quantitative data required to perform a full LCA from cradle-to-grave may challenge such an approach, suggesting that experimental studies under real conditions are still needed to calibrate these models.

A new modular living wall system made of expanded cork agglomerate was proposed in the previous chapter, taking into account several environmental and functional requirements [19]. A full mechanical characterization was also carried out to assist in choosing the most suitable material density. Note that expanded cork agglomerate is a natural material commonly used as thermal insulation for buildings [20], [21], which has shown to have adequate water retention and drainage capabilities when applied in GVS [22].

In the present chapter, it is aimed to extend the characterization of this living wall system regarding its performance in real conditions and taking into account variations introduced by different plant species, geographical orientations and seasons. Four 8 m² façades (facing north, south, east, and west) were built in Coimbra, a city in the central region of Portugal, to serve as a prototype. Two plant species (*Thymus pulegioides* and *Festuca glauca*) with quite distinctive characteristics were chosen to be used as vegetation models. The area of façade covered by vegetation and the amount of biomass accumulated were monitored for over one year (a complete growing season) to assess the performance of the living wall in terms of vegetation development and estimate the carbon sequestration capacity. Additionally, to assess the overall environmental performance of the new living wall, an LCA was carried out. Scenarios for the construction, use, and end of life stages were established based on the prototype characteristics and monitoring results.

4.2. Methodologies

In this section the methodologies and the experimental setups are fully described. This includes the characteristics of all the materials, components and plant species used to build the prototype, as well as information on the dimensions and orientations of the different test façades. It also describes the sampling technique, sample preparation, and chemical analysis carried out to determine the amount of biomass and carbon content. The methodologies and software packages used to evaluate the area of façade covered by vegetation and the LCA modelling are also presented.

4.2.1. Prototype description

The prototype that supports this work was installed in Coimbra, in a Mediterranean climate region characterized by an average maximum temperature of 28.5 °C in the summer and an average minimum temperature of 4.6 °C in the winter [23]. The prototype comprises two testing walls, 4 m wide and 2 m high, one facing north-south and the other east-west. An adhesive mortar, previously characterized, was used to fix the new cork modules to both sides of the bearing walls [24]. The cork troughs were internally protected with a commercially available geotextile filter [25], to prevent fine particles from washing out, and then filled with a technical lightweight substrate (650-700 kg/m³ fully saturated with water). This substrate is commercially available and has a pH in CaCl₂ of 5.5-6.5. It contains less than 70% (w/w) of organic matter and is enriched with a fertilizer NPK 15-05-20 (1 kg/m³) [26]. Drip irrigation lines were placed in all vases to ensure a homogeneous moistening of the test system (8.5 l.h-1m⁻²). Finally, two plant species (*Thymus pulegioides* and *Festuca glauca*), carefully selected to meet the requirements of a living wall and the Mediterranean climate, were planted in each façade, laterally dividing the space in half. Young plants started in a nursery were used. The two plants are perennial species and well adapted to full sun and partial shade conditions, i.e. requiring little irrigation. Additionally, they have relatively simple root systems and a high growing rate. A side view of the new cork-based module with all the components is shown in Figure 4.1. A simplified diagram describing the construction of the prototype is also shown in Figure 4.2.

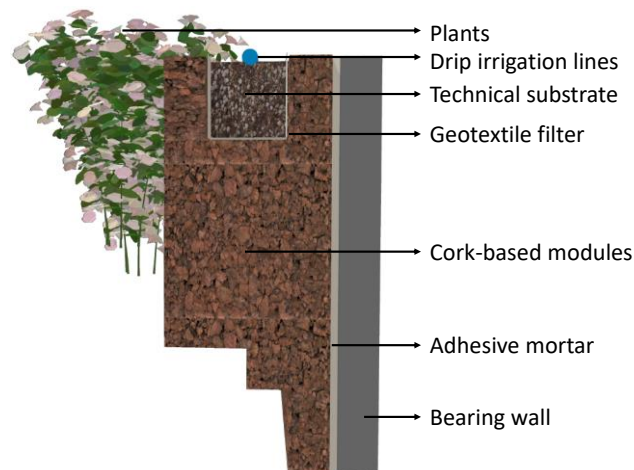


Figure 4.1 - Side view of the new cork-based module with all the components.

Note that a woody plant model (*Thymus pulegioides*) and a hanging plant model (*Festuca glauca*) were deliberately chosen to study the effect of such characteristics on the ability to cover the façade and sequester carbon. A photograph of the south-facing living wall containing both plants (taken in the spring of 2020) is shown in Figure 4.3.

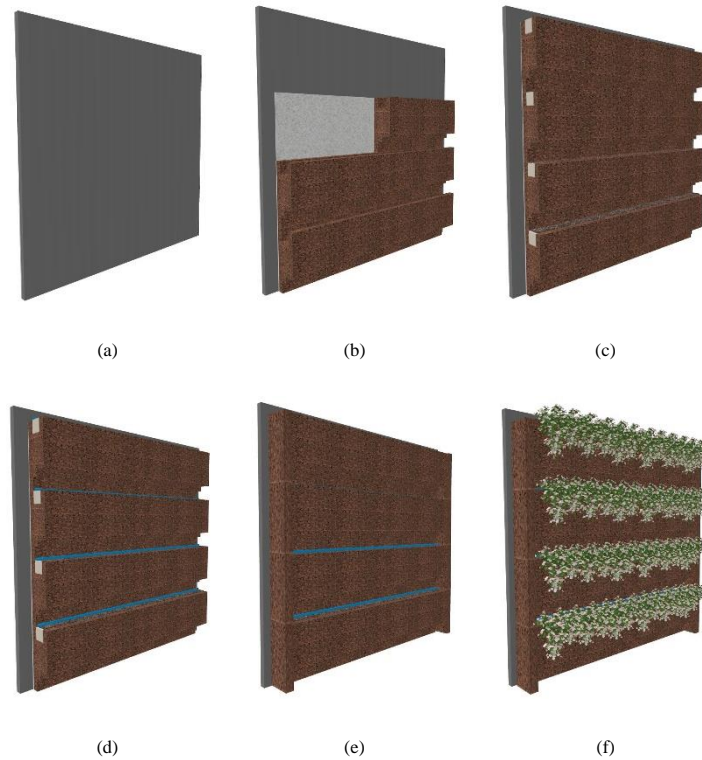


Figure 4.2 - Schematic illustration of the prototype preparation: (a) bearing wall; (b) cork-based modules; (c) geotextile filter and technical substrate; (d) drip irrigation lines; (e) side covers; (f) plants.



Figure 4.3 - Living wall prototype showing *Thymus pulegioides* (left side) and *Festuca glauca* (right side).

4.2.2. Carbon sequestration analysis

Carbon sequestration of each plant model was evaluated by random sampling of aboveground and belowground biomass (spots of 20 cm width of the cork trough) over one year, following a methodology adapted from the work done by Getter et al. [13]. The first samples were collected in April 2019 (week 0), just after planting, to establish a reference scenario. Aboveground biomass

was sampled every two months (April 2019, June 2019, August 2019, October 2019, December 2019, February 2020, and April 2020), while belowground biomass was sampled every 6 months (April 2019, October 2019, and April 2020).

The aboveground biomass was clipped at the substrate level and stored in paper bags, dried in an oven at 70 °C for one week, milled to pass through a 0.25 mm sieve and saved in desiccator until the determination of carbon content. Belowground biomass and substrate were collected and saved in plastic bags. The samples were weighed and left to air dry for two days in order to facilitate the separation of the roots from the substrate. Then, the samples were weighed again and passed through a 4 mm sieve to facilitate the separation of the roots from the substrate. The sieved matter was examined and the fine roots that might escape through the sieving process were also collected. The belowground biomass was then rinsed with deionized water before and after being washed with a phosphate-free dilute detergent. After that, the samples were cleaned with a NaEDTA 0.01M solution for 5 minutes and washed with deionized water. Finally, the samples were gently dried using absorbent paper and any particles of the substrate that might remain after the washing process were removed. The cleaned roots were kept in paper bags and dried at 70 °C for two days. Dried belowground biomass was weighed, milled to pass through a 0.25 mm sieve and saved in desiccator until the carbon content analysis. Carbon content was determined using a vario MACRO cube (Elementar Analysensysteme GmbH) in the CN mode. Note that this instrument was optimized for the analysis of wood and plant material that, for inhomogeneity reasons, requires relatively high sample weights.

4.2.3. Area covered with vegetation

The façade area covered with vegetation was assessed by photographic record every week for a year. The images collected were processed using the Image J software (version 1.52a) to obtain the area of vegetation. This analysis was only applied to the central part of the façades, which was not used in the carbon sequestration tests. Three samples for each image were obtained with the software and the average values considered.

4.2.4. Life cycle assessment of the modular living wall system

The environmental performance of the new modular living wall was evaluated using the life cycle assessment methodology described in the ISO 14000 series of standards. According to this methodology, a functional unit was established, and boundaries were defined for the system under study, quantifying all the mass and energy flows entering and exiting the boundaries. These data were then used to calculate the potential environmental impacts of the new living wall over its life cycle. The calculations were performed using SimaPro (version 9.1). The impact assessment used the CML-IA v.4.7 method [27] with following impact categories: depletion of abiotic resources - elements (ADP-elements), depletion of abiotic resources - fossil (ADP-fossil), global warming

(GWP), ozone depletion (ODP), photochemical ozone creation (PCOP), acidification (AP), and eutrophication (EP).

4.3. Results and discussion

4.3.1. Carbon sequestration

As previously described, samples of below- and aboveground biomass were collected over time and the amount of dry mass and carbon content determined. In the case of the belowground biomass, sampling was carried out less frequently to avoid disturbing the test system as much as possible. In addition, unlike the variations in the amount of aboveground biomass in response to the different seasons, the amount of belowground biomass usually remains constant or slowly increases over time. The results obtained for the above and belowground dry biomass per square meter of façade over time are given in Table 4.1 and Table 4.2, respectively.

Table 4.1 - Dry mass of the aboveground biomass per square meter of façade (g/m²) from week 0 (W0) to week 55 (W55)

Orientation/Plant species	W0	W10	W18	W25	W34	W44	W55	
North	<i>Thymus pulegioides</i>	4.7	18.6	45.5	50.1	42.0	34.4	106.3
	<i>Festuca glauca</i>	22.1	52.4	176.2	252.6	84.9	130.1	376.8
South	<i>Thymus pulegioides</i>	4.7	19.9	39.3	35.7	61.1	19.8	44.7
	<i>Festuca glauca</i>	22.1	138.7	172.8	165.4	151.5	249.1	241.5
East	<i>Thymus pulegioides</i>	4.7	41.4	73.3	46.3	45.2	33.1	68.4
	<i>Festuca glauca</i>	22.1	94.9	107.0	212.0	95.2	66.2	342.4
West	<i>Thymus pulegioides</i>	4.7	11.6	89.7	39.0	21.6	47.5	50.6
	<i>Festuca glauca</i>	22.1	112.4	155.5	181.1	156.6	119.2	126.9

It can be seen that *Festuca glauca* shows a much higher amount of aboveground biomass than *Thymus pulegioides* at any point in time, regardless of the façade orientation. See, for example, the amount of *Festuca glauca* biomass for the south- and east-oriented façades in spring (week 55), which is about 5 times higher than that of *Thymus pulegioides*. As expected, the rate of biomass produced is generally higher from the beginning of spring to the beginning of autumn, with a marked effect for *Festuca glauca* in the north and east orientations.

Table 4.2 - Dry mass of the belowground biomass per square meter of façade (g/m²) from week 0 (W0) to week 55 (W55)

Orientation/ Plant specie		W0	W25	W55
North	<i>Thymus pulegioides</i>	5.1	18.5	39.8
	<i>Festuca glauca</i>	11.5	235.4	165.6
South	<i>Thymus pulegioides</i>	5.1	26.8	32.6
	<i>Festuca glauca</i>	11.5	133.8	199.1
East	<i>Thymus pulegioides</i>	5.1	24.2	27.4
	<i>Festuca glauca</i>	11.5	330.8	382.7
West	<i>Thymus pulegioides</i>	5.1	25.1	25.6
	<i>Festuca glauca</i>	11.5	62.4	70.2

Once again, at any time *Festuca glauca* has a much higher amount of belowground biomass than *Thymus pulegioides*, regardless of the geographical orientation. See, for example, the amount of *Festuca glauca* biomass in spring (week 55) for the south and west façades, which is about 6 and 3 times higher than that of *Thymus pulegioides*, respectively.

The results also show that in general a higher amount of aboveground biomass is obtained, regardless of the geographical orientation or plant species, compared with the amount of belowground biomass. It is believed that a non-representative lower leaf density sample was collected in the case of *Festuca glauca* facing east, that seems to be an exception to this rule.

Chemical analyses carried out further allow to conclude that the carbon content per sample mass is approximately constant (between 44% and 46%) over time for both plant models (*Thymus pulegioides* and *Festuca glauca*) and sources of biomass (aboveground and belowground). Average carbon content and the respective standard deviation values are shown in Table 4.3. Note that, although small differences were found in the results, *Thymus pulegioides* has a carbon content systematically higher than that of *Festuca glauca*, when assessed for corresponding temporal moments and geographic orientations, for both the aboveground and belowground biomass. This is likely to be due to the woodier structure of *Thymus pulegioides* compared with the *Festuca glauca*. Comparable results have been reported in the literature for GVSs containing three different herbaceous plants, with carbon content values varying between 42% and 45% for the aboveground biomass, and 43% and 45% for belowground biomass [14].

Table 4.3 - Carbon content \pm standard deviation, % (m/m)

	Aboveground	Belowground
<i>Thymus pulegioides</i>	44.8 \pm 0.5	45.9 \pm 0.5
<i>Festuca glauca</i>	43.9 \pm 0.8	44.4 \pm 1.2

From the amount of dry biomass and carbon content results, it was possible to calculate the total amount of carbon in the different façades for each plant species and geographical orientation. Figures Figure 4.4 and Figure 4.5 show the total carbon content (g) per square meter of façade in the aboveground branches and leaves and in the belowground root structures, respectively.

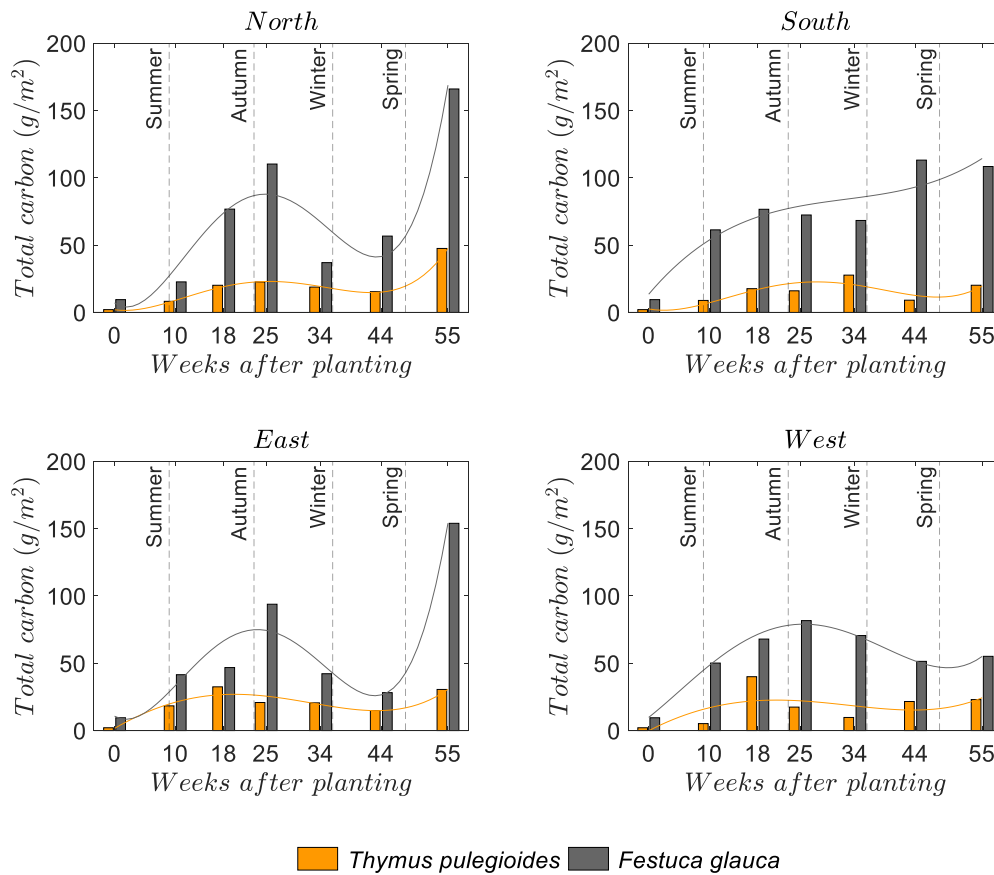


Figure 4.4 - Total carbon content per square meter of façade (g/m²) in the aboveground biomass samples.

As might be expected, the amount of carbon found in the form of aboveground biomass is much higher from the beginning of spring to the beginning of autumn as a consequence of the stronger development that vegetation undergoes these seasons. Moreover, a decrease in the amount of carbon found in the form of aboveground biomass is clearly visible in the autumn and winter due to the fall of leaves and the resulting transfer of biomass to the surroundings. In the case of belowground biomass, the amount of carbon increases over time, as anticipated.

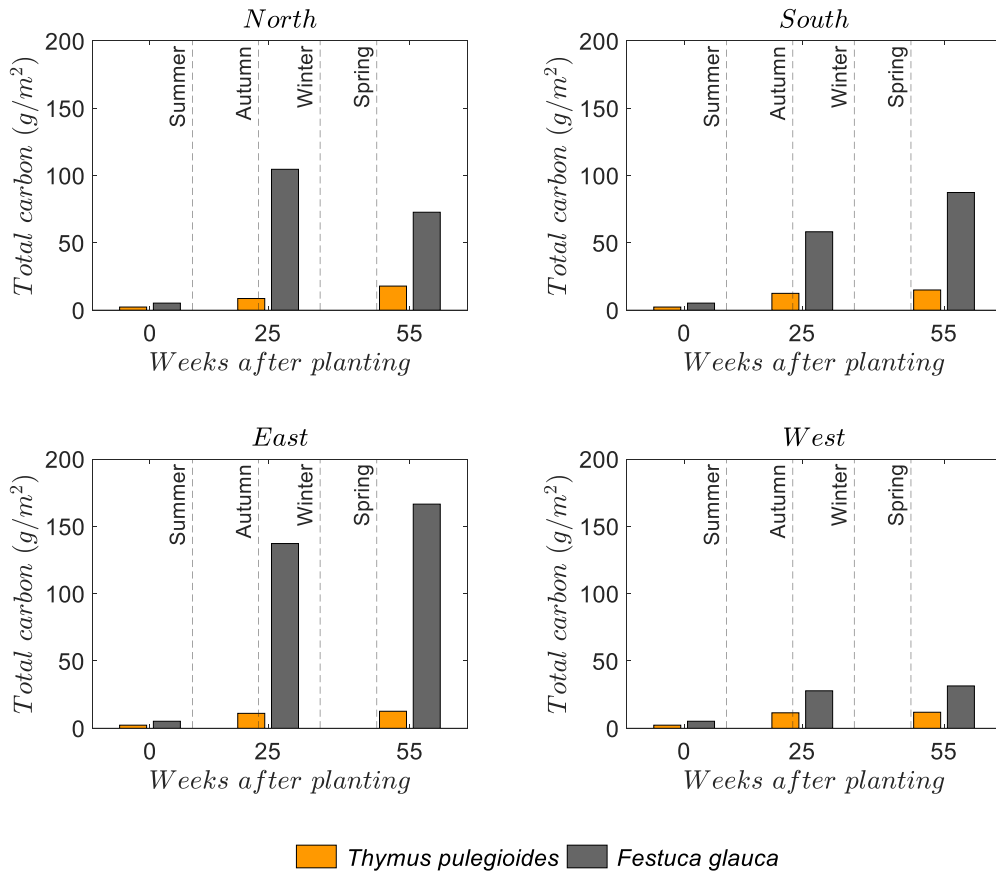


Figure 4.5 - Total carbon content per square meter of façade (g/m²) in the belowground biomass samples.

For easier assessment of the influence of the plant species and geographical orientation on the carbon sequestration, a summary of the cumulative carbon uptake provided by the above- and belowground biomass over a year is shown in Figure 4.6.

The results show that a higher cumulative carbon uptake is provided by the aboveground biomass, regardless of the geographical orientation or plant species. Additionally, the total amount of carbon accumulated (in the belowground and aboveground biomass together) is always higher for *Festuca glauca*, regardless of the geographical orientation, because this species produces a greater amount of biomass.

Regarding geographical orientation, no significant differences were found in the cumulative carbon uptake for the *Thymus pulegioides* (59 gCm⁻², on average). But for *Festuca glauca* the greatest accumulation of carbon seems to have occurred in the north (329 gCm⁻²) and east (371 gCm⁻²) oriented façades, relative to those oriented to the south (194 gCm⁻²) and west (102 gCm⁻²). This is likely to result of the intrinsic characteristics of the selected plant species combined with the environmental conditions provided by the geographical orientation.

Comparable results have been described in the literature. An extensive green roof containing *sedum* species showed a cumulative carbon uptake varying between 64 and 239 gCm⁻² for the aboveground biomass, and 37 and 185 gCm⁻² for belowground biomass [13]. Note, however, that different climatic regions and different plant species are expected to perform differently.

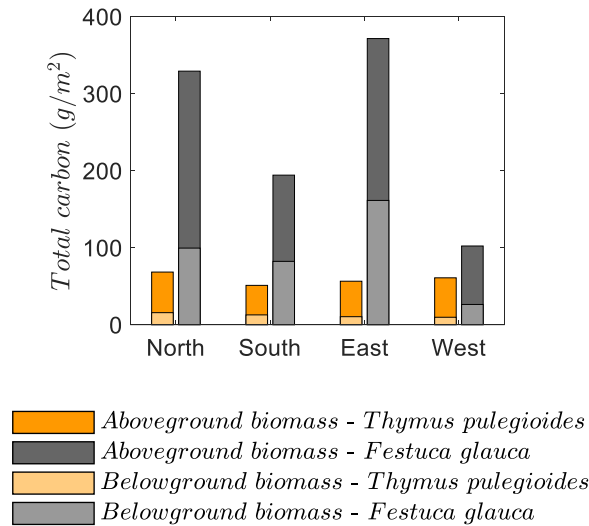


Figure 4.6 - Cumulative carbon uptake in above and belowground biomass over one year.

4.3.2. Covered area

Bearing in mind that the benefits attributed to green façades (with respect not only to the carbon sequestration but also to the retention of other pollutants, thermal insulation, sound absorption, architectural integration, for example) are strongly correlated with the area of vegetated surface, it is important to characterize the covering capacity achieved by the plant models used. Thus, photos were taken of all the test façades over a period of 55 weeks. As previously described, these images were subsequently processed with the objective of systematically and accurately estimating the façade area covered by vegetation. Note that dead or less vigorous vegetation (observed in some phases of the plant's vegetative cycle) was excluded from this analysis since it does not contribute in the same way to the benefits attributed to the plants [28]. For example, representative processed images of the north-facing test façade in the different seasons for *Festuca glauca* and for *Thymus pulegioides* are presented in Figures Figure 4.7 and Figure 4.8, respectively.

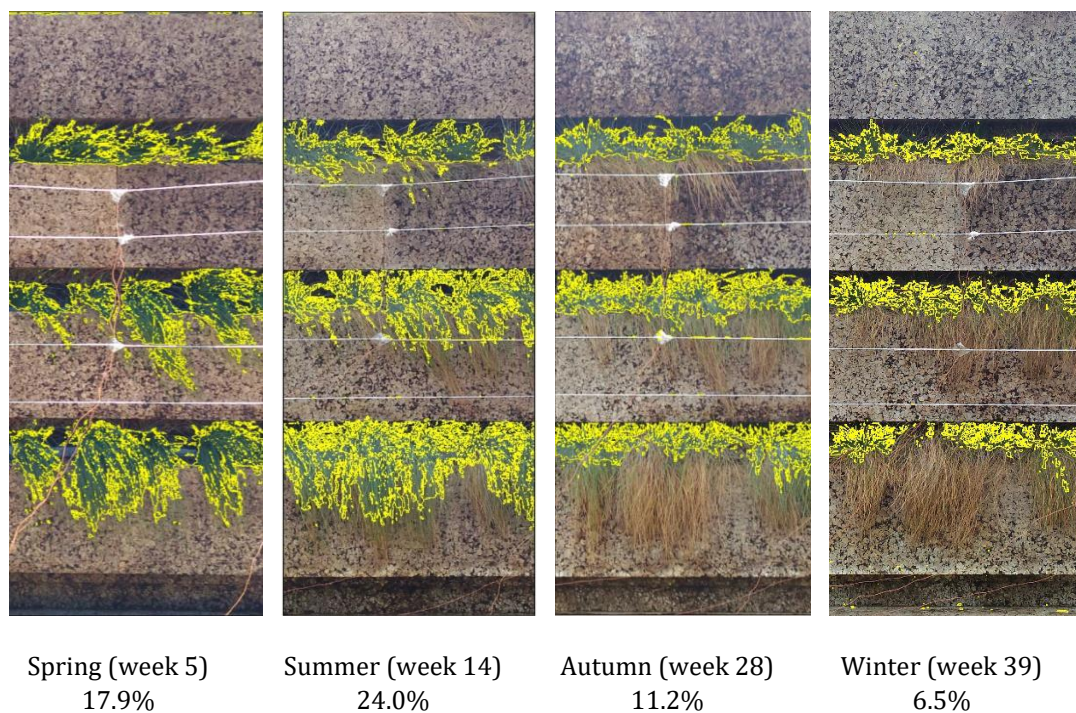


Figure 4.7 - Representative images of the north-facing test façade for *Festuca glauca* processed with the aim of estimating the covering area (%).

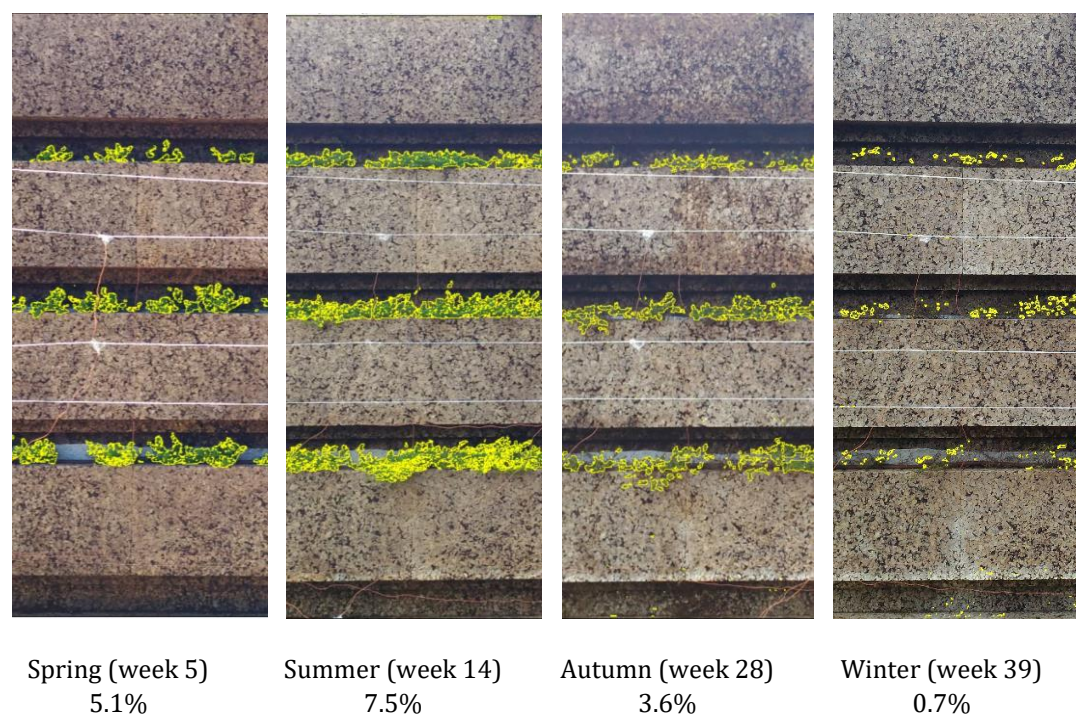


Figure 4.8 - Representative images of the north-facing test façade for *Thymus pulegioides* processed with the aim of estimating the covering area (%).

Figure 4.9 further summarizes the percentage of covered façade area for the different geographical orientations. As expected, larger vegetated areas are found in hot seasons rather than in cold seasons. Additionally, the results show that *Festuca glauca*, which is more of a hanging plant, was able to cover a larger area of the façade throughout the monitored year than the *Thymus pulegioides*. It should be noted, however, that it is expected that a woodier plant, such as *Thymus pulegioides*, would take longer to cover a similar area. This means that several years of monitoring would be necessary to ascertain the long-term differences between the behaviour of the two plant species.

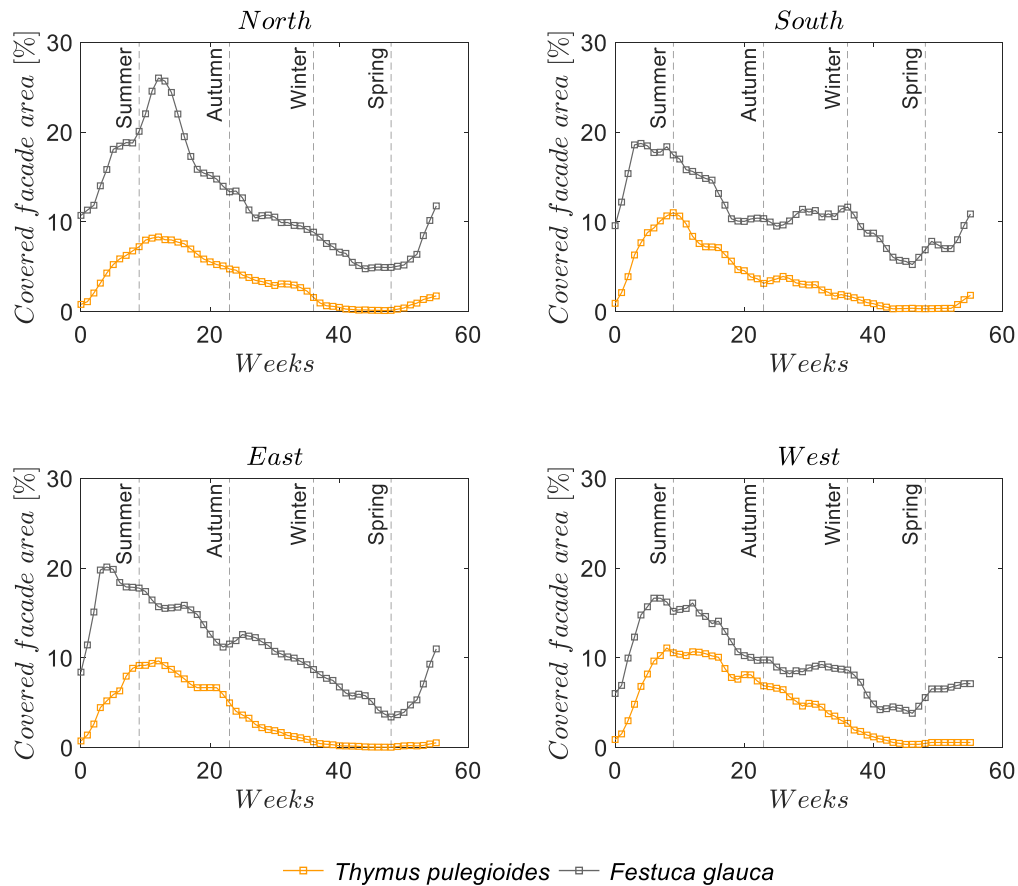


Figure 4.9 - Area of the façade (%) covered by *Thymus pulegioides* and *Festuca glauca* during one year.

It seems that the area of façade covered with vegetation does not exceed 30% for *Festuca glauca*, even at the most favourable times of the year. It is important to note, however, that the discontinuities created in the system to host vegetation also represent only 30% of the total area of the façade. In fact, the system under study was intentionally developed with the aim of combining the benefits of expanded cork agglomerate and vegetation [19]. This strategy means that at times of the year when the vegetation is less vigorous, several of the benefits expected from these façades (thermal and acoustic insulation, architectural integration, etc.) were provided by the expanded cork agglomerate modules.

4.3.3. Environmental performance

LCA of the new modular living wall

This study was aimed to assess the environmental performance of the new modular living wall over its life cycle. A cradle-to-grave approach was adopted that includes all the input and output flows from the raw materials extraction to the end of life of the solution (Figure 4.10). The functional unit established was 1 m² of a modular living wall with a lifetime of 50 years to cover a building façade. This lifetime was defined according to the characteristics of the system and the assumptions of LCA studies carried out for other modular living walls [17], [29], [30], [31].

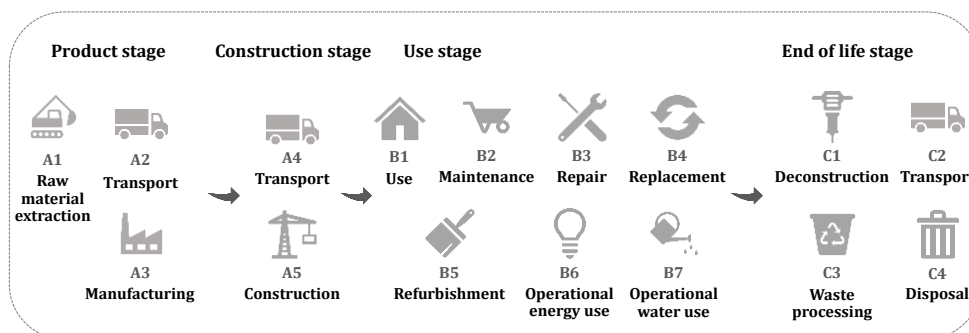


Figure 4.10 - System boundaries of the LCA study.

The inventory data were divided into four sections according to EN 15804: product (A1-A3), construction (A4-A5), use (B1-B7) and end-of-life (C1-C4) stages. Whenever they were available all data related to the construction of the modular living wall were considered. Table 4.4 presents the data inventory for the new modular living wall.

The manufacturing process of all the components was modelled using technical sheets, environmental product declarations, and the Ecoinvent database v3.6. To model the production of the ICB modules industrial data were provided by Amorim Cork Insulation. All the impacts related to the production of the ICB boards and the energy consumption associated with the fabrication of the module were considered, as well as the processing of the waste generated. The electricity production used was the Portuguese mix from 2016 available on the Ecoinvent database v3.6.

Regarding the construction stage, all impacts related to the production and transport of components from the factory site to Coimbra were considered. To model the transport of the materials, distances were measured using Google Maps. The impact associated with fuel combustion was taken into account, but all the impacts related to the infrastructure for the production of vehicles and their maintenance were excluded. The production of the components required for the installation was also taken into account. Concerning the new modular living wall, these components are the adhesive mortar, the water pipes for the connection of the irrigation system and the ICB side covers. The quantities of materials used were calculated based on the construction of the prototype

previously described. The electricity consumed by the mixer to prepare the adhesive mortar was taken into account. The use of mechanical means (such as lifting platforms) was not considered.

Table 4.4 - Input and output flows of the new modular living wall according to the functional unit defined

Life cycle stages	Flows		Unity	Quantity		
Product stage	Inputs	Components	ICB modules	kg	2.10E+01	
			Geotextile filter	m ²	7.20E-01	
		Energy consumption	Substrate	kg	9.50E+00	
			Plants	kg	1.48E+00	
			Irrigation system	kg	1.36E-01	
		Outputs	Waste	Electricity	kwh	1.63E+01
Construction stage	Inputs	Components	ICB wastage	kg	9.00E+00	
			ICB	kg	7.50E-01	
		Transport	Adhesive mortar	kg	4.20E+00	
			PVC pipes	kg	1.24E-01	
			Truck	tkm	7.16E+00	
		Water consumption	Electricity	kwh	9.96E-02	
			Tap water	m ³	8.25E-04	
Outputs	Waste	Mortar wastage	kg	2.00E-01		
Use stage	Inputs	Carbon uptake	CO ₂ sequesterated	kg	7.71E+00	
			Maintenance	Fertilization	kg	9.80E+00
		Replacement	Plants	kg	5.91E+00	
			Irrigation system	kg	8.16E-01	
			Water consumption	Tap water	m ³	1.93E+01
		Transport	Truck	tkm	2.38E+00	
			Outputs	Waste	Plants	kg
Irrigation system	kg	8.16E-01				
End-of-life stage	Inputs	Energy consumption	Electricity	kwh	1.72E+01	
			Truck	tkm	5.07E+00	
		Outputs	Waste	ICB	kg	2.18E+01
				Mortar	kg	4.00E+00
				Plastics	kg	9.80E-01
		Substrate and plants	kg	1.10E+01		

In terms of the use phase, the benefits provided by the new modular living wall with respect to carbon sequestration over 50 years were considered. The experimental results discussed above were used for that purpose. In terms of maintenance, the application of mineral fertilizer four times a year, after the first year, was also considered. According to estimates found in other LCA studies, a replacement rate of 10%/year of the vegetation [16], [17], [31] and the substitution of the irrigation lines at each 7.5 years [16], [17] were also taken into account. The transport, processing and disposal of the residues resulting from these operations were also considered. Additionally, the water consumed for plant irrigation was also taken into account. This value was estimated according to the WUCOLS method [32], considering *Thymus* and *Festuca* as vegetative species and the annual reference evapotranspiration (ET₀) at Coimbra for the year 2019 [33].

Finally, at the end-of-life stage, the electricity consumed during the demolition process was considered, as was the transport of waste from Coimbra to the final destination. In the case of ICB waste, it was assumed that this would be sent back to the factory to be recycled. In the case of mortar, only the collection for final disposal was considered. Regarding the plastics, a Portuguese scenario was assumed where 1% goes for open-air burning, 30% for incineration, and 69% is sent to landfill. In the case of plants and substrate, composting was assumed.

As previously stated, the potential environmental impacts were estimated using the CML-IA v.4.7 method. The results obtained for the product stage are normalized for 100% and presented in Figure 4.11.

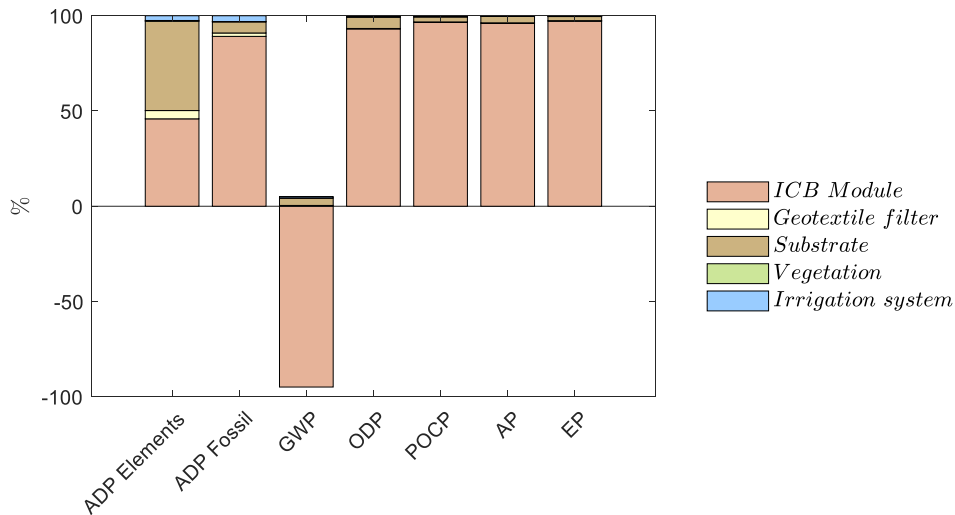


Figure 4.11 - Potential environmental impacts for the product stage of the cork-based living wall normalized for 100%.

The results show that the ICB modules have a strong influence on the overall performance. They make the highest contribution for the great majority of the impact categories assessed (ADP fossil: 89.2%, ODP: 93.1%, POCP: 96.5%, AP: 96.1%, EP: 97.2%), apart from the depletion of abiotic resources – elements where the substrate makes a slightly higher contribution (ICB module: 45.9%, substrate: 46.9%). Note that this could be explained by the large amount of ICB used, which represents about 65% of the total weight of the system. However, since the module is made from a natural material that sequesters carbon as the cork oak grows, it is also responsible for the higher benefit for the global warming potential category (-94.9%).

When these results for the product stage are compared with those previously obtained for different conventional modular living walls [19], the new cork-based system has the best performance for the categories of ADP elements and GWP, the second best for ADP fossil, ODP and POCP and the fourth best for AP and EP.

The potential environmental impacts obtained for the entire life cycle (cradle-to-gate) are presented in Table 4.5 - Potential environmental impacts for the entire life cycle of the cork-based living wall. Once more, to facilitate the analysis they are normalized to 100% and represented in Figure 4.12.

Table 4.5 - Potential environmental impacts for the entire life cycle of the cork-based living wall

Impact categories	Life cycle stages			
	Product	Construction	Use	End-of-life
ADP Elements [kg Sb eq.]	1.38E-04	5.35E-05	2.44E-04	8.70E-05
ADP Fossil [MJ]	3.44E+02	5.91E+01	2.71E+02	1.07E+02
GWP [kg CO ₂ eq.]	-4.27E+01	2.60E+00	8.03E+00	9.45E+00
ODP [kg CFC-11 eq.]	2.25E-06	4.33E-07	9.29E-07	5.84E-07
POCP [kg C ₂ H ₄ eq.]	1.89E-02	1.11E-03	1.21E-02	2.15E-03
AP [kg SO ₂ eq.]	3.62E-01	2.04E-02	6.08E-02	6.62E-02
EP [kg (PO ₄) ³⁻ eq.]	1.10E-01	6.52E-03	2.94E-02	1.89E-02

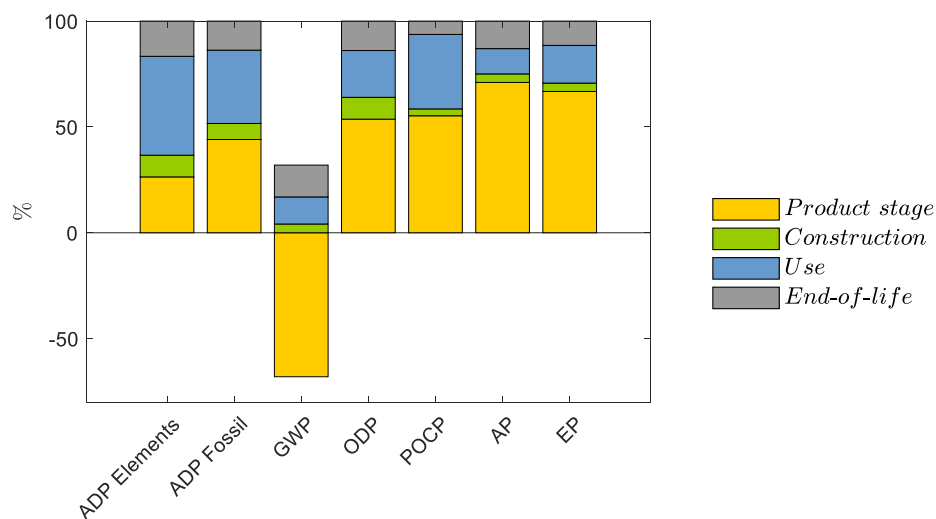


Figure 4.12 - Potential environmental impacts for the entire life cycle of the cork-based living wall normalized for 100%.

It can be seen that the product stage makes the highest contribution to the majority of the impact categories assessed (ADP fossil: 44.1%, ODP: 53.7%, POCP: 55.3%, AP: 71.0%, EP: 66.8%), and also provides the highest benefit for GWP (-68.0%). The use stage is also responsible for the highest contribution from the ADP elements (46.7%) and the second highest from the ADP fossil (34.6%), ODP (22.1%), POCP (35.2%) and EP (17.8%) due in large part to the water consumption for irrigation and the fertilization of the plants during the life cycle of the façade. The results also show that the modular living wall has a negative carbon balance, which means that the carbon embodied in the system not only compensates the carbon emissions produced during the life cycle of the system but also represents a benefit of 22.7 kg CO₂eq.

Comparative LCA

The new modular living wall is expected to further improve the environmental profile of buildings, via carbon sequestration and thermal insulation enhancement, for example. Thus, to evaluate these potential environmental benefits, a comparative life cycle assessment was conducted on a reference wall (RW) and an improved wall containing the new modular living solution (RW + GVS). For that purpose, a conventional building wall made of double-perforated bricks (11 cm + 11 cm) with a 3 cm air layer completely filled with thermal insulation (XPS), with a 3 cm plaster coat on both external surfaces, was used. The functional unit used was 1m² of a wall with a lifetime of 50 years. Once again, the manufacturing of wall components was modelled using technical sheets, environmental product declarations and the Ecoinvent database v3.6. Regarding the transport of the components to the construction site, a scenario of 100 km was assumed. The wastage of mortar and brick in the construction of the wall was considered to be 5%.

Regarding the energy consumption for acclimatization, the usage scenario considered a two-storey building on the outskirts of Coimbra, at an altitude of 50 m, more than 5 km from the coast. This area is part of the Baixo Mondego region and belongs to climatic zone I1, V2. Its geometric and thermal characteristics were established based on the database of the Energy Certification System, provided by the Portuguese Agency for Energy (ADENE). The building under study has façades facing north, east, south, and west, with glazed openings without shading or shutters, with a total area of 15.5 m². The building has floor and wall areas of 155 m² and 83.5 m², respectively. No shading obstructions were considered in its surroundings. To take into account the flat thermal bridges, a 35% increase in the overall thermal transmission coefficient was assumed. At this stage, only the energy needs for heating and cooling the building for 50 years were considered. Other components such as furniture, air conditioning equipment, water heating systems, lighting devices and ventilation systems were excluded. The useful energy needs were estimated using dynamic simulation (multizone) through the DesignBuilder program (version 4.7.0.027), only the results obtained for the 1st floor of the building were taken into account. A layer of ICB covering the building façade with thickness of 200 mm was assumed for calculation purposes. Note that further thermal benefits might be expected with the presence of substrate and vegetation on the building's façade.

In terms of end-of-life, demolition and transport for final disposal was assumed for brick and mortar waste. Regarding XPS, the same Portuguese scenario previously mentioned for plastics was assumed.

The results for the comparative life cycle assessment (cradle-to-grave) of the conventional building wall (RW) and the improved wall containing the new modular living solution (RW+GVS) are presented in Figure 4.13.

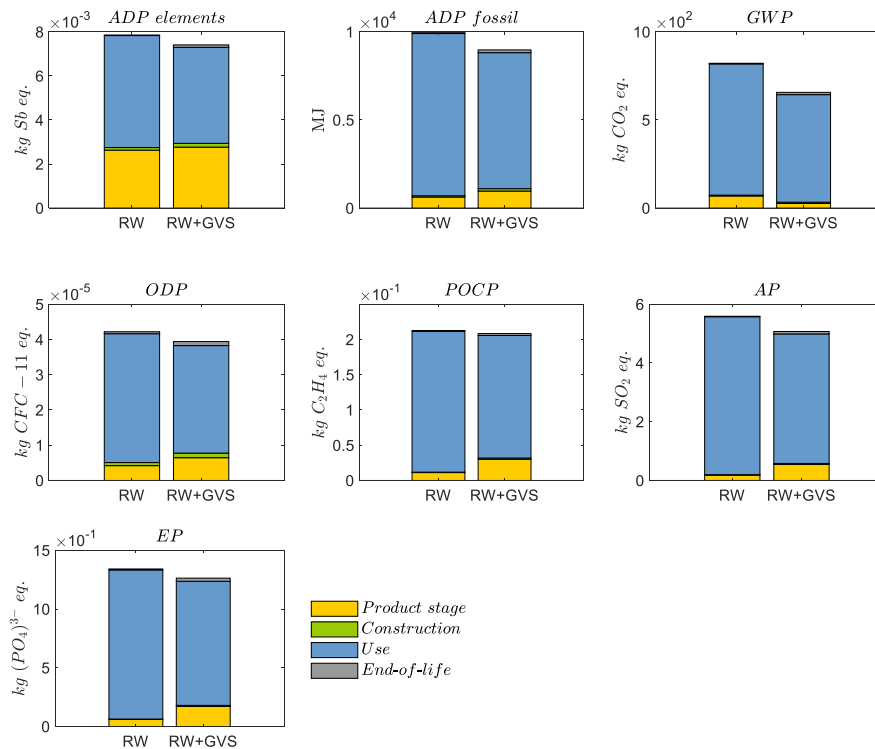


Figure 4.13 - Potential environmental impacts for the entire life cycle for the reference wall (RW) and the wall improved with the new modular living wall (RW+GVS).

The results show that the improved wall containing the new modular living solution has the best environmental performance for all the impact categories assessed, with the differences ranging between 2% for the POCP and 20% for the GWP. In fact, even though the potential environmental impacts increase for all the categories except GWP (due to carbon sequestration) during the product stage with the installation of the new modular living wall, the benefits obtained over time are large and compensate for the environmental burden of adding GVS components to the wall. This indicates that the new cork-based modular living wall can be an eco-friendly choice.

Although not assessed within the LCA, additional benefits (e.g. acoustic insulation, mitigation of urban heat island effect and improvement of the urban biodiversity) are expected to be provided by the new cork based GVS, suggesting that the actual benefits may be even greater.

4.4. Conclusions

In this chapter, the characterization of the performance of the new modular living in real conditions was performed. For this purpose, a prototype was built that consisted of four façades (oriented to north, south, east, and west). Two plant species were selected to be used in the prototype (*Thymus pulegioides* and *Festuca glauca*). The area of façade covered by vegetation and the rate of carbon

sequestration were then monitored for over one year. A cradle-to-grave LCA model based on the characteristics of the prototype and monitoring results, was also carried out to assess the environmental performance of the new modular living wall.

The results showed that although the carbon content is approximately constant (between 44% and 46%) over time for both plant species included in the study, *Festuca glauca* has a much higher amount of biomass than *Thymus pulegioides*, regardless of the façade orientation and season. Consequently, the total carbon uptake provided over one year by *Festuca glauca* (371 gCm⁻²) was much higher than that of *Thymus pulegioides* (68 gCm⁻²), considering the best façade orientation in both cases.

Additionally, the results showed that *Festuca glauca* was able to cover a larger area of the façade during the monitored year, compared with the *Thymus pulegioides*. This was ascribed to the tendency of *Festuca glauca* foliage to hang down as it grows longer. Both plant species perform better in warmer seasons, as expected.

It was also concluded that when assessed from a life cycle perspective the new modular living wall, can be an eco-friendly choice, contributing especially to mitigate global warming. The results showed that the new modular living wall has a negative carbon balance over its life cycle (22.7 kg CO₂eq per square meter). In addition, the benefits of the cork-based solution were shown to offset the environmental burden of installing additional components to the building wall.

References

- [1] European Commission, Towards an EU Research and Innovation policy agenda for Nature-Based Solutions & Re-Naturing Cities. 2015.
- [2] M. Manso and J. Castro-Gomes, “Green wall systems: A review of their characteristics”, *Renewable and Sustainable Energy Reviews*, vol. 41, pp. 863–871, 2015.
- [3] A. Romanova, K. V. Horoshenkov, and A. Hurrell, “An application of a parametric transducer to measure acoustic absorption of a living green wall”, *Applied Acoustics*, vol. 145, pp. 89–97, 2019.
- [4] R. Djedjig, E. Bozonnet, and R. Belarbi, “Modeling green wall interactions with street canyons for building energy simulation in urban context”, *Urban Climate*, vol. 16, pp. 75–85, 2016.
- [5] C. Y. Cheng, K. K. S. Cheung, and L. M. Chu, “Thermal performance of a vegetated cladding system on facade walls”, *Building and Environment*, vol. 45, no. 8, pp. 1779–1787, 2010.

-
- [6] T. Pettit, P. J. Irga, P. Abdo, and F. R. Torpy, “Do the plants in functional green walls contribute to their ability to filter particulate matter?”, *Building and Environment*, vol. 125, pp. 299–307, 2017.
- [7] K. Perini, M. Ottelé, S. Giulini, A. Magliocco, and E. Roccotiello, “Quantification of fine dust deposition on different plant species in a vertical greening system”, *Ecological Engineering*, vol. 100, pp. 268–276, 2017.
- [8] U. Weerakkody, J. W. Dover, P. Mitchell, and K. Reiling, “Particulate matter pollution capture by leaves of seventeen living wall species with special reference to rail-traffic at a metropolitan station”, *Urban Forestry and Urban Greening*, vol. 27, no. July, pp. 173–186, 2017.
- [9] U. Weerakkody, J. W. Dover, P. Mitchell, and K. Reiling, “Quantification of the traffic-generated particulate matter capture by plant species in a living wall and evaluation of the important leaf characteristics”, *Science of the Total Environment*, vol. 635, pp. 1012–1024, 2018.
- [10] U. Weerakkody, J. W. Dover, P. Mitchell, and K. Reiling, “The impact of rainfall in remobilising particulate matter accumulated on leaves of four evergreen species grown on a green screen and a living wall”, *Urban Forestry & Urban Greening*, vol. 35, pp. 21–31, 2018.
- [11] C. Jansson, S. D. Wulschleger, U. C. Kalluri, and G. A. Tuskan, “Phytosequestration: Carbon Biosequestration by Plants and the Prospects of Genetic Engineering”, *BioScience*, vol. 60, no. 9, pp. 685–696, 2010.
- [12] S. M. Zaid, E. Perisamy, H. Hussein, N. E. Myeda, and N. Zainon, “Vertical Greenery System in urban tropical climate and its carbon sequestration potential: A review”, *Ecological Indicators*, vol. 91, no. April, pp. 57–70, 2018.
- [13] K. L. Getter, D. B. Rowe, G. P. Robertson, B. M. Cregg, and J. A. Andresen, “Carbon sequestration potential of extensive green roofs”, *Environmental science & technology*, vol. 43, no. 19, pp. 7564–7570, 2009.
- [14] S. Charoenkit and S. Yiemwattana, “Role of specific plant characteristics on thermal and carbon sequestration properties of living walls in tropical climate”, *Building and Environment*, vol. 115, pp. 67–79, 2017.
- [15] M. Marchi, R. M. Pulselli, N. Marchettini, F. M. Pulselli, and S. Bastianoni, “Carbon dioxide sequestration model of a vertical greenery system”, *Ecological Modelling*, vol. 306, pp. 46–56, 2015.
- [16] M. Ottelé, K. Perini, A. L. A. Fraaij, E. M. Haas, and R. Raiteri, “Comparative life cycle analysis for green façades and living wall systems”, *Energy and Buildings*, vol. 43, pp. 3419–3429, 2011.

- [17] H. Feng and K. Hewage, “Lifecycle assessment of living walls: Air purification and energy performance”, *Journal of Cleaner Production*, vol. 69, pp. 91–99, 2014.
- [18] V. Oquendo-Di Cosola, F. Olivieri, L. Ruiz-García, and J. Bacenetti, “An environmental Life Cycle Assessment of Living Wall Systems”, *Journal of Environmental Management*, vol. 254, p. 109743, 2020.
- [19] A. Cortês, A. Tadeu, M. I. Santos, J. de Brito, and J. Almeida, “Innovative module of expanded cork agglomerate for green vertical systems”, *Building and Environment*, article in Press.
- [20] N. Pargana, M. D. Pinheiro, J. D. Silvestre, and J. de Brito, “Comparative environmental life cycle assessment of thermal insulation materials of buildings”, *Energy and Buildings*, vol. 82, pp. 466–481, 2014.
- [21] J. D. Silvestre, N. Pargana, J. de Brito, M. D. Pinheiro, and V. Durão, “Insulation cork boards-environmental life cycle assessment of an organic construction material”, *Materials*, vol. 9, pp. 1–16, 2016.
- [22] A. Cortês, J. Almeida, J. de Brito, and A. Tadeu, “Water retention and drainage capability of expanded cork agglomerate boards intended for application in green vertical systems”, *Construction and Building Materials*, vol. 224, pp. 439–446, 2019.
- [23] Instituto de meteorologia I.P Portugal, “Ficha Climatológica (1971-2000) Coimbra/Bencanta”.
- [24] “Webertherm flex P - Technical file”, 2018. [Online]. Available: <https://www.pt.weber/revestimento-e-renovacao-de-fachadas/webertherm-flex-p>.
- [25] Atlanlusi Europe, “GeoTexPro - Geotêxtil/Geocompósito”, Ficha Técnica. [Online]. Available: <http://www.atlanlusi.pt/repositorio/projetistas/Bioarquitetura/CoberturasVerdes/FichaTécnica-GeoTexPro.pdf>
- [26] “Siro-roof - Technical file”. [Online]. Available: <https://portal.siro.pt/pt/programs/cindex.aspx>.
- [27] PRé, “SimaPro Database Manual Methods Library”, 4.14.2, 2019.
- [28] R. W. F. Cameron, J. E. Taylor, and M. R. Emmett, “What’s ‘cool’ in the world of green façades? How plant choice influences the cooling properties of green walls”, *Building and Environment*, vol. 73, pp. 198–207, 2014.

-
- [29] M. Manso and J. P. Castro-Gomes, “Thermal analysis of a new modular system for green walls”, *Journal of Building Engineering*, vol. 7, pp. 53–62, 2016.
- [30] L. Pan and L. M. Chu, “Energy saving potential and life cycle environmental impacts of a vertical greenery system in Hong Kong: A case study”, *Building and Environment*, vol. 96, pp. 293–300, 2016.
- [31] M. Manso, J. Castro-Gomes, B. Paulo, I. Bentes, and C. A. Teixeira, “Life cycle analysis of a new modular greening system”, *Science of the Total Environment*, vol. 627, pp. 1146–1153, 2018.
- [32] L. R. Costello and K. S. Jones, “WUCOLS Water use classification of landscape species - A Guide to the Water Needs of Landscape Plants”, 1994.
- [33] Instituto Português do Mar e da Atmosfera I.P., “Boletim meteorológico para a agricultura, No 104, Setembro 2019”.

CHAPTER 5

THE EFFECT OF A CORK-BASED MODULAR LIVING
WALL ON THE ENERGY PERFORMANCE OF
BUILDINGS AND LOCAL MICROCLIMATE

5. The effect of a cork-based modular living wall on the energy performance of buildings and local microclimate

5.1. Introduction

Buildings account for 40% of the energy consumption in Europe and 36% of greenhouse gas emission. Therefore, improving the energy efficiency of buildings is crucial to achieve by 2050 the carbon-neutrality target set by the European Commission [1]. Among several technological proposals, green vertical systems (GVSs) have been recognized as clever solutions to improve thermal insulation of buildings and mitigate the urban heat island effect observed in dense urban territories [2], [3].

The thermal benefits provided by GVSs have been attributed to several heat transfer phenomena, such as those related to the shading and evaporative effects [4]–[6]. The efficiency of the shading effect depends mostly on the foliage thickness and the coverage area provided by the plants. Lee and Jim [7] studied the shading effect of a green façade located in Hong Kong and obtained an average daily energy saving of 0.226 kWh/m². The phenomena that govern the heat transfer are complex and involves several mechanisms. In general terms, plants can reflect and transmit long-wave radiation (about 50% of the solar radiation), absorbing the short-wave radiation in photosynthetic processes. However, the absorptance capacity may vary depending on the water content, plant characteristics, and radiation wavebands [5]. Additionally, plants could also

exchange heat with air by convection and with the substrate by conduction. Heat losses from the plant to the surrounding air could also occur due to transpiration. It was estimated that about 60% of the heat stored in plant leaves can be dissipated, depending on the wind speed, moisture content of the air and plant species [5], [8], [9]. In turn, the surrounding air could further exchange heat by convection with ambient air [10].

Thermal performance of GVSs is also strongly influenced by the characteristics of plants, system design, geographical orientation, local climate conditions, and seasons. The morphology and physiology of plants play an important role on the thermal performance of GVSs. Plants with larger number of leaves, denser foliage, higher leaf area index and smaller leaves have been referred as preferable options to improve the cooling performance of façades [11], [12]. In addition, leaf texture and shape should be considered. Plant leaves with dense hairs and unlobed shape could difficult the transference of heat [12]. A study performed with three different plant species, revealed a reduction of up to 5.7 °C for *Hedera helix* compared with a bare wall exposed to the same conditions [13]. Another study conducted with three different canopy thicknesses (7.2 cm, 19.8 cm and 30.5 cm) of the same plant species (Boston ivy) revealed that the best cooling performance is achieved with an intermediate canopy thickness, suggesting that the thicker canopy was responsible for blocking the air circulation and so the convective heat transfer [14].

Since the design and materials used to build a GVS may strongly influence its final thermal performance, care should be taken in selecting the best solutions. An experimental study compared two completely different systems: a green façade and a living wall. While the first solution makes use of climbing plants that grow attached to a supporting structure, the living wall uses plastic modules filled with substrate where the plants are rooted. The results showed that the living wall could provide an energy saving of 58.9% during the cooling season, while the green façade could only offer 33.8%. Regarding the heating season, only the green wall solution provides energy savings (around 4.2%) [15]. Another experimental study conducted in Hong Kong with two GVSs with an air gap of 1.0 m and 0.3 m between the GVS and the building's façade suggested that a deeper air cavity could help on cooling the building façade [16]. Similar conclusions were found in other study conducted in Malaysia that evaluated two air gap thicknesses (30 cm and 15 cm) [17].

As well known, the radiation that reaches building façades greatly varies according to geographic orientation. A study performed under the Mediterranean continental climate compared south-, east- and west-oriented GVSs, concluding that all of them are able to reduce more than 15 °C the maximum surface temperature, but at different times of the day [18]. Other authors also compared the thermal performance of south- and west-oriented GVSs located in the city of Madrid, concluding that the maximum temperature variation occurred for the south-oriented wall both in summer and winter [19]. A study performed in China, during winter, also indicated that a north-oriented GVS is a suitable choice for buildings mainly occupied during the day time or the entire

day, while both north- and south-facing GVSs are good options for buildings with mainly night-time occupancy [20].

Another dynamic variable that governs the thermal performance of GVSs is related with the seasons of the year. Several studies in the literature highlight the benefits provided by GVSs in the cooling season. For example, an experimental study conducted in Shanghai reported indoor air temperature reductions of 1.2 °C with an indirect green façade oriented to the south [21]. Another study performed in the Mediterranean climate, evidenced a reduction of 26% in the energy cooling needs during the summer season [22]. Other authors studying a prototype located in Portugal were able to minimize 75% and maximize 60% the income and outgoing heat flux, respectively [23]. Another experimental study conducted over two years in Italy found that, during warm days, the temperatures of a wall covered with the GVS were lower than the bare walls up to 9 °C while during cold days the night temperatures of the wall covered with the GVS were high than the bare walls up to 3.5 °C [24].

The ability of GVSs to reduce the surrounding air temperatures, helping to mitigate the urban heat island effect, has also been reported. An experimental study conducted with two GVSs in Singapore measured the mean radiant temperature and found out that for the situation with only one GVS, the peak temperature was 10.9 to 12.9 °C at 0.5 m away from the wall higher when compared with the situation with both GVSs present [25]. Another study performed in Spain found that the GVS could reduce air temperatures between 2.5 °C and 2.9 °C during the summer period [3]. A study performed using a model with six idealized urban blocks and 30 different scenarios also found cooling effects with high-rise and high-density sites [26].

In this chapter the effect of a new modular living wall on the energy performance of buildings and local microclimate was evaluated. This system, already described in chapter 3 [27], is made of insulation cork boards (ICB) commonly used in thermal and acoustic insulation of buildings. The hygrothermal performance of ICB when applied as an external coating solution was already assessed, showing that the insulation capacity of ICB was not highly affected by the water content [28], [29]. The ability of ICB to retain water, contributing to reduce the irrigation needs, was also previously demonstrated [30]. Regarding the modules of ICB, they were fixed to the bearing wall with an appropriated mortar (permeable to vapour but impermeable to water), covered with a geotextile felt, and then filled with a technical substrate where the plants will be rooted.

A prototype of this new cork-based solution composed of four façades with 8m² each (oriented to north, south, east, and west) was built and properly instrumented to measure temperatures across the system and in the vicinity of it. Two plant species (*Thymus pulegioides* and *Festuca glauca*) with distinct characteristics were selected to be used. Temperature data were collected over a year to allow the assessment of its performance under the different seasons. For comparison purposes,

two walls containing an external thermal insulation composite system (ETICS) were also monitored.

The characteristics of the prototype, including thermocouple positioning and data acquisition system, are detailed in the next section. The recorded temperatures are further discussed, firstly in terms of geographical orientations, plant species and seasons, and then in terms of evaporative effects. The results are further compared with those recorded in the reference walls with ETICS. Finally, real climatic data were used to update a model in the Design-builder and the results obtained discussed in terms of energy savings. The main conclusions are summarized at the end.

5.2. Methodology

In this chapter, it was intended to evaluate the thermal behaviour of the new modular living wall under real conditions. For this purpose, a prototype consisting of two walls (2.0 m high and 4.0 m wide) containing four façades oriented to north, south, east, and west were installed in Coimbra, in the centre region of Portugal.

The cork modules were designed to create a trough 100 mm wide with side walls 50 mm thick, where the plants and the growing medium are placed. A continuous insulation layer 50 mm thick is provided to the bearing wall. The cork modules were fixed to bearing walls by an adhesive mortar commercially available [31]. A geotextile felt [32] was then used to protect the cork trough by preventing fine particles to be washed out. The troughs were then filled with a technical lightweight substrate where the vegetation was rooted. A drip irrigation line with a water flow of $8.5 \text{ l}\cdot\text{h}^{-1}\cdot\text{m}^{-2}$ was installed in each through to guarantee an adequate supply of water for irrigation. Note that no watering was supplied during the winter, while in the summer the system was watered at night (10 pm) for 15 min, every day. A schematic cross-section of the cork-based module is presented in Figure 5.1.

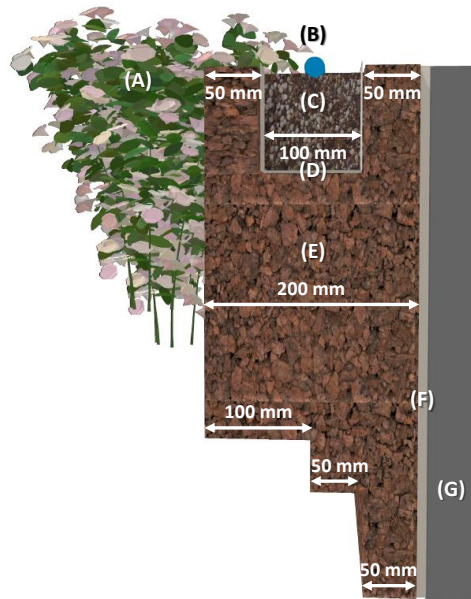


Figure 5.1 - Schematic representation of the cork-based module: (A) Plants; (B) Drip irrigation lines; (C) Technical substrate; (D) Geotextile filter; (E) Cork-based modules; (F) Adhesive mortar; (G) Bearing wall.

To study the influence of vegetation on the thermal performance of the system, each façade was divided horizontally in half, planting in one part *Thymus pulegioides* (Figure 5.2a) and in the other *Festuca glauca* (Figure 5.2b). These plants are perennial species and were carefully selected to meet some important requirements, namely lower irrigation needs and lower development of the radicular system. Each façade was instrumented with 10 thermocouples (divided in equal parts by the *Thymus pulegioides* and *Festuca glauca* areas) to measure temperatures across the system, and 3 additional thermocouples positioned in the façade and in front of it to measure the surface and air temperatures in the vicinity of the system.



Figure 5.2 - Plant species used: a) *Thymus pulegioides*; b) *Festuca glauca*.

As illustrated in Figure 5.3, thermocouples T1, T2, and T3 were placed at the interface between the ICB and the mortar layer at different heights of the module. The thermocouple T4 was located at the bottom of the trough (below the geotextile). The thermocouples T5 and T6 were located on the external surface of the ICB in the external and internal parts of the module, respectively. Finally,

the thermocouples T7 and T8 were placed in the air at the same height, but horizontally displaced 42 cm and 56 cm from the thermocouple T6, respectively. All thermocouples were connected to a datalogger, recording temperatures every 30 min. Data regarding air temperature, relative humidity, wind direction and speed, and solar radiation were also gathered with a meteorological station.

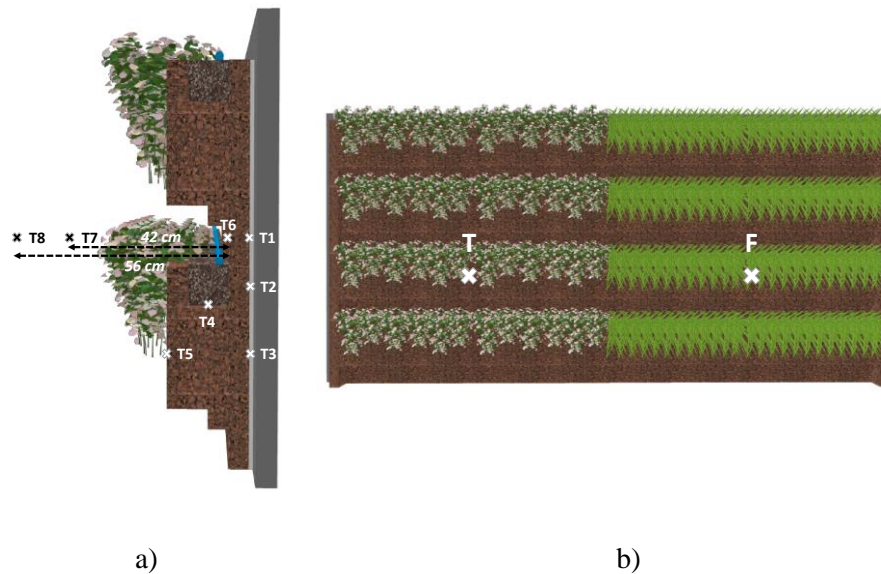


Figure 5.3 - Schematic representation of the thermocouples positions: a) Cross-section view b) Longitudinal view: T – *Thymus pulegioides* area and F – *Festuca glauca* area.

As mentioned above, the monitoring campaign was conducted over one year to study the performance of system in both winter and summer conditions. Additionally, to evaluate the cooling benefits provided by evaporative effects in summer, the outer surface of the ICB layer was sprayed with water (28°C) for 5 minutes when the ambient temperatures were above 30°C. A line of three sprinklers with a flow rate of 5.8 l/min was used.

For comparison purposes, two additional walls covered on both sides with a conventional ETICS solution (containing an insulation layer of ICB 80 mm thick) were used. One of the walls was painted in white, representing a higher reflective solution, and the other in black, representing a higher absorptive solution, expected to approach better the ICB colour. Both walls contain façades north- and south-oriented. Two thermocouples were installed in each façade, one in the external surface and the other at the interface between the support and the insulation layer (TR_w and TR_B , for white and black wall, respectively).

Finally, to evaluate the impact of the new cork-based living wall on the energy savings, a reference building was dynamically simulated using the Design-Builder software (version 4.7.0.027). For this, a reference building representing the detached houses built between 1991 and 2012 in Portugal was used. The geometric and thermal characteristics were established based on the database Energy Certification System, provided by the Portuguese National Agency for Energy (ADENE). The

building, a 3-bedroom single-family dwelling with a floor area of 155 m², consists of two floors with four façades oriented to north, south, east, and west, a rooftop and a sanitary gap. Each facade has a glass area of 7.75 m². The outer walls are made of double masonry of perforated brick (11 cm + 11 cm), with a 3 cm air layer completely filled with thermal insulation (XPS), plastered on both sides, with a thickness of 3 cm. An increase of 35% in the thermal transmittance value (U-value [W/(m².°C)]) of the walls was considered to take into account the structural thermal bridges, obtaining an U = 0.87 W/(m².°C). The U- value for the roof and floors are 0.94 and 0.78 [W/(m² C)], respectively. The glazed openings are sliding, with aluminum frames without thermal break with double current glass, with a solar factor of 0.75 and U = 3.1 W/(m².°C). Light-colored blinds from outside were considered. For the simulations a climatic file for the city of Coimbra created in the SCE.CLIMA V.1.0 was used [33] for an altitude of 59 m. Only the simulation results obtained for the 1st floor of the building are presented in this work, once this is the floor with greater energy losses in winter and with summer majors energy gains. To evaluate the impact of the ICB external coating provided by the living wall solution in the building thermal behavior, the outer walls of the building were covered with ICB boards of 50 mm and 200 mm thickness. As the thermal insulation is continuous, the U value of the constructive solutions is no longer increased by 35%. To simulate the impact of the water on the building thermal behaviour, due to both rainwater and irrigation, simulations were also performed with ICB in wet state, i.e. defining $\lambda=0.047$ W/(m.K). To simulate the expected evaporative effect [3], a climatic file (CF-2), based on the climatic file generated for the city of Coimbra, in which the air temperatures were reduced 2.0°C whenever the outdoor air temperature was higher than 22 °C during the daytime was further created.

5.3. Results

Firstly, the temperatures gathered from the prototype for three representative days of winter and summer are presented and discussed in terms of geographical orientation and plant species. Additionally, the temperatures collected in summer with and without water spraying are analysed. The results are further compared with those of a set of two reference walls with ETICS. Finally, to evaluate the impact of the new cork-based living wall on the energy savings, a reference building was dynamically simulated using the Design-builder and the results obtained discussed in terms of energy savings.

5.3.1. Temperature profiles

The temperatures registered in the thermocouples T1 to T5 in three typical days of winter for each orientation and plant species (*Thymus pulegioides* and *Festuca glauca*) are represented in Figure 5.4.

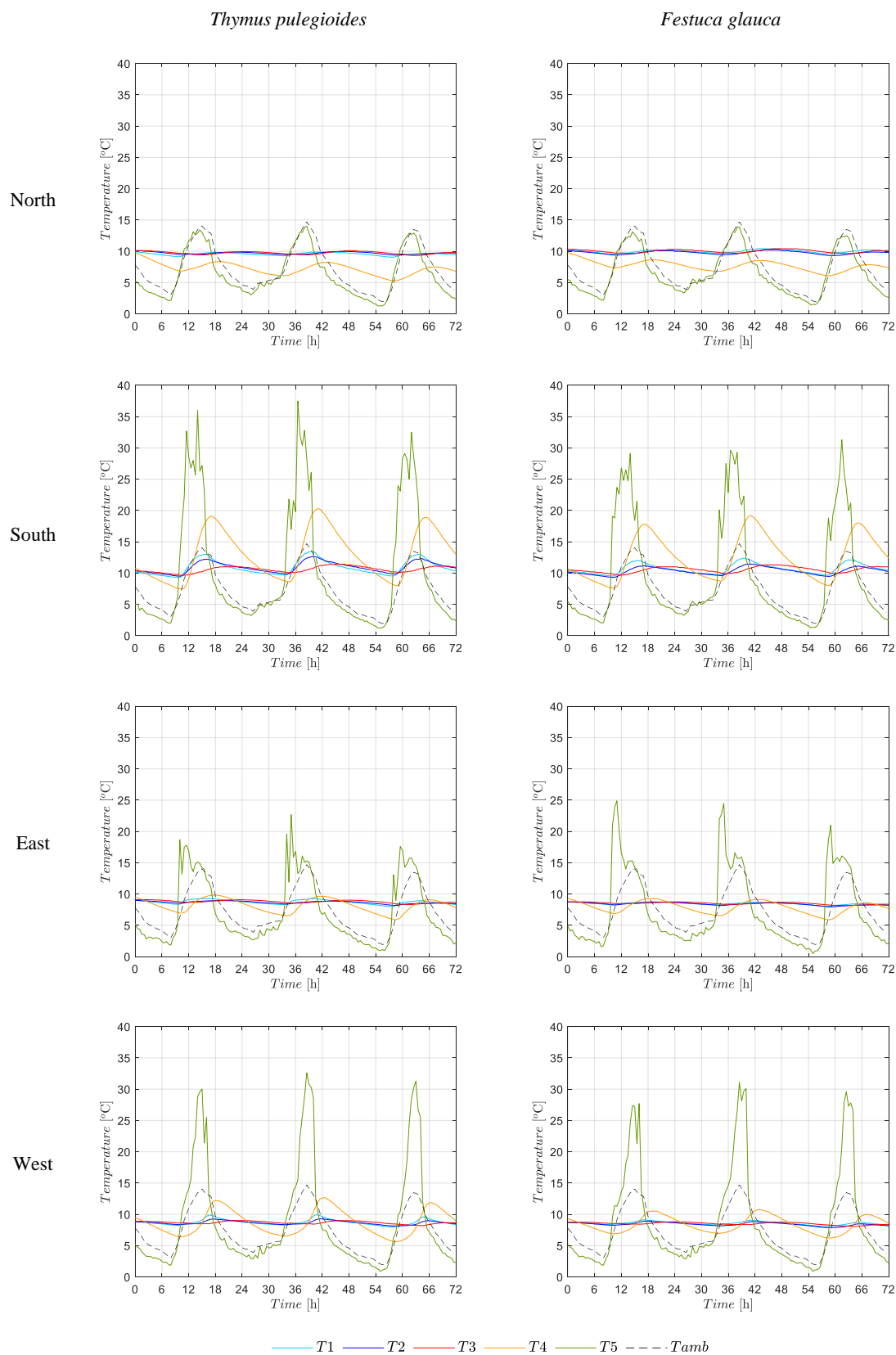


Figure 5.4 - Temperatures recorded during three consecutive days representative of winter season (January 2020).

The average maximum and minimum ambient temperatures recorded in these three days are 14.1 °C and 3.0 °C, respectively. Table 5.1 presents the average maximum and minimum temperatures obtained for each thermocouple for the same period of time.

Table 5.1 - Average maximum and minimum temperatures recorded during three consecutive days in January 2020

Orientation		<i>Thymus pulegioides</i>					<i>Festuca glauca</i>				
		T1	T2	T3	T4	T5	T1	T2	T3	T4	T5
North	Max	9.8	10.0	10.1	8.0	13.4	10.3	10.1	10.4	8.4	13.2
	Min	9.2	9.4	9.4	6.1	2.1	9.6	9.4	9.7	6.7	2.3
South	Max	13.1	12.4	11.3	19.4	35.3	12.2	11.2	11.2	18.3	30.0
	Min	9.5	9.7	10.0	8.0	2.1	9.6	9.5	9.8	8.1	2.2
East	Max	9.2	8.9	9.1	9.5	19.7	8.7	8.6	8.7	9.0	23.5
	Min	8.2	8.4	8.5	6.5	1.8	8.2	8.1	8.3	6.5	1.5
West	Max	9.8	9.2	9.0	12.3	31.3	9.0	8.8	8.8	10.4	29.5
	Min	8.2	8.3	8.4	6.2	1.9	8.3	8.1	8.3	6.7	1.9

As expected, higher temperatures are recorded during daytime in façades south- and west-oriented as a result of direct solar radiation in the warmer hours of the day. For the east façade, it is yet possible to observe that maximum surface temperatures are higher in the first hours of the day, when this facade receives direct solar radiation. See, for example, temperatures recorded by the thermocouple T5 and T4 located on the outer surface of the ICB modules and at half depth at the bottom of the through, respectively. Maximum surface temperatures are registered in the west and south façades (up to 22.8°C higher than the maximum ambient temperature). Differences of temperature in the outer surface between the north and south façades can reach 23.6°C. As might be expected, a significant thermal delay is further observed in temperatures recorded at half depth of the ICB by the thermocouple T4 for all geographical orientations (reaching 4h in the north and 2h in the south façades).

Regarding the thermocouples located behind the ICB layer (T1, T2 and T3), higher maximum temperatures are systematically observed for the south-oriented façade, that receives higher direct solar radiation, in comparison to the other orientations (differences up to 4°C are found). Comparing now the temperatures recorded by the thermocouples T1, T2 and T3, no significant differences are found for the north, east and west façades. In contrast, small variations are observed for the south façade. In this case, higher temperatures are observed in the thermocouple T1 (where the ICB is thinner), with differences for the remaining two thermocouples that can reach 2.8°C.

Inspecting now the influence of the plant species, small differences were found between the temperature profiles of both systems, with *Festuca glauca* contributing to a more significant

decrease of the surface temperatures in the south- and west-oriented façades directed exposed to solar radiation. Note, however, that plants are less vigorous in winter, which means that fewer leaves are covering the façade. It is thus likely that temperature profile in this season be mainly governed by the ICB layer.

Following the same approach, the temperature profiles obtained in three representative days of summer are presented in Figure 5.5.

The average maximum and minimum ambient temperatures recorded in these three days of summer is 30.3 °C and 19.3 °C, respectively. Table 5.2 presents the average maximum and minimum temperatures obtained for each thermocouple for the same period of time.

Once again, as expected, higher temperatures are recorded in the south and west orientations. In this case, the maximum surface temperatures were registered for the west-and south-oriented façades (up to 17.5°C higher than the maximum ambient temperature). Note, however, that this difference is lower than that obtained in winter conditions, which may be attributed to the more vigorous vegetation that are responsible for shading and evapotranspiration effects. Differences of temperature in the outer surface between the north and south façades can reach 14.3 °C. Again, these differences are lower than those obtained for winter. As in winter, a thermal delay is also possible to observe in the temperatures recorded with the thermocouple T4 (reaching 5 h 30 min in the north and 4 h 30 min in the south façades). Note that the ICB and substrate are expected to have lower thermal conductivities due to lower water contents.

Temperatures behind the ICB layer (given by the thermocouples T1, T2 and T3) do not vary much as a consequence of the different geographical orientations. Additionally, very small variations are found between the three thermocouples when applied in the same façade, suggesting that the decrease of insulation due to the smaller ICB thickness in T1 (50 mm) and T2 (100 mm), comparing with T3 (200 mm), is compensated by the presence of substrate and vegetation.

Once more, differences were found between the temperature profiles of both plants, with *Festuca glauca* contributing again to a more significant decrease of the surface temperatures in the south- and west-oriented façades. This is likely to occur because of the higher pending morphology of this plant, which covers a larger area of the façade.

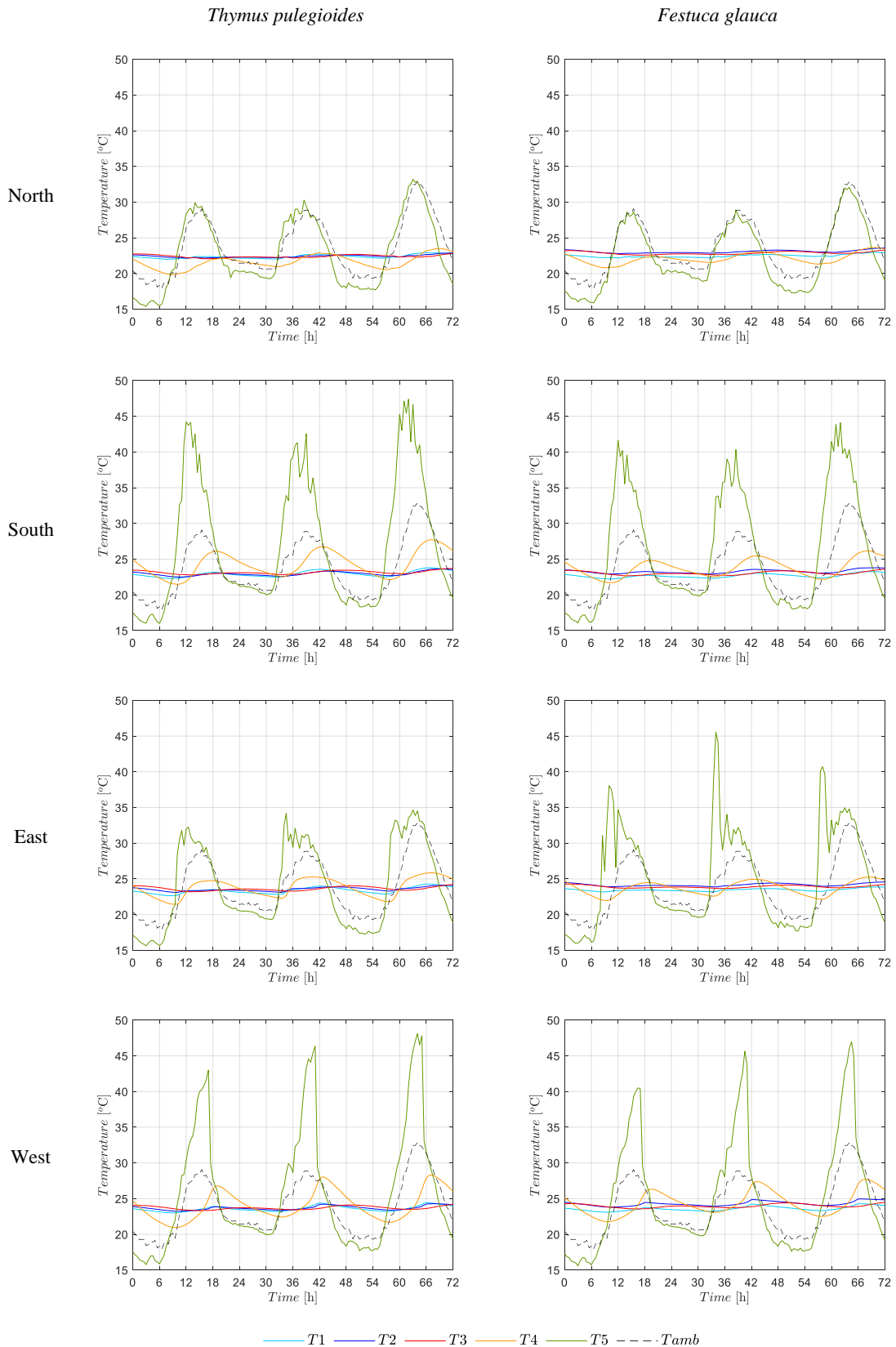


Figure 5.5 - Temperatures recorded during three consecutive days representative of summer season (July 2020).

Table 5.2 - Average maximum and minimum temperatures recorded during three consecutive days in July 2020

Orientation		<i>Thymus pulegioides</i>					<i>Festuca glauca</i>				
		T1	T2	T3	T4	T5	T1	T2	T3	T4	T5
North	Max	22.7	22.7	22.7	22.8	31.1	22.7	23.4	23.2	23.0	29.9
	Min	22.1	22.2	22.2	20.5	17.1	22.3	22.9	22.7	21.2	17.3
South	Max	23.5	23.4	23.5	26.9	44.7	23.0	23.6	23.4	25.5	42.0
	Min	22.4	22.6	22.9	22.1	17.8	22.3	22.9	22.7	22.1	17.6
East	Max	23.9	23.9	24.1	25.3	33.7	23.7	24.5	24.2	24.9	41.4
	Min	22.8	23.2	23.3	21.8	17.1	23.2	23.9	23.7	22.2	17.5
West	Max	24.2	24.1	24.1	27.7	45.8	24.1	24.8	24.4	27.1	44.4
	Min	23.1	23.3	23.4	21.7	17.4	23.2	23.9	23.7	22.4	17.3

5.3.2. Microclimate effect

Beyond the previous described effects, the new modular living wall is also expected to slightly decrease the air temperature in the vicinity of the façade, contributing to mitigate the urban heat island effect if applied in large scale. Normally, this is due to the shading and evapotranspiration processes provided by the presence of plants in the façade. However, in this case, since ICB has the ability to retain liquid water and release it in vapour form over time, the evaporative effect may be enhanced by watering the ICB layer.

To get an insight of this effect, two consecutive summer days with temperatures above 30°C were selected. On the first day, the external layer of cork modules was kept dry. On the second day, near to the highest ambient temperature of the day, water (T=28°C) was sprayed to the façade, moistening the outer surface of ICB layer. Four thermocouples located on the external surface of the ICB in the external and internal parts of the module (T5 and T6) and in front of the façade at two different distances (T7 and T8) were used to assess the temperatures in the vicinity of the system (positioning of the thermocouples is detailed in Figure 5.3).

The temperature profile obtained in the first day, when no watering was provided to the ICB layer, is represented in Figure 5.6. For simplicity, only the results obtained in the north and south orientations are presented, since they correspond to the most distinct cases. Additionally, discussion is made only for *Festuca glauca*, since no significant differences were found between the two plant species.

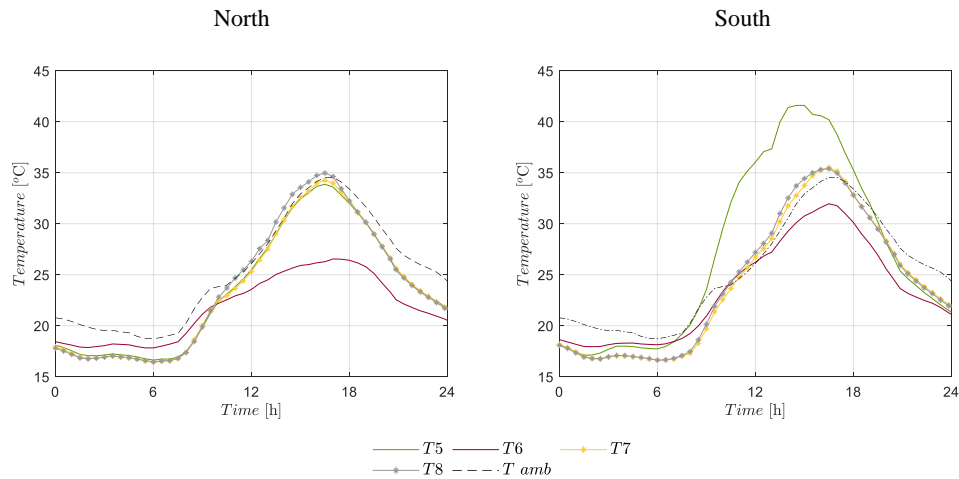


Figure 5.6 - Temperatures recorded in a summer day, when the outer surface of the ICB layer was kept dry.

Based on the results of the north-facing system, it is possible to observe that the thermocouple located on the surface of the ICB behind the plants (T6) presents a maximum temperature 9°C lower than the ambient temperature. In turn, the temperatures registered in the thermocouples positioned on the surface of ICB (T5) and in front of the façade (T7 and T8) are not distinct from the ambient temperature. Observing now the south-oriented façade, a smaller decrease of the maximum temperature is observed in T6 (about 3°C) and the maximum temperatures of T7 and T8 are slightly higher than the ambient temperature. A maximum temperature 7°C higher than the ambient temperature was also recorded for T5.

The temperature profile obtained for the second day, when the outer surface of the ICB layer was sprayed with water, is now represented in Figure 5.7.

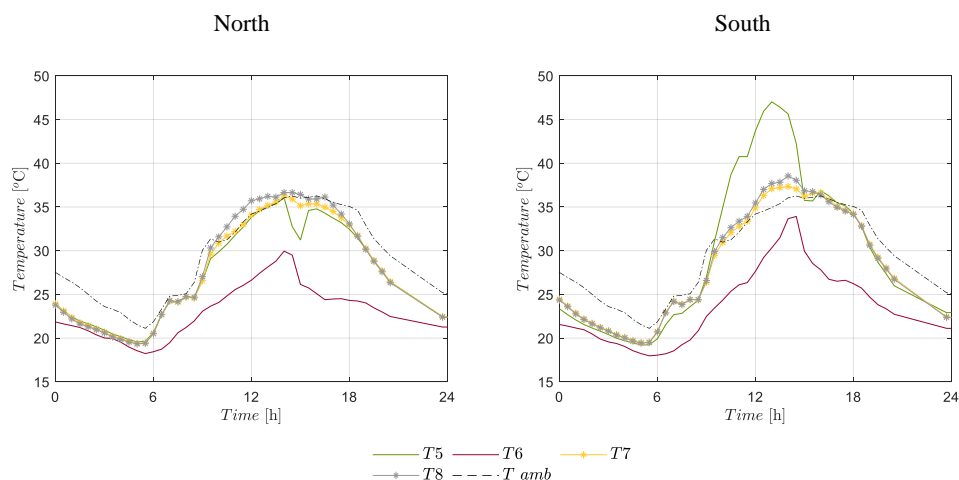


Figure 5.7 - Temperatures recorded in a summer day with, when the outer surface of the ICB layer was sprayed with water.

Now, immediately after water spraying, a decrease of 5°C was observed in the north façade at T5, probably due to the presence of a film of water in the outer surface of the ICB layer. However, after

drying, a lower temperature in T5 is still visible, when compared with the ambient temperature. Regarding the thermocouple T6, a sharp decrease of 3°C was also recorded immediately after watering. In contrast, very slightly variations of temperature were observed for the thermocouples T7 and T8. A similar behaviour is observed for the south façade. In this case, a drop of 11°C and 4°C is observed at T5 and T6, respectively. However, for this orientation, the maximum temperatures of T7 and T8 suffer a quite perceptible decrease of temperature of about 2°C.

Note, as it will be detailed in the next subsection, that the drop of temperature in the vicinity of the façade is expected to be even higher when comparing these temperatures with those of a reference wall without any vegetation. A similar effect was reported by other authors for an identical climate [3].

5.3.3. Comparison with an ETICS insulated wall

Two walls oriented to north and south, containing a conventional ETICS solution made of ICB (80 mm), were used to compare the thermal performance of the new living wall system. As stated before, one of the walls was painted in white (TR_w) and the other in black (TR_B).

The surface temperatures obtained for the same three days of summer previously analysed are now presented (Figure 5.8).

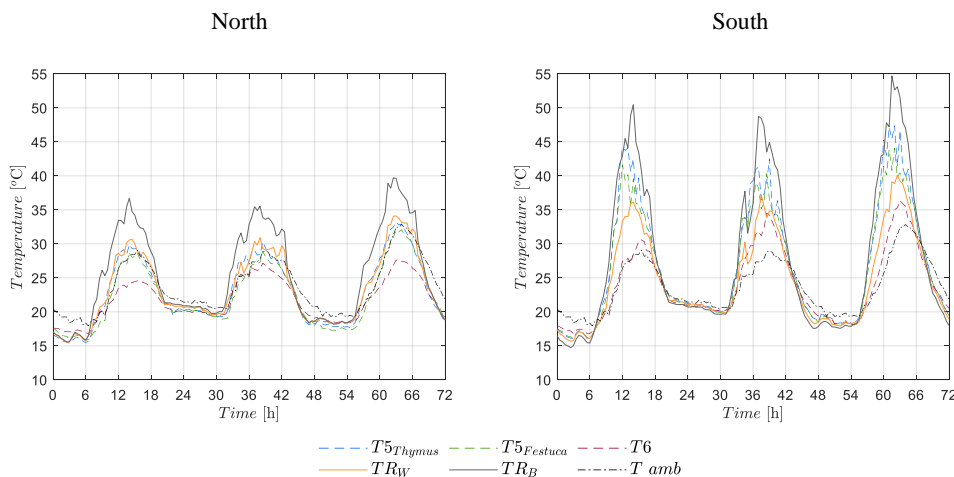


Figure 5.8 - Surface temperatures of the modular living walls and of the reference walls with ETICS (summer).

For the north-oriented façades, the surface temperatures of the living wall are quite similar to those recorded on the white reference wall, but significantly lower (up to 8°C) than those recorded on the black reference wall. Surface temperatures even lower were recorded for the living wall oriented to the south, when compared to the corresponding black reference wall (up to 11°C). In contrast,

higher surface temperatures were registered in the living wall than in the reference wall painted in white.

Analysing now the surface temperatures in the groove where the plants are rooted and the ICB is thinner (T6), one can find much lower values. Thus, for the north façade, temperatures 6.5°C and 12.2°C lower than those obtained respectively on the surface of the white and black walls were achieved. In turn, for the south façade, differences of 5.6°C and 19.9°C were found when comparing T6 with the surface temperatures of the white and black walls, respectively.

When comparing these results with those obtained when the outer surface of the ICB layer was sprayed with water (Figure 5.9), an enhanced cooling effect is achieved.

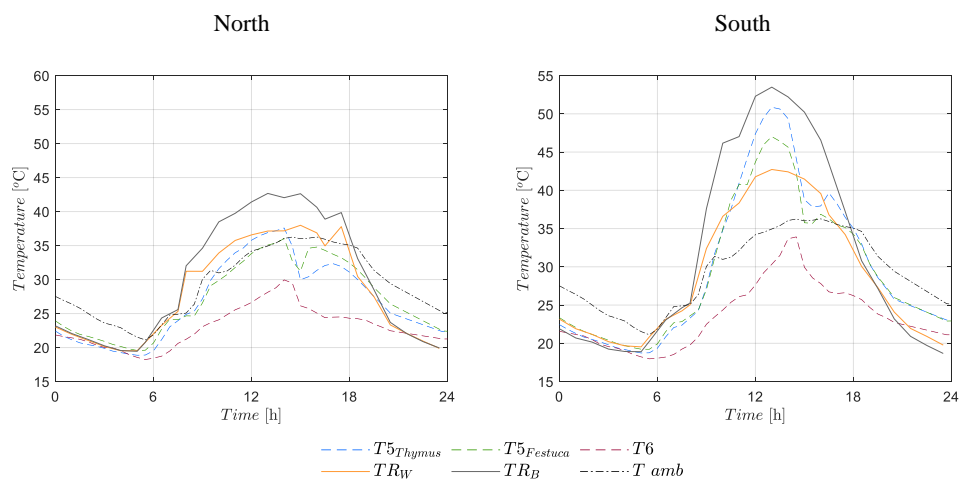


Figure 5.9 - Surface temperatures of the modular living walls, when the outer surface of the ICB layer was sprayed with water, and of the reference walls with ETICS (summer).

Thus, after spraying the ICB layer with water, a sharp drop was observed in the surface temperatures of the living wall oriented to north (up to 8°C and 13°C lower than those measured on the white and black reference façades, respectively). A similar behaviour was obtained for the south façade. In this case, the surface temperatures of the living wall were up to 6°C and 14°C lower than those measured on the white and black reference façades, respectively.

Once again, the surface temperatures in the groove are lower than those registered on the surface of the white and black reference walls. For the north façade, temperatures 11.8°C and 16.5°C lower than those obtained on the surface of the white and black walls, respectively, were measured. For the south façade, differences of 11.5°C and 20.3°C were found when comparing the same thermocouples. The strong drop of temperatures in these grooved areas are expected to contribute to a major cooling effect of the building.

Additionally, when inspecting the temperatures at the interface between the insulation layer and the support, both the white and black reference walls oriented to the south present higher temperatures than those obtained in the modular living wall (up to 4°C and 7°C for the white and black reference walls, respectively), suggesting a good thermal performance of the living wall. Note that the cork-based ETICS 80 mm thick are considered good solutions in terms of buildings insulation.

5.3.4. Simulation of energy savings

As mentioned above, to evaluate the impact of the new cork-based living wall on the energy savings, simulations were performed for a reference building using the Design-Builder package. The obtained results are presented in Table 5.3.

Table 5.3 - Heating and cooling needs for a reference building and a modified building containing ICB boards of 50 mm and 200 mm thickness covering the outer walls

Unit	Heating needs	Cooling needs	Δ Heating needs		Δ Cooling needs	
	[kWh]	[kWh]	[kWh]	[%]	[kWh]	[%]
Reference building (RB)	1129	1949	-	-	-	-
RB + 50 mm ICB ($\lambda=0.041$ W/m°C)	762	1897	-366	-32%	-52	-3%
RB + 50 mm ICB ($\lambda=0.047$ W/m°C); CF (-2°C)	784	1183	-345	-31%	-766	-39%
RB + 200 mm ICB ($\lambda=0.041$ W/m°C)	589	1923	-539	-48%	-26	-1%
RB + 200 mm ICB ($\lambda=0.047$ W/m°C); CF (-2°C)	618	1252	-511	-45%	-698	-36%

It can be seen that the reference building presents significant heating (Hneeds) and cooling (Cneeds) needs, with Cneeds significantly higher than the Hneeds. When applying an external coating of 50 mm of ICB, considering the thermal conductivity of the ICB in the reference conditions, the Hneeds reduce significantly (32%), while the Cneeds show a residual decrease (3%). However, when considering the ICB in wet conditions and the climate file CF-2, for the same thickness, the reduction in Cneeds becomes significant, suffering a 39% decrease in relation to the Cneeds of the reference solution.

The solution under development is intended to reduce the energy needs in the cooling season, but at the same time behaves as an external thermal insulation, in the heating season. It is therefore essential that the ICB in wet conditions does not significantly increase heating needs. According to the results, the heating needs for CF-2, in which the 50 mm of ICB is considered to be permanently wet ($\lambda = 0.047$ W/m°C), slightly increase in relation to the solution with 50 mm of ICB in the

reference condition ($\lambda = 0.041 \text{ W/m}^{\circ}\text{C}$). Note that the most unfavourable situation was considered, once the ICB will be wet during only the rain periods. It is thus expected that, for a real situation, this increase in heating needs is actually less than the value obtained in the simulations.

For 200 mm thick ICB, the conclusions are in all similar, varying only in magnitude. Thus, the heating needs decrease 48% in relation to the reference building. With regard to cooling needs, they show a slight increase as the insulation thickness increase, assuming a value -1%. Comparing the results obtained for ICB in wet conditions and CF-2, it appears that the heating needs decreases, now, with an increase of ICB thickness, but not significantly. For the cooling situation, it appears that the increase in the thickness of the ICB induces a slight increase in cooling needs, as would be expected, due to the greater difficulty of the building losing heat.

From the results presented, it can be concluded that the solution under development has good thermal behaviour in the heating season and, with regard to the cooling station, the proposed solution allows to significantly reduce the building cooling needs.

5.4. Conclusions

The effect of a new cork-based living wall on the energy performance of buildings and local microclimate was evaluated in this chapter. For this purpose, a prototype containing four façades (directed to the north, south, east and west) and two plant species (*Thymus pulegioides* and *Festuca glauca*) was installed in Coimbra, Portugal. Temperatures across each living wall façade and in the vicinity of them were measured over one year. Two additional walls containing a conventional ETICS were used for comparison purposes. Real climatic data were eventually used to update a building model, discussing the results in terms of energy savings.

Although significantly different surface temperatures were measured in the façades facing different orientations, temperatures behind the ICB layer did not vary much, suggesting that the living wall performs well in terms of thermal insulation. Additionally, in the south- and west-oriented façades, which receive higher direct solar radiation, *Festuca glauca* leads to lower surface temperatures than *Thymus pulegioides*, which is likely to be related with the pending morphology of the former plant species.

When inspecting the surface temperatures in the grooves, behind the plants, lower values than those registered on the surface of the white and black reference walls are attained. Differences up to 20°C

were found, for example, when comparing temperatures for the south-oriented façades. Additionally, very small variations are found in the thermocouples located at different heights behind the ICB layer, suggesting that the decrease of insulation in the groove is compensated by the shading and evaporative effects. Results have also shown that the evaporative effects may be enhanced by water spaying the ICB layer.

Simulations carried out against a reference building resorting to Design Builder have further shown lower heating and cooling needs when an external coating of ICB is applied to the reference building, even with the lower thickness ICB (50 mm) in wet conditions. According to this model, the heating and cooling needs decrease 31% and 39%, respectively, when 50 mm thick ICB is added to the reference building, wet conditions are considered and evaporative effects of the system were taken into account.

References

- [1] European Commission, “Energy efficiency in buildings”, Department: Energy – In focus, no. February, 2020.
- [2] European Commission, Towards an EU Research and Innovation policy agenda for Nature-Based Solutions & Re-Naturing Cities. 2015.
- [3] M. P. de Jesus, J. M. Lourenço, R. M. Arce, and M. Macias, “Green façades and in situ measurements of outdoor building thermal behaviour”, *Building and Environment*, vol. 119, pp. 11–19, 2017.
- [4] B. Raji, M. J. Tenpierik, and A. Van Den Dobbelen, “The impact of greening systems on building energy performance: A literature review”, *Renewable and Sustainable Energy Reviews*, vol. 45, pp. 610–623, 2015.
- [5] S. Charoenkit and S. Yiemwattana, “Living walls and their contribution to improved thermal comfort and carbon emission reduction: A review”, *Building and Environment*, vol. 105, pp. 82–94, 2016.
- [6] T. Safikhani, A. M. Abdullah, D. R. Ossen, and M. Baharvand, “A review of energy characteristic of vertical greenery systems”, *Renewable and Sustainable Energy Reviews*, vol. 40, pp. 450–462, 2014.

-
- [7] L. S. H. Lee and C. Y. Jim, “Energy benefits of green-wall shading based on novel-accurate apportionment of short-wave radiation components”, *Applied Energy*, vol. 238, pp. 1506–1518, 2019.
- [8] I. Susorova, M. Angulo, P. Bahrami, and Brent Stephens, “A model of vegetated exterior facades for evaluation of wall thermal performance”, *Building and Environment*, vol. 67, pp. 1–13, 2013.
- [9] L. Malys, M. Musy, and C. Inard, “A hydrothermal model to assess the impact of green walls on urban microclimate and building energy consumption”, *Building and Environment*, vol. 73, pp. 187–197, 2014.
- [10] L. Škerget, A. Tadeu, and C. A. Brebbia, “Transient numerical simulation of coupled heat and moisture flow through a green roof”, *Engineering Analysis with Boundary Elements*, 2018. [Online]. Available: <https://www.dgeg.gov.pt/pt/areas-setoriais/energia/energias-renovaveis-e-sustentabilidade/sce-er/>.
- [11] R. W. F. Cameron, J. E. Taylor, and M. R. Emmett, “What’s ‘cool’ in the world of green façades? How plant choice influences the cooling properties of green walls”, *Building and Environment*, vol. 73, pp. 198–207, 2014.
- [12] S. Charoenkit and S. Yiemwattana, “Role of specific plant characteristics on thermal and carbon sequestration properties of living walls in tropical climate”, *Building and Environment*, vol. 115, pp. 67–79, 2017.
- [13] F. Thomsit-Ireland, E. A. Essah, P. Hadley, and T. Blanuša, “The impact of green facades and vegetative cover on the temperature and relative humidity within model buildings”, *Building and Environment*, vol. 181, no. July, 2020.
- [14] C. Li, J. Wei, and C. Li, “Influence of foliage thickness on thermal performance of green façades in hot and humid climate”, *Energy and Buildings*, vol. 199, pp. 72–87, 2019.
- [15] J. Coma, G. Pérez, A. de Gracia, S. Burés, M. Urrestarazu, and L. F. Cabeza, “Vertical greenery systems for energy savings in buildings: A comparative study between green walls and green facades”, *Building and Environment*, vol. 111, pp. 228–237, 2017.
- [16] L. S. H. Lee and C. Y. Jim, “Subtropical summer thermal effects of wirerope climber green walls with different air-gap depths”, *Building and Environment*, vol. 126, pp. 1–12, 2017.
- [17] T. Safikhani and M. Baharvand, “Evaluating the effective distance between living walls and wall surfaces”, *Energy and Buildings*, vol. 150, pp. 498–506, 2017.

- [18] G. Pérez, J. Coma, S. Sol, and L. F. Cabeza, “Green facade for energy savings in buildings: The influence of leaf area index and facade orientation on the shadow effect”, *Applied Energy*, vol. 187, pp. 424–437, 2017.
- [19] R. Sendra-Arranz, V. Oquendo, L. Olivieri, F. Olivieri, C. Bedoya, and A. Gutiérrez, “Monitorization and statistical analysis of south and west green walls in a retrofitted building in Madrid”, *Building and Environment*, vol. 183, no. March, 2020.
- [20] X. Nan, H. Yan, R. Wu, Y. Shi, and Z. Bao, “Assessing the thermal performance of living wall systems in wet and cold climates during the winter”, *Energy and Buildings*, vol. 208, p. 109680, 2020.
- [21] F. Yang, F. Yuan, F. Qian, Z. Zhuang, and J. Yao, “Summertime thermal and energy performance of a double-skin green facade: A case study in Shanghai”, *Sustainable Cities and Society*, vol. 39, no. January, pp. 43–51, 2018.
- [22] K. Perini, F. Bazzocchi, L. Croci, A. Magliocco, and E. Cattaneo, “The use of vertical greening systems to reduce the energy demand for air conditioning. Field monitoring in Mediterranean climate”, *Energy and Buildings*, vol. 143, pp. 35–42, 2017.
- [23] M. Manso and J. P. Castro-Gomes, “Thermal analysis of a new modular system for green walls”, *Journal of Building Engineering*, vol. 7, pp. 53–62, 2016.
- [24] G. Vox, I. Blanco, and E. Schettini, “Green façades to control wall surface temperature in buildings”, *Building and Environment*, vol. 129, no. September 2017, pp. 154–166, 2018.
- [25] C. L. Tan, N. H. Wong, and S. K. Jusuf, “Effects of vertical greenery on mean radiant temperature in the tropical urban environment”, *Landscape and Urban Planning*, vol. 127, pp. 52–64, 2014.
- [26] L. L. H. Peng, Z. Jiang, X. Yang, Y. He, T. Xu, and S. S. Chen, “Cooling effects of block-scale facade greening and their relationship with urban form”, *Building and Environment*, vol. 169, no. November 2019, p. 106552, 2020.
- [27] A. Cortês, A. Tadeu, M. I. Santos, J. de Brito, and J. Almeida, “Innovative module of expanded cork agglomerate for green vertical systems”, *Building and Environment*, article in press.
- [28] N. Simões, R. Fino, and A. Tadeu, “Uncoated medium density expanded cork boards for building façades and roofs: Mechanical, hygrothermal and durability characterization”, *Construction and Building Materials*, vol. 200, pp. 447–464, 2019.

-
- [29] R. Fino, A. Tadeu, and N. Simões, “Influence of a period of wet weather on the heat transfer across a wall covered with uncoated medium density expanded cork”, *Energy and Buildings*, vol. 165, pp. 118–131, 2018.
- [30] A. Cortês, J. Almeida, J. de Brito, and A. Tadeu, “Water retention and drainage capability of expanded cork agglomerate boards intended for application in green vertical systems”, *Construction and Building Materials*, vol. 224, pp. 439–446, 2019.
- [31] “Webertherm flex P - Technical file”, 2018. [Online]. Available: <https://www.pt.weber/revestimento-e-renovacao-de-fachadas/webertherm-flex-p>.
- [32] Atlanlusi Europe, “GeoTexPro - Geotêxtil/Geocompósito”, Ficha Técnica. [Online]. Available: <http://www.atlanlusi.pt/repositorio/projetistas/Bioarquitetura/CoberturasVerdes/FichaTécnica-GeoTexPro.pdf>.
- [33] “Direção Geral de Energia e Geologia (DGEG)”. [Online]. Available: <https://www.dgeg.gov.pt/pt/areas-setoriais/energia/energias-renovaveis-e-sustentabilidade/sce-er/>.

CHAPTER 6

FINAL REMARKS

6. Final remarks

6.1. Overview and main conclusions

Green vertical systems can provide several recognized benefits to the buildings and urban environment. However, numerous questions have been raised regarding their sustainability, particularly with respect to the materials they use, and their irrigation and maintenance needs. Consequently, the main objective of this research work was to design and develop an innovative green vertical system with an improved environmental performance throughout its life cycle. For that purpose, the expanded cork agglomerate, a natural material with recognized thermal insulation and water retention capacities, was used. This material is made of by-products of the cork industry and the waste resulting from pruning the cork oak, all of which is agglomerated with the resins naturally present in the cork granules.

The work began with the experimental evaluation of the water retention and the drainage capacity of the expanded cork agglomerate (Chapter 2). This involved performing tests on board specimens of varying density, height, and thickness. Drainage profiles were obtained for fully confined and partially confined boards and were further tested for water retention and runoff time. The results suggest that expanded cork agglomerate has a suitable moistening and a retention capacity up to 20 kg/m³, and can also quickly drain the excess water (even if denser specimens are used) which will prevent soil saturation. These results confirmed that the expanded cork agglomerate is suitable for use in green vertical systems.

Then this work presented the process to design a new ICB module for building eco-friendlier living walls (Chapter 3). To support that, a comparative life cycle analysis of five distinct modular living

wall systems was performed in a cradle-to-gate perspective. The results showed that the metal and plastic materials used for the fastening components and vegetation support elements have the biggest impact on the overall environmental performance. To further assist the design process, several additional functional requirements have also been discussed, including aspects related to protecting the bearing wall, and the mechanical resistance to face loads generated by the dead weight, wind, maintenance operations, and other potential actions. Concerning these aspects, the design proposed uses ICB modules instead of plastic components to support the vegetation layer. The modules were also developed so that they could be fastened directly to the bearing wall using a waterproofing adhesive mortar avoiding metal fixing components. The modules were carefully designed to ensure that the supporting wall would benefit from a continuous layer (at least 50 mm) that has both thermal and acoustic insulation properties, and protection functions. Finally, to help choose the most suitable ICB density and to evaluate the behaviour of the proposed solutions in wet conditions and after wetting-drying cycles, a full mechanical characterization was performed. The results suggest that the medium-density (140 - 160 kg/m³) ICB modular system could be an appropriate eco-friendlier alternative to the plastic- and metal-based GVS currently used, and it would meet the environmental and functional requirements expected of a living wall system.

The new modular living wall was then characterized in real conditions (Chapter 3). For this purpose, a prototype consisting of four façades (facing north, south, east, and west) was built and two plant species were selected to be used (*Thymus pulegioides* and *Festuca glauca*). The area of façade covered by vegetation and the rate of carbon sequestration were monitored for over one year. The results showed that although the carbon content is approximately constant (between 44% and 46%) over time for both plant species, *Festuca glauca* has a much higher amount of biomass than *Thymus pulegioides*, regardless of the façade orientation and season. Consequently, the total carbon uptake provided over one year by *Festuca glauca* (371 gCm⁻²) was much higher than that of *Thymus pulegioides* (68 gCm⁻²), considering the best façade orientation in both cases. In terms of coverage area, the results showed that *Festuca glauca* was able to cover a larger area of the façade during the monitored year, compared with *Thymus pulegioides* performing both plant species well in warmer seasons. Finally, a cradle-to-grave LCA based on the characteristics of the prototype and monitoring results was also carried out to assess the environmental performance of the new modular living wall. The results showed that the new modular living wall can be an eco-friendly choice, contributing especially to mitigate global warming since it has a negative carbon balance of 22.7 kg CO₂eq per square metre over its life cycle. Additionally, the results of a comparative LCA showed that the benefits of the cork-based solution were able to offset the environmental burden of installing additional components to the building wall.

Finally, the effect of the new cork-based living wall on the energy performance of buildings and the local microclimate was evaluated (Chapter 5). For this, the same prototype as that described previously was used to monitor temperatures across each living wall façade and in their vicinity for

one year. The results show that although different surface temperatures were obtained in façades with different orientations, the temperatures behind the ICB layer do not vary much, suggesting that the living wall performs well in terms of thermal insulation. For comparison purposes, two additional walls containing an external thermal insulation composite system (ETICS) were also monitored over the same period. One was painted white, representing a higher reflective solution, and the other black, representing a higher absorptive solution, expected to better approach the ICB colour. The results showed that the surface temperatures in the troughs behind the plants were lower than those measured at the surface of the white and black reference walls. Furthermore, very small variations are found in the thermocouples, located at different heights behind the ICB layer, which suggests that the decrease of insulation in the trough is offset by the shading and evaporative effects. The results have also shown that the evaporative effects of the living wall can be enhanced by spraying the ICB layer with water. The simulations compared against a reference building (using DesignBuilder software) have further shown lower heating and cooling needs when an external coating of ICB is applied to the reference building, even using the lower thickness ICB (50 mm) in wet conditions.

This research work has shown that the modules designed with expanded cork agglomerate are a suitable solution to build modular living walls that fulfil the functional and environmental requirements. Expanded cork agglomerate has also been found to be beneficial in terms of water retention, drainage capability, and carbon sequestration. The design created with this natural material avoids the use of plastic and metal components. The new modular living wall solution showed a good performance in terms of the plants' carbon sequestration and thermal insulation, and proved to be an eco-friendly solution over its life-cycle.

6.2. Future work

An innovative green vertical system using the expanded cork agglomerate with improved environmental performance was successfully designed and developed in this research work. The objectives initially established were achieved, but it is recognized that further research on the following aspects should be conducted:

- Evaluation of the water retention of the new modular living wall in field conditions and monitoring the humidity of the substrate to help to establish values to automate the irrigation systems.
- Experimental analysis of the carbon sequestration and coverage area of the vegetation with different types of plants and simulating the climate conditions typical of other regions.

- Assessment of the thermal performance of the system under different climate conditions. This study could be performed in bioclimatic chambers that allow simulating different climate scenarios.
- Develop and/or adapt numerical models to simulate the hygrothermal behaviour of the new modular living wall under different climatic conditions.
- Comparison of the environmental performance of the new modular living wall with other existing solutions from a cradle-to-grave perspective.